Title
Liver and pancreas development in the zebrafish, Danio rerio

Author
Field, Holly Ann

Publication Date
2003

Peer reviewed|Thesis/dissertation

Liver and Pancreas Development in the Zebrafish, Danio rerio

by

Holly Ann Field

DISSERTATION

Submitted in partial satisfaction of the requirements for the degree of

DOCTOR OF PHILOSOPHY

in

Genetics

in the

GRADUATE DIVISION

of the

UNIVERSITY OF CALIFORNIA, SAN FRANCISCO

For Robert and Cheryl

and

For Peter

PREFACE

I would like to take this opportunity to acknowledge:

Didier Y. R. Stainier, an outstanding advisor. He has taught me the skill of scientific inquiry and approach, and has gained my sincere respect as a mentor.

Gail Martin and Matthias Hebrok, members of my thesis committee. They have provided insight and guidance, and offered me a great deal of their time to make my graduate career successful.

Members of the Stainier Lab, past and present. They have promoted my intellectual growth as individuals and as an unparalleled collective.

Regina Burris, friend and editor. She has given me great friendship and helped edit my recent written works, including this thesis.

Robert and Cheryl Field, my parents. They are always loving, encouraging and supportive.

Peter Chien, my partner. He has gone out of his way to learn about developmental biology, and supports me in every aspect of my life.

Page 1 is a reproduction of the cover of *Mechanisms of Development* 120, (2003) for which I contributed the image.

Page 25 is a reproduction of the cover of *Developmental Biology* 253(2), 2003 for which I contributed the image.

Chapter 2 represents data and text previously published as:

Formation of the digestive system in zebrafish: I. Liver morphogenesis.

Developmental Biology (2003) 253:279-290.

By H. A. Field, E. A. Ober, T. Roeser, D. Y. R. Stainier

Page 63 is a reproduction of the cover of *Developmental Biology* 261(1), 2003 for which I contributed the image.

Chapter 3 represents data and text previously published as:

Formation of the digestive system in zebrafish: II. Pancreas Morphogenesis.

Developmental Biology (2003) 261:197-208.

By H. A. Field, P. D. Si Dong and D. Y. R. Stainier

ABSTRACT

My thesis work has been focused on understanding the processes involved in liver and pancreas organogenesis. With its amenability to forward genetic screens and external fertilization of its eggs, the zebrafish is a useful and practical model system in which to investigate aspects of liver and pancreas development. Taking advantage of the embryos' optical clarity and a transgenic line that expresses GFP throughout the endoderm, I have been able to characterize the morphogenesis of these organs in zebrafish embryos.

Liver development has not previously been characterized in the zebrafish. Using confocal microscopy with the GFP transgenic line mentioned above I identified three morphologically distinct stages of liver budding and characterized the behavior of the hepatocytes as the liver undergoes organogenesis.

Morphogenesis of the zebrafish pancreas has been previously described, with all studies indicating that pancreas development in zebrafish occurs from a single pancreatic anlage. My work has led to the realization that there are in fact two pancreatic anlagen that join to form the pancreas. The posterior bud contains only endocrine tissue, and the anterior bud gives rise to the pancreatic duct and exocrine cells. Interestingly, at later stages the anterior bud also gives rise to a small number of endocrine cells that can be seen near the pancreatic duct. Observations regarding the location and timing of endocrine cell development have led us to hypothesize that there are two distinct origins for endocrine cells in the zebrafish. Future directions of the lab will include genetic analyses to determine whether these populations do indeed come from different precursor populations, and whether different genetic programs regulate their differentiation.

Table of Contents

List of Tables

List of Figures

MECHANISMS of DEVELOPMENT

Volume 120, issue 1 JANUARY 2003 ISSN 0925-4773

Reviews on Molecular Mechanisms of Liver and Pancreas Development edited by Ken Zaret

ELSEVIER

Chapter 1.

Introduction

Liver Development

An overview of adult liver anatomy and physiology

The human adult liver has many characteristic anatomical features. Endodermally derived hepatocytes are the main functional component of the liver. They produce numerous important molecules involved in carbohydrate and lipid storage, transportation of plasma proteins, and metabolism. Hepatocytes in the liver form spongy units called lobules. Each lobule has an extensive network of sinusoids, channels throughout the hepatic parenchyme lined by highly fenestrated endothelial cells and populated by Kupffer cells . Blood from capillaries surrounding the intestine travels into the liver via the hepatic portal vein and drains into these sinusoids where phagocytic Kupffer cells help detoxify the blood. Arterial blood, supplied to the liver through the hepatic artery, also drains into the sinusoids. Blood plasma flows into the space between the endothelial lining and hepatocytes, the space of Disse, where it is in direct contact with hepatocytes and can drain into the lymph system for further detoxification (Vassy and Kraemer, 1993). Blood exiting the liver drains from the hepatic sinusoids into central veins, and then blood exits the liver through the hepatic vein. In addition to their roles in blood detoxification, hepatocytes secrete bile into bile canaliculi. The bile drains into intrahepatic bile ducts and subsequently to the gall bladder where it is stored until signals from the intestine stimulate its release into the duodenum for aid in digestion of fats.

Hepatocytes achieve their diversity of roles by sequestering functional proteins to established plasma membrane domains. A single hepatocyte is polarized such that it

possesses three specialized membrane domains (reviewed in Stamatoglou and Hughes, 1994; Vassy and Kraemer, 1993). The bile canalicular domain (apical) faces and projects microvilli into the bile canaliculi. This face of the cell is responsible for secretion of bile. The lateral domains contact other hepatocytes. These cell faces contains tight junctions for cell adhesion and gap junctions for cell communication. The third membrane domain is the blood sinusoidal domain (basal). Like the bile canalicular domain, this cell face also forms microvilli. The large surface area of the blood sinusoidal domain is involved in extensive interactions with the blood, which include receiving information via receptor-mediated binding of hormones, and secreting plasma proteins (Vassy and Kraemer, 1993).

Liver anatomy has also been studied in different fish species. Studies on the brown trout and the sea bass have found liver sinusoids lined by reticuloendothelial cells and surrounded by five to eight hepatocytes in transverse section. Bile canaliculi collect bile from adjacent hepatocytes. The larger bile ducts, into which these canaliculi drain, are lined by a cuboidal epithelium (Gromon, 1982). As in mammals, microvilli project into both the bile canaliculi and the space of Disse (Rocha et al., 1994). Hepatic function is also at least partially conserved between mammals and fishes as the hepatocytes of both contain glycogen and lipid stores (Gromon, 1982; Rocha et al., 1994).

Early embryology and fate mapping

Fate mapping studies are carried out to determine the location of the endodermal cells that give rise to the liver before these endodermal cells show signs of hepatic specification and differentiation. Fate mapping is achieved by marking an undifferentiated cell with a permanent label, such as carbon particles or a tracer dye, taking note of where the cell is throughout development, and finally determining what organ or tissue type that cell becomes. Through this style of analysis, one can determine the location of cells that will contribute to the liver. It is important to remember that fate mapping studies do not provide information on whether a given cell is committed to a certain fate when it is labeled, just that a cell in a given location will eventually receive all the information through the normal course of development to differentiate.

Fate mapping studies in both chick (Le Douarin, 1975) and zebrafish embryos (Warga and Nusslein-Volhard, 1999) have tracked cells that eventually contribute to the liver. These data are summarized in Fig. 1.1. In a Stage 5 chick, pre-hepatic cells are located in bilateral patches of the endoderm. These patches start to migrate into the head fold at Stage 6 of development. By the 5 somite stage, these patches have not fused, but are becoming incorporated into the ventral floor of the anterior intestinal portal (AIP), also called the foregut pocket. At Stage 11 of chick development, the pre-hepatic endodermal cells are in a single cluster on the ventral floor of the AIP (Le Douarin, 1975) (Fig. 1.1A).

Cells contributing to the liver in zebrafish have not been tracked through so many stages of development. However, their location at 40% epiboly is mapped to regions within 4 cell diameters from the blastoderm margin between 120 and 150 degrees from

dorsal on one side and around 30 degrees from dorsal on the other side of the embryo (Warga and Nusslein-Volhard, 1999) (Fig. 1.1B).

Influence of adjacent tissues

Liver development, from hepatocyte determination to differentiation, proliferation and maintenance of hepatocytes, requires signals from surrounding tissues. This endoderm's dependence on other tissues for hepatocyte development is not surprising when the nature of liver structure is considered. Since the adult structure is an organized mixture of cells originating from both endoderm and mesoderm, it comes as little surprise that these tissues interact during organogenesis. To understand these interactions fully, it is necessary to have a clear picture of where mesoderm and endoderm are juxtaposed during the stages preceding determination through differentiation.

In quail, when the hepatic endoderm begins to evaginate, at the 20 somite stage, it is in close contact with the endothelium of the omphalomesenteric vein and splanchnic mesenchyme (Fukuda, 1979). Endoderm and endothelial cells proliferate and invade a loose mesenchymal tissue that develops around the ductus venosus (Fukuda, 1979).

Endoderm develops on the ventral surface of the developing mouse embryo during gastrulation, displacing the visceral endoderm. At approximately E8 of embryonic development, the endoderm folds dorsally at the region of the headfold to produce a blind ended cavity lined by a single layer of endodermal cells, the AIP. As gut morphogenesis continues, bringing more lateral endodermal tissue toward the midline to extend the developing gut tube posteriorly, the heart tissues develop into a tube sitting ventral to the endoderm of the foregut pocket. The heart remains adjacent to the ventral foregut endoderm as pre-hepatic cells begin to proliferate. Gut morphogenesis brings these ventral foregut cells more posterior along the developing gut tube and their association with the cardiac mesoderm is lost by 9.5 days (Zaret, 1996). At this point, the

presumptive liver bud is in contact with the septum transversum mesenchyme, but there is a basement membrane which separates the liver bud from the adjacent septum transversum mesenchyme (Houssaint, 1980). This basement membrane breaks down around the 28 somite stage allowing liver cells to invade the septum transversum mesenchyme.

As described above, the cells that will give rise to the liver start out in bilateral patches in the endoderm in contact with pre-cardiac mesoderm cells which sit dorsal to the endoderm. The first morphological sign of heart formation in chick occurs at the 3 to 5 somite stage. The splanchnopleure that is slightly lateral to the hind-brain begins to thicken and this tissue will eventually form the myocardium (Willier and Rawles, 1984). As the splanchnopleure folds toward the midline, the two populations of pre-cardiac tissue fuse (occurring around the 6 somite stage) (Willier and Rawles, 1984). At this stage cells that will contribute to the liver are located along the ventro-lateral edges of the AIP (Fig. 1.1A, C). By about the 10 to 12 somite stage, the heart is a single tubular organ with its venous end resting upon the anterior intestinal portal. The omphalomesenteric veins, which are connected to the venous end of the heart, lay along the edges of the AIP (Willier and Rawles, 1984). The endoderm in this region of the AIP will develop into hepatocytes.

Tissue grafting studies noted a strong correlation between the development of the liver and the heart (Willier and Rawles, 1984). While performing grafts of chick blastoderm to the chorio-allantoic membrane, Willier and Rawles notice that in no cases did a liver develop in these grafts without the presence of a heart. In addition, when two hearts were formed in these grafts, two corresponding livers were also seen.

The necessity of the mesoderm for hepatocyte development was more specifically demonstrated in chick, by isolating regions of the endoderm fate-mapped to become liver and determining what conditions can lead to hepatocyte differentiation. For these studies, a ruling of differentiation was usually based on cell morphology, sub-cellular organization of organelles, or the ability of the cell to perform the functions of hepatocytes, namely to store glycogen and lipids. If pre-hepatic endoderm is isolated before the 4 – 5 somite stage in chick or the 2 somite stage in quail, it does not develop into hepatocytes, even if associated with mesoderm that supports the differentiation of older pre-hepatic endoderm into hepatocytes (Fukuda, 1979; Le Douarin, 1970). Endoderm at this early stage becomes determined only in the presence of the adjacent mesoderm, the pre-cardiac mesoderm (Fukuda, 1979; Le Douarin, 1970).

Interestingly, the ability of the pre-cardiac mesoderm to induce endoderm toward a hepatic fate does not work on all endoderm. Fukuda tested the ability of posterior endoderm to respond to inductive signals from the cardiac mesoderm. At no stage, from the definitive streak to the 21-35 somite stage, did posterior endoderm differentiate into hepatocytes regardless of the presence or absence of pre-cardiac mesoderm (Fukuda, 1979).

In mouse, there is also an apparent necessity of the cardiac mesoderm for liver development. Ventral foregut endoderm isolated from 4 to 6 somite stage mouse embryos fails to differentiate *in vitro* after 2 days unless cultured with cardiac mesoderm (Gualdi et al., 1996). In these studies, differentiation was defined as the expression of the liver gene albumin. Normal albumin expression occurs at a stage in mouse liver development that precedes any cell or tissue morphology change. Later it was discovered

that these explants, both those with and those without cardiac mesoderm, contained a considerable amount of septum transversum mesenchyme adding another dimension to exactly which tissues are responsible for different aspects of hepatic development (Rossi et al., 2001).

In the zebrafish the heart is far from the location of the liver bud upon its first signs of morphogenesis. This would suggest that initial morphogenesis of the liver is not controlled by direct contact with the heart tube. In addition, in cases where the bilateral cardiac tissues do not migrate to the midline and result in cardia bifida, the liver still forms as a single, well formed organ (Nick Osborne, personal communications). However, an earlier instructive interaction between pre-hepatic endoderm and pre-cardiac mesoderm has not yet been ruled out, and fate mapping studies have not been performed to look at the location of pre-hepatic endoderm after gastrulation and before liver morphogenesis begins. Based on the current knowledge of heart and liver location one must conclude that if the pre-cardiac mesoderm is necessary for liver induction in zebrafish, other mesodermal populations must be supplying signals for hepatic differentiation and morphogenesis, or the ability of the pre-hepatic tissue to further develop is inherent.

The inherent potential of induced hepatic endoderm has undergone some debate. Chick endoderm isolated from the anterior intestinal portal when the liver rudiment is forming (20 to 22 somite stage) does not differentiate and rapidly degenerates when grown alone *in vitro* or if grafted into the coelom (Le Douarin, 1970). However, hepatocyte survival is rescued when these cells are cultured with isolated mesoderm of the same stage or older embryos (Le Douarin, 1970). Different populations of mesoderm

can promote hepatocyte differentiation and morphogenesis from specified endoderm in chick. Specified endoderm from the AIP differentiates properly when co-cultured with either somatic or splanchnic lateral plate mesoderm (LPM) at various levels between the limb buds (Le Douarin, 1970). It also differentiates when cultured with the hepatic mesenchyme – an area of mesoderm, presumably of splanchnic LPM origin, into which the proliferating hepatocytes migrate (Le Douarin, 1970). Renal mesenchyme, on the other hand, can only stimulate pre-hepatic endoderm to proliferate, but does not induce these cells to differentiate (Le Douarin, 1970).

In quail the data suggest that after induction by the cardiac mesoderm the pre-hepatic tissue possesses an autonomous ability to differentiate. Anterior endoderm isolated between the 2 and 5 somite stages differentiates into hepatocytes with or without contact from different mesodermal tissues (Fukuda, 1979). Similar results were observed in mouse (Gualdi et al., 1996). However, it was later discovered, using the expression of *Mrg1* as a marker for septum transversum mesenchyme, that the mouse explants contained a considerable amount of septum transversum mesenchyme (Rossi et al., 2001). If the mouse and quail explants did and the chick explants did not contain this population of mesenchyme, it could explain why chick explants of induced but not differentiated endoderm rapidly degraded in culture unless in the presence of mesoderm (Le Douarin, 1970), while mouse tissue of the same class was able to survive and express hepatic genes (Gualdi et al., 1996). In this explanation, the mouse and quail tissue cultures unknowingly had a sufficient population of mesoderm to sustain hepatic development.

From studies in chick, quail and mouse, one can conclude that initial specification of hepatic endoderm requires signals from similarly staged pre-cardiac mesoderm, although the timing of this induction varies by organism occurring by the 4 to 5 somite stage in chick, the 2 somite stage in quail and the 7 somite stage in mouse. Experiments have not been performed to determine whether older cardiac mesoderm can also perform this function. Once the hepatic endoderm is specified, mesoderm may or may not be necessary to maintain hepatocyte identity and promote morphogenesis of the endodermal component of the liver. Lateral or ventral (including pre-cardiac) mesoderm are all sufficient to perform this task. Yet the question remains as to whether other tissues, such as the vascular endothelium which is present in all regions that were shown to support hepatic differentiation, are actually the necessary tissue. In fact, Fukuda hints at this:

> It must be noted that the time of appearance of self-differentiation potency in the endoderm for the hepatic epithelium, coincides with that of the first differentiation of embryonic endothelium in the anterior intestinal portal region. The endothelium of this region is generally considered as the most important in hepatic morphogenesis (Fukuda, 1979).

Thus, until the molecular factors necessary for liver development are isolated, one can not be sure which tissue supplies those signals to liver during normal embryonic development.

Molecular analyses in vitro

in vitro analysis of tissue potentials can assist in understanding the interactions sufficient for hepatocyte development. As discussed above, mouse explant experiments have shown that culturing pre-hepatic tissue with cardiac mesoderm *in vitro* directs the endoderm to express the liver marker albumin, a sign of hepatic differentiation. Jung et al. took advantage of this tissue culture system to examine the potential molecular cues responsible for this developmental progression (Jung et al., 1999). They used albumin expression, which is first detectable by RT-PCR at the 7 to 8 somite stage, to assay hepatocyte differentiation. Isolated ventral foregut endoderm from 2 to 6 somite stage mice was cultured for two days in the presence of different fibroblast growth factors (FGFs) and a heparin sulfate carrier. These tissue cultures were then tested by RT-PCR for albumin expression. FGF1 reliably induces albumin expression at concentrations above 50 ng/ml, but is effective in only 50% of the explants when supplied at a concentration of 5 ng/ml. FGF2 effectively induces albumin expression at 5 ng/ml but not at higher concentrations. FGF8b is marginally effective at high and low concentrations, only inducing about 33% of cultures to express albumin. One caveat of *in vitro* studies is that they show whether a molecule can induce hepatic gene expression, but do not prove that these are the same molecules acting *in vivo* during development. In this case, each FGF protein tested – FGF1, FGF2 and FGF8b – is present at the 7 to 8 somite stage in the cardiac mesoderm, although the dynamics of their expression vary: FGF1 is just beginning to appear, FGF2 is prevalent, and FGF8 protein persists although gene expression is beginning to decline (Jung et al., 1999).

In a later study by the same group, Sonic Hedgehog (Shh) is shown to be expressed in domains of explanted ventral foregut endoderm adjacent to cardiac mesoderm and in ventral foregut endoderm cultured *in vitro* with 5ng/ml of FgF2 (Deutsch et al., 2001). Shh is absent from ventral foregut endoderm cultured in the absence of cardiac mesoderm (Deutsch et al., 2001). If cardiac mesoderm or FGF2 induces Shh expression in ventral foregut endoderm, and cardiac mesoderm or FGF2 can induce albumin expression in ventral foregut endoderm, then one might expect Shh expression to be an intermediate signal between FGF2 and albumin expression. However, Shh added to cultures of ventral foregut endoderm does not result in the expression of albumin in this tissue (Deutsch et al., 2001). Therefore, it appears that cardiac mesoderm can induce expression of both Shh and albumin in ventral foregut endoderm explants (perhaps even in the same cells) but that Shh signaling is most likely not acting upstream of albumin expression.

As described above, FGF molecules are able to induce albumin expression in cultured pre-hepatic tissue. Interestingly, they are not sufficient to support any further progression of the endoderm toward hepatocyte differentiation and morphogenesis. Neither FGF1 nor FGF8b induce endodermal outgrowth in explants as occurs when co-cultured with cardiac mesoderm (Jung et al., 1999). However, blocking FGF8b signaling does affect endodermal outgrowth. Recall that 2 to 4 somite staged ventral foregut endoderm, dissected along with the associated cardiac mesoderm, develop into albumin-expressing hepatocytes and clusters of beating cardiac cells, respectively. Blocking FGF8b signaling in these co-cultures with a dominant negative FGFR4 protein diminishes the levels of albumin expression, and dramatically affects the outgrowth of

the endoderm. It has been suggested that FGF8b is therefore necessary for endoderm to respond to some outgrowth signal. However, there is no data indicating whether the co-cultures exposed to dominant negative FGF receptors contained beating cardiac cells. Evidence showing the role of FGF8 in heart development (Reifers et al., 2000) may suggest that blocking FGF8 in these cultures is primarily affecting the cardiac mesoderm which leads to problems in hepatocyte differentiation and morphogenesis. Further studies are needed to sort the actual hierarchy of interactions.

The role of BMPs has also been examined in liver differentiation. *in vitro* cultures of what was thought to be isolated pre-hepatic ventral foregut endoderm were later shown to contain BMP4 expressing septum transversum mesenchymal cells (Rossi et al., 2001). These cultures do not express albumin in the endoderm suggesting that BMP4 is not able to induce hepatic differentiation (Rossi et al., 2001). However, if endoderm is removed from the embryo after the initial stages of hepatocyte induction, and cultured only with these septum transversum derived BMP4 positive cells, the endoderm survives and maintains albumin expression for many days in culture (Gualdi et al., 1996; Rossi et al., 2001). These data suggests a direct role for BMP4 in maintaining hepatocyte identity or promoting further differentiation of already specified hepatocytes. Alternatively, there may be other molecules generated by the BMP4 expressing tissue that are acting on induced hepatic endoderm (both cardiac and septum transversum mesoderm express BMP4, between the 12 and 17 somite stages just preceding liver budding and outgrowth (Rossi et al., 2001)).

A great deal of work has been done to identify the external conditions necessary for all stages of hepatocyte induction, differentiation and morphogenesis. However,

every method of study has its limits and *in vitro* tissue culture is no exception. The next wave of insight into the mechanisms controlling liver development will most likely be generated through a combination of forward genetic screens, to identify the molecules involved, and tissue specific reverse genetics, to identify in which tissues these molecules function.

Pancreas Development

A number of extensive reviews exist on pancreas development (Kim and Hebrok, 2001, Edlund, 2002, Slack, 1995). Therefore, I will refer the reader to these sources for review of the wealth of knowledge available for pancreas development. However, due to its relevance to information in Chapter 3 of this thesis, I will review pancreas morphogenesis and the influence of adjacent tissues on pancreas development.

Influence of adjacent tissues

In mouse, after gastrulation the endoderm that will give rise to the dorsal pancreatic bud is midline and contacts the notochord until the 13 somite stage (Wessells and Cohen, 1967). At the 13 somite stage, the dorsal aorta fuses at the midline separating the notochord from this midline endoderm (Wessells and Cohen, 1967). The midline endoderm maintains direct contact with the dorsal aorta until about the 22 somite stage when the mesodermal mesenchyme, which has been accumulating lateral to the dorsal aorta since about 12 somites, invades the midline separating the dorsal aorta from the endoderm(Wessells and Cohen, 1967). No signs of dorsal bud morphogenesis are detectable until about the 22 – 25 somite stage when the endoderm starts to evaginate forming the dorsal pancreatic bud (reviewed in Kim and Hebrok, 2001).

Endoderm that will give rise to the ventral pancreatic bud in mouse is located at the lip of the anterior intestinal portal by the 7 to 8 somite stage, at which time it begins expressing pancreatic and duodenal homeobox gene 1 (pdx1) detectable by RT-PCR (Deutsch et al., 2001). In the chick embryo, the endoderm that will give rise to the ventral pancreas is still bilateral at the level of somites 7 – 9 (Kumar et al., 2003). Pdx1

can first be detected in this region of endoderm at the 9 to 10 somite stage (Kumar et al., 2003).

Tissue recombination studies, both *in vivo* and *in vitro* were used to determine the role and timing of tissue interactions in ventral pancreatic bud development. Lateral endoderm at various levels posterior to the anterior intestinal portal was tested for competence to express pancreas genes and for morphogenetic capabilities (Kumar et al., 2003). If endoderm from the 7 to 9 somite level of a chick embryo is isolated from a 5 somite stage embryo, a 10 somite stage embryo or a 15 somite stage embryo and cultured alone *in vitro*, Pdx1 expression is not detectable after 48 hours. When this same endoderm from a 10 somite stage embryo is cultured with the adjacent mesoderm for 48 hours, not only is Pdx1 expressed, but also Glucagon, Insulin, and p48. If this endoderm is transplanted anteriorly to the 2 to 4 somite level any time ranging from the 6 to 14 somite stage, it is still able to initiate and maintain Pdx1, Glucagon and p48 expression after 2 days, although insulin expression is lost. The same is true when this endoderm is cultured with mesoderm from the 2 to 4 somite level. When transplanted posteriorly or cultured with mesoderm from the 12 to 14 somite level, the posterior mesoderm induces Cdx expression in the endoderm and expression of all pancreatic genes is lost.

These data strongly suggest that the mesoderm adjacent to lateral endoderm from an A/P level corresponding to the 7^{th} to 9^{th} somite sends an instructive signal to the endoderm by the 6 somite stage and is then necessary for maintaining tissue identity. More anterior mesoderm seems to be sufficient for maintenance.

Pdx1 expression in the ventral pancreatic domain is initiated in mouse embryos by E9 only in endoderm adjacent to the vitelline veins (Lammert et al., 2001). In chick,

however, the ventral pancreatic tissue is located in bilateral patches at the level of the 7th to 9th somite when they first start to express Pdx1, around the 9 – 10 somite stage (Kumar et al., 2003). This does not exclude the possibility that the endoderm in chick is receiving information from endothelium other than that of the vitelline veins. At E10.5 in mouse, after the dorsal pancreas has initiated budding, differentiated β-cells are found in contact with endothelium of the portal vein (Lammert et al., 2001).

Although the interaction of the pancreatic endoderm and the endothelium is coincident with the initiation of Pdx1 expression, the question remains whether the endothelium is being recruited by the endoderm as it differentiates, or the endothelium is necessary for the differentiation of the endoderm into pancreas. To answer this question, Lammert et al. focused on the interactions between the dorsal pancreas and the dorsal aorta (Lammert et al., 2001). Tissues were isolated from E8.25 to E8.5 embryos, a stage before the dorsal aorta is in contact with the presumptive dorsal pancreatic endoderm and before this endoderm expresses pdx1. When grown in culture alone for 6 days, this endoderm survives and forms a tube-like structure, but does not express pdx1 or insulin. When cultured for 6 days with isolated dorsal aorta from the same stage, both pdx1 and insulin expression are detectable by *in situ* hybridization.

This rescue of insulin and pdx1 expression can be achieved also by recombining the endoderm with the umbilical artery or the LPM. These data demonstrate that endothelium is sufficient to support the expression of pdx1 and insulin in induced, competent pancreatic endoderm. However, since LPM can also support expression of insulin and pdx1, perhaps many different mesodermal derivatives can have this effect.

Alternatively, the isolated LPM may have been contaminated with endothelial cells, complicating any conclusions that are drawn.

The data from Lammert et al. make a convincing argument for the necessity of vascular endothelium in endocrine pancreas differentiation. One might wonder whether studies showing the necessity of lateral plate mesoderm for induction, differentiation and morphogenesis of the pancreas were misleading in that they may have had endothelium contaminating their isolated mesoderm samples. However, studies in zebrafish embryos lacking vascular endothelium suggest that the vascular endothelial cells are not necessary for normal pancreas differentiation and morphogenesis (Field et al., 2003).

Some studies have demonstrated that the mesoderm is needed to provide an environment conducive to pancreas induction, differentiation and morphogenesis. Other studies show a need for vascular endothelial cells. Having already mentioned the difficulties associated with isolating clean populations of mesoderm or endothelium, one must also consider the influence of these two tissues on one another. The vascular endothelial cells may be responsible for survival of mesoderm and thus only indirectly affect pancreas differentiation through maintenance of these mesodermal cells. The most definitive experiment to ascertain which are primary and which are secondary interactions would be to identify the molecules responsible for induction and differentiation of the pancreatic buds. Once the necessary signaling molecules are identified, their expression patterns and the normal course of tissue interactions will make it clear which tissue is normally responsible for the developing pancreas and which tissues are sufficient to compensate in perturbed situations.

REFERENCES

Argenton, F., Zecchin, E., and Bortolussi, M. (1999). Early appearance of pancreatic hormone-expressing cells in the zebrafish embryo. *Mech Dev* **87,** 217-21.

Biemar, F., Argenton, F., Schmidtke, R., Epperlein, S., Peers, B., and Driever, W. (2001). Pancreas development in zebrafish: early dispersed appearance of endocrine hormone expressing cells and their convergence to form the definitive islet. *Dev Biol* **230,** 189-203.

Deutsch, G., Jung, J., Zheng, M., Lora, J., and Zaret, K. S. (2001). A bipotential precursor population for pancreas and liver within the embryonic endoderm. *Development* **128,** 871-81.

Edlund, H. (2002). Pancreatic organogenesis--developmental mechanisms and implications for therapy. *Nat Rev Genet* **3,** 524-32.

Field, H. A., Dong, P. D., Beis, D., and Stainier, D. Y. (2003). Formation of the digestive system in zebrafish. II. Pancreas morphogenesis. *Dev Biol* **261,** 197-208.

Fukuda, S. (1979). The development of hepatogenic potency in the endoderm of quail embryos. *J Embryol Exp Morphol* **52,** 49-62.

Golosow, N., and Grobstein, C. (1962). Epitheliomesenchymal interaction in pancreatic morphogenesis. *Dev Biol* **4,** 242-55.

Gromon, D. B. (1982). "Histology of the Striped Bass."

Gualdi, R., Bossard, P., Zheng, M., Hamada, Y., Coleman, J. R., and Zaret, K. S. (1996). Hepatic specification of the gut endoderm in vitro: cell signaling and transcriptional control. *Genes Dev* **10,** 1670-82.

Houssaint, E. (1980). Differentiation of the mouse hepatic primordium. I. An analysis of tissue interactions in hepatocyte differentiation. *Cell Differ* **9,** 269-79.

Jung, J., Zheng, M., Goldfarb, M., and Zaret, K. S. (1999). Initiation of mammalian liver development from endoderm by fibroblast growth factors. *Science* **284,** 1998-2003.

Kim, S. K., and Hebrok, M. (2001). Intercellular signals regulating pancreas development and function. *Genes Dev* **15,** 111-27.

Kumar, M., Jordan, N., Melton, D., and Grapin-Botton, A. (2003). Signals from lateral plate mesoderm instruct endoderm toward a pancreatic fate. *Dev Biol* **259,** 109-22.

Lammert, E., Cleaver, O., and Melton, D. (2001). Induction of pancreatic differentiation by signals from blood vessels. *Science* **294,** 564-7.

Le Douarin, N. (1970). Induction of determination and induction of differentiation during development of the liver and certain organs of endomesodermal origin. *In* "Documents on biology: Tissue interactions during organogenesis" (E. Wolff, Ed.), Vol. 1, pp. xiv, 225. Gordon and Breach, New York,.

Le Douarin, N. M. (1975). An experimental analysis of liver development. *Med Biol* **53,** 427-55.

Mathews, W. W. (1982). "Atlas of Descriptive Embryology." Englewood Cliffs, NJ.

Reifers, F., Walsh, E. C., Leger, S., Stainier, D. Y., and Brand, M. (2000). Induction and differentiation of the zebrafish heart requires fibroblast growth factor 8 (fgf8/acerebellar). *Development* **127,** 225-35.

Rocha, E., Monteiro, R. A. F., and Pereira, C. A. (1994). The liver of the brown trout, *Salmo trutta fario*: a light and electron microscope study. *J Anat* **185,** 241 - 249.

Rossi, J. M., Dunn, N. R., Hogan, B. L., and Zaret, K. S. (2001). Distinct mesodermal signals, including BMPs from the septum transversum mesenchyme, are required in combination for hepatogenesis from the endoderm. *Genes Dev* **15,** 1998-2009.

Slack, J. M. (1995). Developmental biology of the pancreas. *Development* **121,** 1569-80.

Stamatoglou, S. C., and Hughes, R. C. (1994). Cell adhesion molecules in liver function and pattern formation. *Faseb J* **8,** 420-7.

Vassy, J., and Kraemer, M. (1993). Fetal and Postnatal Growth. *In* "Molecular and Cell Biology of the Liver" (A. V. LeBouton, Ed.), pp. 265 - 307. CRC Press, Boca Raton, Florida.

Warga, R. M., and Nusslein-Volhard, C. (1999). Origin and development of the zebrafish endoderm. *Development* **126,** 827-38.

Wessells, N. K., and Cohen, J. H. (1967). Early pancreas organogenesis: morphogenesis, tissue interactions and mass effects. *Dev Biol* **15,** 237 - 270.

Willier, B. H., and Rawles, M. E. (1984). Developmental Relations of the heart and liver in chorio-allantoic grafts of whole chick blastoderms. *The Anatomical Record* **48,** 277 - 301.

Zaret, K. S. (1996). Molecular genetics of early liver development. *Annu Rev Physiol* **58,** 231-51.

FIGURE LEGENDS

Fig. 1.1. Schematic representation of liver fate map data from chick (ventral views) (A) and zebrafish (B), with sketches of transverse (C1.) and sagittal (C2.) sections through chick embryos to show the close association of the ventral foregut endoderm and mesoderm. (A) Shaded regions represent endodermal cells fated to contribute to the liver. The bilateral patches of pre-hepatic endoderm migrate into the headfold and are positioned in the ventro-lateral lip of the anterior intestinal portal by the 5 somite stage. By Stage 11, all pre-hepatic endoderm is located in a single population of cells in the ventral foregut endoderm of the AIP. (B) Schematics representing the location of cells fated to contribute to the liver. Domes represent the cellular component of embryos at 40% epiboly. "0" marks the most dorsal point on the embryo. (B1.) Lateral view with dorsal to the right. (B2.) Dorsal view. Pre-hepatic cells map to within 4 cell diameters from the blastoderm margin between 120 and 150 degrees from dorsal on one side and around 30 degrees from dorsal on the other side of the embryo. (C1.) Representation of a transverse section through a 5 somite staged chick embryo at the level depicted by the arrow marked "C1" in (A). (C2.) Representation of a sagittal section through a 5 somite staged chick embryo at the level depicted by the arrow marked "C2" in A. Sections show the close association between the pre-hepatic endoderm and the mesoderm. AIP, anterior intestinal portal.

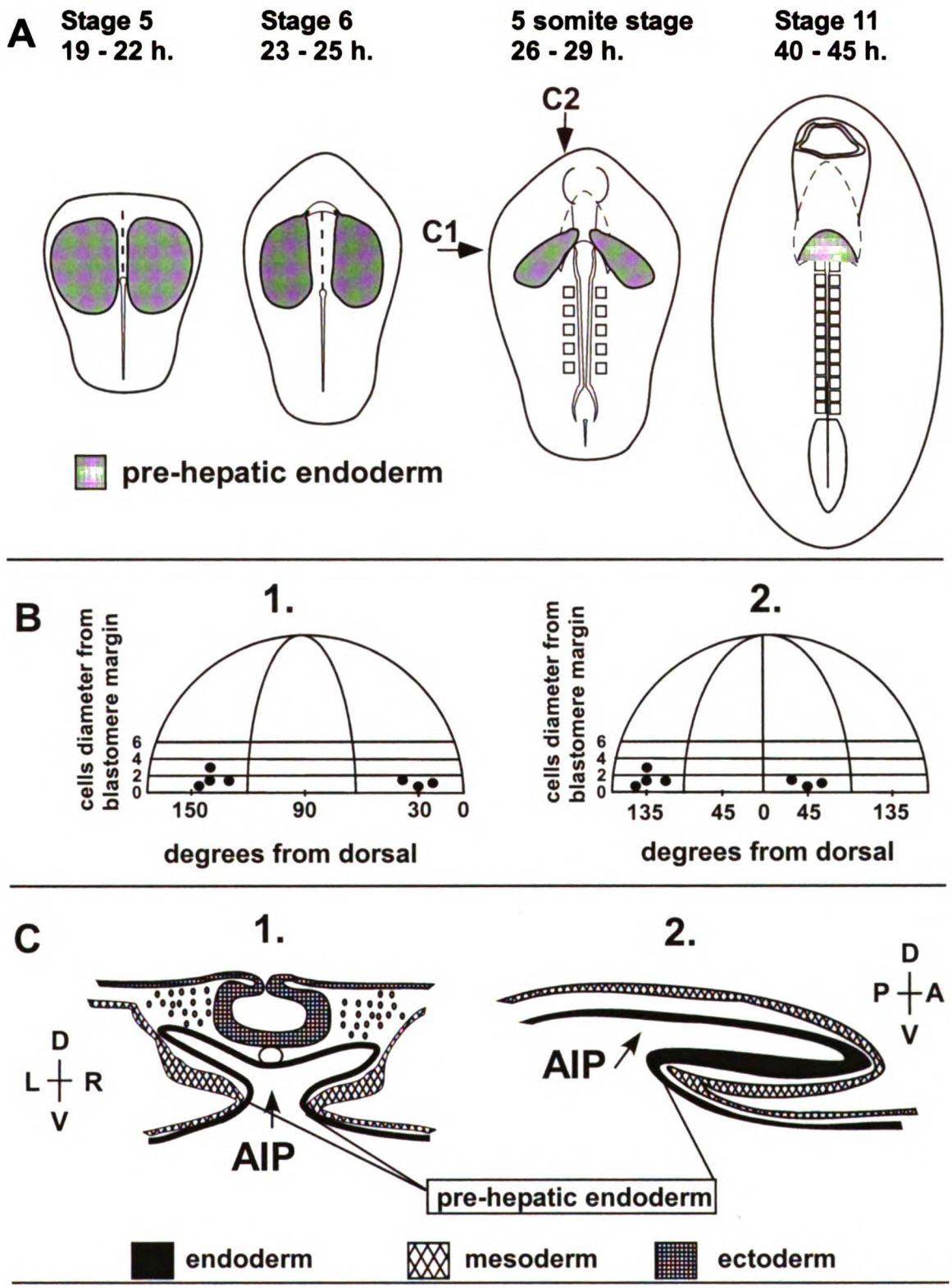

Figure 1.1. Schematic representation of liver fate map data from chick (A) and zebrafish (B), with sketches of transverse (C1.) and sagital (C2.) sections through chick embryos to show the close association of the ventral foregut endoderm and mesoderm.

DEBIAO
ISSN 0012-1606
This Number Completes Volume 253
Volume 253, Number 2, January 15, 2003

DEVELOPMENTAL BIOLOGY

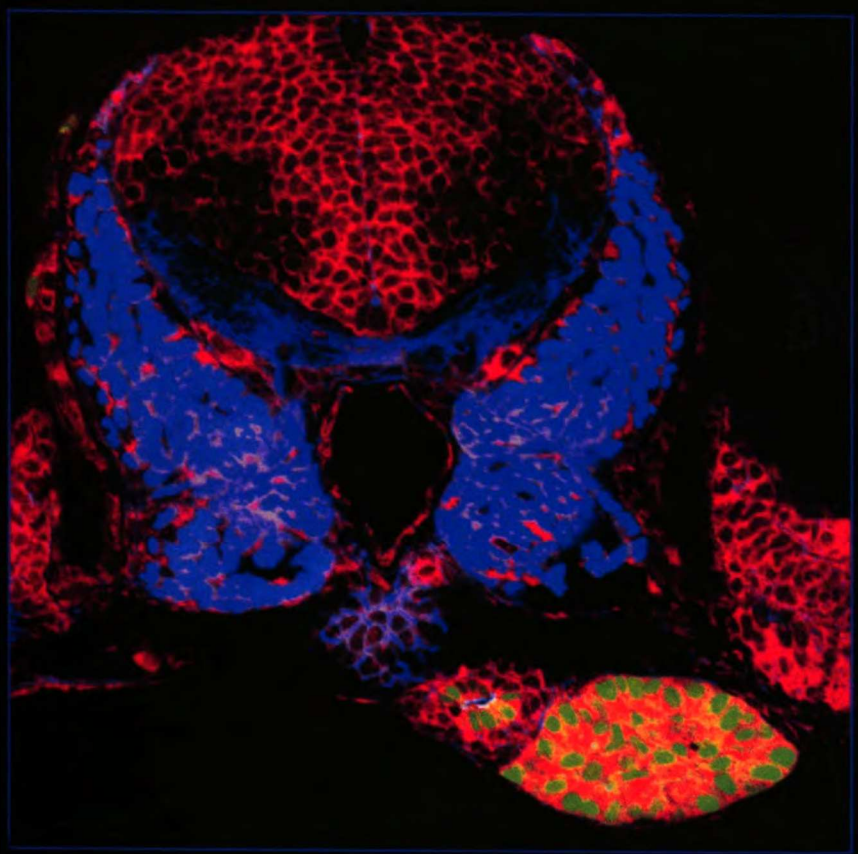

ACADEMIC PRESS
An imprint of Elsevier Science

"In order to study the development of the liver objectively, the first requirement is to forget all prejudices. . . The problem of liver embryology must be approached with a complete absence of any opinion whatsoever." – Hans Elias, 1955

Chapter 2.
Formation of the Digestive System in Zebrafish: I. Liver Morphogenesis

Holly A. Field, Elke A. Ober, Tobias Roeser+ and Didier Y. R. Stainier*

Department of Biochemistry and Biophysics, Programs in Developmental Biology, Genetics and Human Genetics, University of California, San Francisco, San Francisco, California 94143, USA

[+] Department of Physiology, University of California, San Francisco, San Francisco, California 94143, USA

*Author for correspondence:

Didier Stainier
Dept. of Biochemistry and Biophysics, HSE 1530C
Box 0448
513 Parnassus Ave.
San Francisco, CA 94143-0448
e-mail: didier_stainier@biochem.ucsf.edu
phone: (415) 502-5679
fax: (415) 476-3892

Running title: Zebrafish liver development

ABSTRACT

Despite the essential functions of the digestive system, much remains to be learned about the cellular and molecular mechanisms responsible for digestive organ morphogenesis and patterning. We introduce a novel zebrafish transgenic line, the gutGFP line, that expresses GFP throughout the digestive system, and use this tool to analyze the development of the liver. Our studies reveal two phases of liver morphogenesis: budding and growth. The budding period, which can be further subdivided into three stages, starts when hepatocytes first aggregate, shortly after 24 hours post fertilization (hpf), and ends with the formation of a hepatic duct at 50 hpf. The growth phase immediately follows and is responsible for a dramatic alteration of liver size and shape. We also analyze gene expression in the developing liver and find a correlation between the expression of certain transcription factor genes and the morphologically defined stages of liver budding. To further expand our understanding of budding morphogenesis, we use loss-of-function analyses to investigate factors potentially involved in this process. It had been reported that *no tail* mutant embryos appear to lack a liver primordium, as assessed by *gata6* expression (Chin et al., 2000). However, analysis of gutGFP embryos lacking Ntl show that the liver is in fact present. We also find that in these embryos the direction of liver budding does not correlate with the direction of intestinal looping, indicating that the left/right behavior of these tissues can be uncoupled. In addition, we use the *cloche* mutation to analyze the role of endothelial cells in liver morphogenesis, and find that in zebrafish, unlike what has been reported in mouse (Matsumoto et al., 2001), endothelial cells do not appear to be necessary for the budding of this organ.

Key words: Endoderm, hepatocytes, chirality, *cloche*

INTRODUCTION

The digestive system consists of an alimentary canal and its associated organs, the liver, gallbladder and pancreas. Although pancreas development has received a lot of attention in different organisms (Slack, 1995; Biemar et al., 2001; Edlund, 2002), formation of the liver is relatively understudied. Hepatocytes make up the majority of the liver and carry out most of the liver's function, including bile production, blood detoxification, the production of critical plasma proteins and clotting factors, and the storage of many substances such as lipids, amino acids, iron, and glycogen. The liver develops as an outgrowth of the anterior intestine. Tissue explant studies have demonstrated the necessity of adjacent mesoderm for hepatocyte differentiation and maintenance (Le Douarin, 1970; Le Douarin, 1975; Cascio and Zaret, 1991; Gauldi et al., 1996). More recent studies have implicated FGFs (Jung et al., 1999) as well as BMPs (Rossi et al., 2001) in these tissue interactions (reviewed by Zaret, 2002). Although the molecular details of hepatocyte differentiation are beginning to emerge, much remains to be learned. Even less is known about the mechanisms responsible for liver morphogenesis. For example, while *Prox1* is known to be necessary for the migration of hepatocytes into the septum transversum in mouse (Sosa-Pineda et al., 2000), its specific mechanism of action remains to be determined.

The zebrafish has emerged as a valuable organism for genetic studies of vertebrate organ formation and promises to be a significant addition to the model organisms currently used to study liver development. Since the liver is an early hematopoietic organ in mammals, mutations affecting its development in mouse lead to early lethality from anemia (Reimold et al., 2000), thus making prolonged in vivo studies of mouse liver

morphogenesis difficult. Hematopoiesis in zebrafish takes place in the intermediate cell mass (ICM) and subsequently in the kidney, not the liver (reviewed by Thisse and Zon, 2002), thus liver defects do not lead to anemia. In addition, zebrafish embryos lacking circulation receive enough oxygen through diffusion to allow embryonic development to proceed relatively normally for several days (reviewed by Stainier, 2001), eliminating some of the problems encountered with mammalian model organisms. The relative optical clarity of zebrafish embryos is another advantage for studies of internal organs, especially in conjunction with the use of GFP transgenes, which allow analysis of fluorescing tissues throughout development in the living embryo.

Here we introduce a transgenic zebrafish line, the gutGFP line, that expresses GFP throughout the developing digestive system. This unique tool can be used to examine, in living and fixed embryos, endodermal organs otherwise obscured by the yolk ball and dorsal tissues. In the present study, we investigate liver morphogenesis both in wildtype and in a selective and informative set of mutant embryos. Our analyses reveal the timing and nature of the morphogenetic movements, as well as gene expression patterns, associated with liver budding. We also find that directional outgrowth of the liver can be uncoupled from the direction of intestinal looping, and that, surprisingly and contrary to what has been reported in mouse (Matsumoto et al., 2001), endothelial cells do not appear to be required for budding morphogenesis of the liver in zebrafish.

MATERIALS AND METHODS

Embryo culture and zebrafish stocks

Fish and embryos were maintained, collected and staged as described (Westerfield, 1995). We collected embryos homozygous for the *clo*^{s5} mutation (Wayne Liao and D.Y.R.S., unpublished), and used wildtype siblings as controls.

Transgenic animals

To visualize the gut and associated organs, we used a new stable transgenic strain referred to as the gutGFP line. This line was generated by Tobias Roeser in Herwig Baier's group in the lab of Christiane Nüsslein-Volhard, Tübingen, Germany, using a DNA construct that consists of a Xenopus EF-1α promoter regulating GFP expression. Characterization of the inserted transgene and the insertion site is ongoing and will be published elsewhere. The gutGFP line will be available through the Zebrafish Stock Center.

To visualize endothelial cells, we used a stable transgenic line that expresses GFP under the control of the mouse Tie2 enhancer (Motoike et al., 2000).

RNA in situ localization

In situ hybridization was performed with digoxigenin-labeled RNA anti-sense probes for the following genes: foxA2/axial/hnf3β, foxA3/fkd2 (Odenthal and Nüsslein-Volhard, 1998), prox1 (Glasgow and Tomarev, 1998), selenoprotein Pb (sePb) (Kryukov and Gladyshev, 2000; Kudoh et al., 2001), hnf4 (Kudoh et al., 2001), and sox17 (Alexander and Stainier, 1999).

Wholemount in situ hybridization was performed as described (Alexander et al., 1998) with the following modifications. Embryos older than 24 hpf were raised in

0.003% 1-phenyl-2-thiourea (PTU, Sigma) in egg water to inhibit the production of pigment and, after fixation, were treated with 10 μg/ml proteinase K (Roche Diagnostics).

Images were acquired using either a Zeiss StemiSV11 stereomicroscope or a Zeiss Axioplan, equipped with a Zeiss color Axiocam digital camera running Axiovision 3.0 software.

Immunofluorescence and histological stains

Immunofluorescent analysis of protein expression was performed with a rabbit anti-Prox1 antibody (Wigle et al., 1999). Embryos were fixed in 4% paraformaldehyde for 1 hour at room temperature then manually de-yolked, washed with PBS and incubated in a 1:100 dilution of antibody in PBS with 1% TritonX and 2% sheep serum for approximately 40 hours at 4oC. Embryos were mounted in 4% SeaPlaque agarose (BioWhittaker Molecular Applications) in PBS. Bound antibody was detected on transverse vibratome sections (100 μm thick) using Alexa Fluor-594 goat anti-rabbit IgG H + L antibody (1:200, Molecular Probes). To visualize actin, transverse vibratome sections were incubated in rhodamine-labeled phalloidin (1:100, Molecular Probes).

Confocal images were acquired using a Leica TCS NT confocal microscope. Image overlays were assembled using Adobe Photoshop 5.0 LE. Two dimensional projections were generated using Scion Image version 4.0.2.

Morpholino injection

We designed morpholino oligonucleotides to overlap the translational start site of no tail, 5'-GACTTGAGGCAGGCATATTTCCGAT-3', and they were injected essentially as described (Heasman et al., 2000). Briefly, morpholinos were solubilized in 10 mM HEPES, pH 7.6, to create a 1 mM stock. Stock was diluted with a 5 mM HEPES, pH 7.6,

solution that contained 0.05% phenol red for visual detection of successfully injected embryos. A total of 3.2 ng of morpholino was injected per embryo. Non-injected, HEPES injected and embryos injected with morpholinos designed against other genes served as controls.

RESULTS

Introduction of the gutGFP line

To investigate liver development in zebrafish, we used a novel GFP-expressing transgenic line which facilitates observation of the digestive tract and its associated organs in living (data not shown) as well as fixed embryos (Fig. 2.1A). This gutGFP line was generated by random integration of a GFP-containing construct (see materials and methods). Initially ubiquitous, GFP expression becomes restricted to the endoderm by approximately 22 hours post fertilization (hpf). Expression is also observed in the notochord until approximately 30 hpf, and in the eye and hatching gland (data not shown). GFP expression is sometimes variable in heterozygous animals (data not shown) but uniform throughout the endoderm of embryos homozygous for the transgene. Homozygous animals are viable and have no observable phenotype.

At 52 hpf, when the internal organs are easily recognizable, GFP expression is present along the entire alimentary canal: the pharynx, oesophagus, intestinal bulb, and the posterior intestine up to and including the anus (Fig. 2.1B). Additionally, expression is observed in the endodermal component of all accessory organs: the liver, pancreas, gall bladder (visible by 72 hpf, data not shown), the duct systems of these organs, and the swim bladder (Fig. 2.1B).

Liver morphogenesis

To characterize the progression of liver morphogenesis, we analyzed the pattern of GFP expression in homozygous gutGFP embryos at multiple time points between 24 hpf and 46 hpf. We describe liver morphogenesis in two phases: 1. budding, which is further divided into three stages based on distinct liver morphology, and 2. growth. Confocal analysis of 24 hpf embryos revealed the endoderm as a flat sheet in the pharyngeal region that constricts into a solid rod of midline cells, the intestinal rod, just rostral to the first somite (Fig. 2.2A). By 28 hpf, two thickened regions are present on the intestinal rod (Fig. 2.2B). The posterior thickening, situated dorsally on the intestinal rod at the level of the fourth somite, expresses Somatostatin and will contribute to the pancreas (unpublished observations). The anterior thickening is positioned slightly left of the midline and projects from the ventral side of the rod at the level of the first somite. This aggregation of cells marks the first morphogenetic movements of liver organogenesis and is defined as budding stage I. The timing of this first stage of budding varies slightly, but was consistently seen between 24 and 28 hpf.

During stage II, the intestinal bulb primordium undergoes a leftward bend at the level of the developing liver. The aggregate of liver cells increases in size resulting in a smooth, thickened area along the outer curvature of the intestinal bulb primordium by 30 hpf (Fig. 2.2C). We define this process as budding stage II, since the appearance of the nascent liver is distinct from that observed in stage I (Figs. 2.2C, D).

Stage III of budding begins at approximately 34 hpf when a furrow starts to form between the liver bud and the adjacent oesophagus (Fig. 2.2E). This furrow expands posteriorly over time, restricting the connection between the liver and the intestinal bulb

primordium (Figs. 2.2E, F). By 50 hpf, cells connecting these two organs have formed the hepatic duct. Transverse sections through the hepatic duct at this time show between five and 10 cells, with pronounced apical actin staining, arranged around a small central lumen to form a simple tubular duct (data not shown). Hepatic duct formation marks the end of stage III and the end of the budding process.

Upon completion of budding, the liver is a well defined structure that increases in size and modifies its shape and placement. We refer to this subsequent size increase as the growth phase of liver development. By 72 hpf, the size of the liver has increased moderately but the shape has not altered. By 96 hpf, liver growth has resulted in a medial expansion so that it extends from the left side of the embryo all the way across the midline ventral to the oesophagus (data not shown).

During budding, hepatocytes emerge from the intestinal rod and protrude to the left as a disorganized but cohesive mass of cells (Fig. 2.2G - I). The hepatocytes maintain very close apposition with one another as the liver expands to the left. Throughout the budding phase, mesodermal cells are observed adjacent to the intestine and dorsal to the liver (Fig. 2.2G - I). As the furrow between the liver and oesophagus expands, mesodermal cells can be seen in the resulting gap (Fig. 2.2I). The liver is directly adjacent to the yolk ball, and we observed no mesodermal cells in contact with the ventral face of the liver at any stage of liver budding (Fig. 2.2G - I). The necessity of adjacent mesoderm on liver development has been shown in other vertebrates (Le Douarin, 1970; Le Douarin, 1975; Cascio and Zaret, 1991; Gauldi et al., 1996), but in zebrafish the influence of surrounding tissues has never been studied. The proximity of the developing

liver to the yolk and mesoderm make these tissues likely candidates to be involved in the budding process.

In addition to investigating the location of the liver with respect to adjacent tissues, it is important to note the position of the liver with respect to the entire embryo. During budding, the anterior edge of the liver aligns with the duct of Cuvier, and extends caudally to the mid-level of the fin bud (Fig. 2.3A). By the completion of the budding process at 50 hpf, the liver protrudes slightly beyond the lateral edge of the left somites. A left lateral view shows its anterior edge situated immediately posterior to the duct of Cuvier, and its posterior edge extending half-way through the level of the fin bud (Fig. 2.3B). By 4 days post fertilization (dpf) (96 hpf), the liver is in the growth phase. A left lateral view of the embryo shows the liver overlying the anterior portion of the remaining yolk ball, and the anterior edge of the liver in contact with the pericardial cavity (Fig. 2.3C).

Gene expression in the digestive system

To identify genes that may be involved in the morphological transitions described above, we performed in situ hybridization of endodermally expressed genes at multiple time points between 24 and 48 hpf. Although the general expression pattern of these genes has been previously reported (see materials and methods), we present them here specifically in the context of the developing digestive system. Interestingly we found that some genes appear to initiate or halt their expression at specific morphological transitions during liver development. For example, *prox1* (Glasgow and Tomarev, 1998) expression first appears in the liver around 24 hpf, concurrent with the onset of the first stage of

budding, while initiation of *hnf4* (Kudoh et al., 2001) expression appears to coincide with the onset of stage II.

Initial *prox1* expression appears at the level of the first somite in a subset of medial endodermal cells that will bud to form the liver (data not shown). *prox1* expression persists throughout liver development (Fig. 2.4A, K). From its onset of expression, *hnf4* is found in the liver bud and the intestinal primordium posterior to the oesophagus, and this pattern of expression is observed throughout the budding process (Fig. 2.4B, K). Endodermal *foxA2* expression first appears by the 10-somite stage (Odenthal and Nüsslein-Volhard, 1998). By 24 hpf, *foxA2* expression stretches from the rostral end of the digestive system to the boundary between the intestinal bulb and posterior intestine (Odenthal and Nüsslein-Volhard, 1998). Shortly after the onset of budding stage II, *foxA2* expression in the liver decreases, and it is nearly absent from this organ at 32 hpf (Fig. 2.4K). At 48 hpf, *foxA2* expression is elevated in the hepatic and pancreatic ducts, pancreas, swim bladder, oesophagus and pharynx, and very low in other parts of the digestive tract (Fig. 2.4C).

To extend the set of molecular markers valuable to the study of the zebrafish digestive system, we also examined the expression pattern of *selenoprotein Pb* (*sePb*) (Kryukov and Gladyshev, 2000; Kudoh et al., 2001) and *sox17* (Alexander and Stainier, 1999) which are restricted to specific tissues. Expression of *sePb*, which encodes a serum protein produced by the liver, is first detected during stage II of liver budding, and is restricted to the liver throughout the budding process (Fig. 2.4D). At 48 hpf, expression of *sox17* is detected at a low level throughout the digestive system with heightened expression in a subset of liver cells adjacent to the hepatic duct (Fig. 2.4E). In Xenopus,

sox17α expression is down-regulated in all but the gallbladder (Zorn and Mason, 2001) suggesting that the cells with heightened *sox17* expression in zebrafish may also represent the gallbladder precursors.

foxA3 (Odenthal and Nüsslein-Volhard, 1998) expression is detected in the digestive tract throughout the duration of liver budding (Fig. 2.4F-J). The expression pattern of *foxA3* nearly mimics that of GFP in the gutGFP line, with the exclusion of pharyngeal expression, and provides a valuable alternative for visualizing the morphology of the digestive system in fixed embryos. Using this marker, liver development, as well as the development of other endodermally-derived organs, can be clearly examined in the context of the digestive system.

Uncoupling the left/right positioning of the liver and intestinal bulb

Chin et al. (2000) reported that in *no tail* (*ntl*) mutant embryos, liver primordia could not be detected at 30 hpf by looking at *gata6* expression, prompting us to further investigate the role of *ntl* in liver formation. In order to visualize the liver in the context of the entire digestive system, we injected *ntl* morpholino into the gutGFP line. We found that 95% of the morpholino-injected embryos perfectly phenocopied *ntl* mutants as assessed morphologically (data not shown), consistent with what has been previously reported (Feldman and Stemple, 2001). Surprisingly, we observed a distinct liver in all embryos showing *ntl* phenocopy, indicating that the liver does form, but may not differentiate properly, in embryos lacking Ntl.

In addition, we noticed that the position of the liver in Ntl deficient embryos did not always correlate with the chirality of the intestinal bulb. Although uncoupled

laterality has been observed between structures in different organ systems such as the heart and gut (Schilling et al., 1999; Bisgrove et al., 2000), altered situs of organs within a single organ system has not been reported in zebrafish. We further investigated this phenomenon of uncoupled digestive organ position by recording the position of the liver in embryos where the intestinal bulb had looped to either the left or right. We observed that at 52 hpf, the intestinal bulb of 72.6% of the embryos showing a *ntl* phenotype (n=124) had looped to either the left or right. [The intestinal bulbs of the other 27.4% had remained midline.] Of the 90 embryos that showed intestinal bulb looping, 65 (72%) exhibited a liver that stretched to both the left and right of the midline with a single hepatic duct connecting it to the alimentary canal (Fig. 2.5B, D), while the rest showed a liver that overlapped the midline but usually budded off the outer curvature of the intestinal bulb (data not shown). We observed the same phenotypes in *ntl* mutant embryos stained for *foxA3* expression (data not shown). These data show that in the absence of Ntl, the directional outgrowth of the liver can be uncoupled from the direction of intestinal bulb looping.

Role of endothelial cells in liver budding morphogenesis

The adult liver is a highly vascularized organ, and this vascularization is critical for liver function. Recent work in mouse has indicated that endothelial cells are additionally required for liver morphogenesis, even before a vascular network is formed (Matsumoto et al., 2001). These studies showed that in *Vegfr2/Flk-1* mutant mice, which lack endothelial cells, liver budding fails to occur altogether. Here we investigate whether liver budding in zebrafish is also dependent on endothelial cells.

To examine the timing and nature of liver vascularization in zebrafish, we performed a time course of vascular development in the liver using the Tie2-GFP transgenic line to visualize endothelial cells (Motoike et al., 2000), and an anti-Prox1 antibody to label the hepatocytes (Wigle et al., 1999). GFP expressing endothelial cells are positioned adjacent to, but not completely encasing, the liver bud at 36 hpf (data not shown) and 48 hpf (Fig. 2.6A). By 60 hpf, endothelial cells remain present around the liver as seen earlier, but are also found between surface hepatocytes of the liver (Fig. 2.6B). By 72 hpf, endothelial cells permeate the entire liver (Fig. 2.6C).

To analyze the potential role of endothelial cells in liver morphogenesis, we examined liver formation in embryos homozygous for the *cloche* (*clo*) mutation, which appear to lack all endothelial cells from an early stage (Stainier et al., 1995; Liao et al., 1997; Thompson et al., 1998). Liver budding and differentiation is indistinguishable in *clo* mutant embryos and their wildtype siblings, as assessed by *foxA3* (n=56) (Fig. 2.6D, E), and *sePb* expression (n=48) at 48 hpf (Fig. 2.6F, G). [*clo* mutant embryos were distinguished from their wildtype siblings by their distinct heart phenotype.] These observations suggest that in zebrafish endothelial cells are not required for liver budding morphogenesis or hepatocyte differentiation.

DISCUSSION

Anatomy of the zebrafish digestive system

We have analyzed the morphogenesis of the developing zebrafish liver using a unique GFP transgenic line to facilitate observations of the endoderm. While collecting data presented in this paper, we were faced with the difficulty of choosing the correct

terminology. To date, there has been no convention in the nomenclature used for zebrafish digestive anatomy, resulting in multiple terms being used to identify a single structure. With the ability to observe the entire digestive tract in the gutGFP line, we took the opportunity to define a nomenclature for the digestive anatomy of the zebrafish.

Our observations suggest that the zebrafish gut is divided into the pharynx, oesophagus, intestinal bulb, and posterior intestine, as depicted in Figure 2.1. This nomenclature partitions the gut based on distinct topographical characteristics. The pharynx is the region of the alimentary canal posterior to the oral opening. The oesophagus is identified as the constricted region posterior to the pharynx. The dorsal wall of the oesophagus opens into the pneumatic duct which connects to the endodermal lining of the swim bladder. Although not part of the digestive system, the lining of the swim bladder is included here to show a complete diagram of the endodermally-derived organs that express GFP in the gutGFP line. The connection of the hepatic duct to the alimentary canal demarcates the caudal boundary of the oesophagus.

The region of the digestive tract posterior to the hepatic duct has had multiple designations. It has been referred to as the stomach, the duodenum, the anterior intestine and the foregut. The term foregut usually refers to the region of the digestive system rostral to the hepatic duct. Histological studies have been performed on both the adult and developing zebrafish digestive tract (Pack et al., 1996), and identity of this region is not exclusively analogous to the stomach or small intestine. Members of the *Cyprinidae* family, which includes zebrafish, lack stomachs, and the widened anterior portion of the intestine is referred to as the pseudogaster (Harder, 1975). However, we employed the term "intestinal bulb" to label this structure since it had previously been used for this

region in adult zebrafish (Westerfield, 1995), and more precisely describes the anatomical structure.

The intestinal bulb, distinguishable primarily by its bulbous appearance, begins to develop a lumen around 42hpf (Horne-Badovinac et al., 2001). Increases in the diameter of this lumen, amongst other events, lead to a clearly inflated structure by 3 dpf. The intestinal bulb extends caudally to the level where the gut re-aligns with the midline of the embryo. Posterior to the intestinal bulb lies the posterior intestine which continues down the midline of the embryo and ends at the anal opening.

The terms foregut, midgut and hindgut are commonly used when referring to regions along the digestive tract. However, using this terminology in zebrafish is deceptive; many of the structures used to define these regions in other organisms (Langman and Sadler, 1985) are not present in zebrafish and thus there is no consensus for where the boundaries should be. These subdivisions have been used to label the digestive tract in other fishes, although the definition of borders between regions in those organisms is again ambiguous (Harder, 1975). Given this confusion in precise anatomical terminology, we suggest that this vocabulary be used very carefully in zebrafish, and only in conjunction with terms that refer to the specific structures of the digestive system.

Early in development, before a hepatic duct is formed, the boundaries of the oesophagus, intestinal bulb, and posterior intestine are not as clear. When the endoderm is a solid rod of midline cells, before the liver primordium has formed, all endoderm posterior to the constricted caudal end of the pharynx can be referred to as the intestinal rod. Once the liver primordium is present, the intestinal rod can be subdivided into three

regions. The oesophagus stretches from the caudal end of the pharynx to the anterior extent of the liver bud. The intestinal bulb primordium begins at the caudal end of the oesophagus. The exact border between the intestinal bulb primordium and the posterior intestine is not easy to distinguish at this stage based on anatomy alone. Careful histological analyses will be necessary to define this boundary. Further analyses of the developing digestive system in zebrafish will undoubtedly refine the terminology proposed here.

Morphological characteristics separate liver development into two phases

To chart the timing and location of liver morphogenesis, we performed a developmental time course using the gutGFP transgenic line which allowed us to visualize the liver in the context of the entire digestive system.

We divided liver morphogenesis into two phases: budding and growth. Budding is the phase of liver development when the organ emerges from the intestinal rod to become a separate and distinct structure on the embryo's left. Based on different shapes of the liver throughout budding, we further divided this process into three stages. Stage I begins around 24 hpf, when we first noticed an aggregation of pre-hepatic cells on the ventral surface of the intestinal rod. Stage II begins once the pre-hepatic region is a smooth thickening projecting to the left of, but still contiguous with, the intestinal bulb primordium. Stage III begins when a furrow starts forming between the anterior edge of the liver and the adjacent oesophagus, and ends when the stalk of cells connecting the liver and intestinal bulb primordium forms an ordered hepatic duct with columnar epithelial cells. The behavior of hepatocytes during the budding process was somewhat

surprising when compared to that described in mammals, but consistent with that seen in other fishes. In mammals, the hepatocytes appear to dissociate from one another and migrate into the mesenchyme of the adjacent septum transversum. This process is referred to by Elias (1955) as "interstitial invasion". In sea bream, as we observed in zebrafish, interstitial invasion does not appear to occur (Guyot et al., 1995). The cells of the nascent liver are closely juxtaposed forming a single mass on the left side of the digestive tract.

The growth phase follows the completion of budding and is characterized by a dramatic change in liver size and shape. As a result of this growth phase, the liver comes to occupy a substantial portion of the abdominal cavity and spreads across the midline. Further analysis of this phase will be extremely informative since it is during this time that the liver becomes vascularized and presumably begins its physiological functions.

In addition to this detailed analysis of liver morphogenesis, we also examined the spatiotemporal expression patterns of specific molecular markers. The expression patterns of the transcription factor genes *foxA2*, *prox1* and *hnf4*, appear to correlate with stages of liver budding as defined by the morphological criteria, and may represent part of the molecular network necessary for these stages to proceed. For example, *prox1* expression is initiated at the onset of stage I, consistent with data in the mouse showing a requirement for this gene in the migration of hepatocytes into the surrounding mesenchyme (Sosa-Pineda et al., 2000). *hnf4*, whose expression is initiated at the onset of stage II, has also been implicated in liver development in mouse (Li et al., 2000). Of course, there may be other molecular transitions that do not correspond to overt morphogenetic differences. These presently unobservable transitions may be identifiable

through mutational analysis, and we are currently undertaking a forward genetic screen, using the gutGFP line, to identify genes regulating liver morphogenesis. Therefore, by keeping the definition of developmental phases broad at this time, we leave open the possibility of further subdividing the process of liver morphogenesis as mutant analysis uncovers additional critical transitions during liver budding and growth.

Left/right asymmetry of the liver can be uncoupled from the direction of intestinal bulb looping

The relationship between intestinal bulb chirality and the direction of liver budding has not been previously analyzed. We observed that in wildtype liver morphogenesis the direction of liver budding and that of intestinal bulb looping are correlated, resulting in both organs being positioned on the embryo's left. In naturally occurring cases of reversed chirality of the intestinal bulb (observed in approximately 0.1 % to 1% of wildtype embryos depending on the genetic background), the liver always buds off the outer curvature of the intestinal bulb primordium (unpublished observations). These observations have led to the hypothesis that the direction of liver outgrowth is dictated by the direction of looping of the intestinal bulb primordium.

Surprisingly, we found that in the absence of Ntl, the directions of intestinal bulb looping and liver budding are frequently uncoupled; the intestinal bulb usually loops but the liver fails to bud exclusively to the left or right. The opposite phenotype has been observed in *hands-off* mutant embryos in which the intestinal bulb does not loop, yet the liver usually buds to the left or right (Sally Horne-Badovinac, E. A. O. and D. Y. R. S., unpublished). These data indicate that the behavior of the liver primordium is not dictated by the orientation of the intestinal bulb primordium, and that the morphogenetic

movements of these two organs are separable. Furthermore, these results suggest a role for the midline in the proper placement of the liver, and it will be most interesting to further investigate the mechanisms that regulate the directionality of liver budding.

Endothelial cells do not appear to be essential for liver budding morphogenesis in zebrafish

It has been reported recently that endothelial cells are required for liver budding in mouse (Matsumoto et al., 2001). Before investigating the role of endothelial cells in zebrafish liver morphogenesis, we first wanted to determine the timing and nature of endothelial/hepatic associations. We found that endothelial cells are closely associated with the liver periphery by 36 hpf and that they maintain this close apposition until approximately 60 hpf, when they begin to invade the outer layers of hepatocytes. These endothelial cells are likely part of nascent branches from the sub-intestinal vessels, and will eventually form the hepatic vasculature (Isogai et al., 2001). By 72 hpf, endothelial cells are found throughout the entire liver, leading us to conclude that vascularization of the zebrafish liver is achieved by endothelial invasion after budding is complete. This process of vascularization appears to be different from that classically reported in mouse, where hepatocytes undergo interstitial invasion of the adjacent mesenchyme and arrange themselves around the vascular network already present (Elias, 1955).

In *Vegfr2/Flk-1* -/- mouse embryos, which lack mature endothelial cells, the liver never progresses beyond an early thickening of hepatic endoderm on the gut tube (Matsumoto et al., 2001). The zebrafish *clo* mutation, which appears to disrupt endothelial cell differentiation at a stage upstream of *Vegfr2/Flk-1* expression (Liao et al., 1997; Thompson et al., 1998), provides a tool in zebrafish for studying the behavior of

hepatocytes in the apparent absence of endothelial cells. If the primary conserved role of endothelial cells in liver development is to initiate morphogenesis, one would expect the liver of *clo* mutant embryos to arrest during stage I of budding. We performed a qualitative analysis of the size and shape of the liver in *clo* mutant embryos. Surprisingly, liver budding and differentiation in *clo* mutant embryos appear to proceed normally. The discrepancy of these findings with those described in *Vegfr2/Flk-1* -/- mouse embryos may be explained in several ways including by a difference in cell behavior during liver outgrowth between these species. One possibility is that signals from the endothelial cells may be necessary for the breakdown of cell adhesion between hepatocytes. In mouse, this function would be concomitant with initiation of hepatocyte migration. However, since cell dissociation does not occur in zebrafish liver morphogenesis, the presence of endothelium would be dispensable for budding. This model would suggest that the growth phase, during which endothelial cells invade the liver, may be affected in *clo* mutant embryos. However, due to an increased severity of the cardiac edema, we were not able to analyze these later time points. An alternative explanation for the discrepancy between mouse and zebrafish is that signals provided by the endothelial cells in mouse may be produced by a different cell type in zebrafish. Other explanations are of course possible.

The zebrafish has the potential to contribute significantly to studies of the vertebrate digestive system. With its proven usefulness for large scale forward genetics screens and embryological studies, and with the addition of the gutGFP line, we hope that this model

organism will become invaluable to investigate the molecular and cellular mechanisms of endodermal organ development.

ACKNOWLEDGEMENTS

We would like to thank Steve Waldron for expertly maintaining the zebrafish stocks; Herwig Baier for the invaluable gift of the gutGFP zebrafish line; Juan Engel and the UCSF Liver Center for training and assistance on the confocal microscope; Guillermo Oliver for the generous gift of anti-Prox1 antibody; Tetsuhiro Kudoh and Michael Tsang for sharing plasmids encoding Selenoprotein Pb and Hnf4 before publication; Peter Chien, Sally Horne-Badovinac, Matthias Hebrok, Karen Borst-Rothe, and the Stainier lab for discussion and critical comments on the manuscript. E. A. O. was supported by an AHA fellowship. This work was supported in part by grants from the NIH (NIDDK) and the Packard Foundation to D.Y.R.S. .

REFERENCES

Alexander, J. and Stainier, D. Y. (1999). A molecular pathway leading to endoderm formation in zebrafish. *Curr Biol* **9**, 1147-57.

Alexander, J., Stainier, D. Y. and Yelon, D. (1998). Screening mosaic F1 females for mutations affecting zebrafish heart induction and patterning. *Dev Genet* **22**, 288-99.

Biemar, F., Argenton, F., Schmidtke, R., Epperlein, S., Peers, B. and Driever, W. (2001). Pancreas development in zebrafish: early dispersed appearance of endocrine

hormone expressing cells and their convergence to form the definitive islet. *Dev Biol* **230**, 189-203.

Bisgrove, B. W., Essner, J. J. and Yost, H. J. (2000). Multiple pathways in the midline regulate concordant brain, heart and gut left-right asymmetry. *Development* **127**, 3567-79.

Cascio, S. and Zaret, K. S. (1991). Hepatocyte differentiation initiates during endodermal-mesenchymal interactions prior to liver formation. *Development* **113**, 217-25.

Chin, A. J., Tsang, M. and Weinberg, E. S. (2000). Heart and gut chiralities are controlled independently from initial heart position in the developing zebrafish. *Dev Biol* **227**, 403-21.

Edlund, H. (2002). Pancreatic organogenesis – developmental mechanisms and implications for therapy. *Nat Rev Genet* **3**, 524-32.

Elias, H. (1955). Origin and early development of the liver in various vertebrates. *Acta Hepatologica*, 1-57.

Feldman, B. and Stemple, D. L. (2001). Morpholino phenocopies of *sqt*, *oep*, and *ntl* mutations. *Genesis* **30**, 175-7.

Gualdi, R., Bossard, P., Zheng, M., Hamada, Y., Coleman, J. R. and Zaret, K. S. (1996). Hepatic specification of the gut endoderm in vitro: cell signaling and transcriptional control. *Genes Dev* **10**, 1670-82.

Glasgow, E. and Tomarev, S. I. (1998). Restricted expression of the homeobox gene *prox 1* in developing zebrafish. *Mech Dev* **76**, 175-8.

Guyot, E., Diaz, J. P. and Connes, R. (1995). Organogenesis of the liver in sea bream. *The Fisheries Society of the British Isles* **47**, 427-37.

Harder, W. (1975). Anatomy of fishes. Stuttgart: Schweizerbart.

Heasman, J., Kofron, M., Wylie C. (2000). Beta-catenin signaling activity dissected in the early *Xenopus* embryo: a novel antisense approach. *Dev Biol* **222**, 124-34.

Horne-Badovinac, S., Lin, D., Waldron, S., Schwarz, M., Mbamalu, G., Pawson, T., Jan, Y., Stainier, D. Y. and Abdelilah-Seyfried, S. (2001). Positional cloning of *heart and soul* reveals multiple roles for PKCλ in zebrafish organogenesis. *Curr Biol* **11**, 1492-502.

Isogai, S., Horiguchi, M. and Weinstein, B. M. (2001). The vascular anatomy of the developing zebrafish: an atlas of embryonic and early larval development. *Dev Biol* **230**, 278-301.

Jung, J., Zheng, M., Goldfarb, M. and Zaret, K. S. (1999). Initiation of mammalian liver development from endoderm by fibroblast growth factors. *Science* **284**, 1998-2003.

Krauss, S., Johansen, T., Korzh, V., Moens, U., Ericson, J. and Fjose, A. (1991). Zebrafish pax[zf-a]: a paired box-containing gene expressed in the neural tube. *EMBO J.* **10**, 3609-3619.

Kryukov, G. V. and Gladyshev, V. N. (2000). Selenium metabolism in zebrafish: multiplicity of selenoprotein genes and expression of a protein containing 17 selenocysteine residues. *Genes Cells* **5** (12), 1049-1060.

Kudoh, T., Tsang, M., Hukriede, N. A., Chen, X., Dedekian, M., Clarke, C. J., Kiang, A., Schultz, S., Epstein, J. A., Toyama, R. et al. (2001). A gene expression screen in zebrafish embryogenesis. *Genome Res* **11**, 1979-87.

Langman, J. and Sadler, T. W. (1985). Langman's Medical embryology. Baltimore: Williams & Wilkins.

Le Douarin, N. M. (1970). Induction of determination and induction of differentiation during development of the liver and certain organs of endomesodermal origin. In "Tissue interactions during organogenesis" (E. Wolff, Ed.), pp. 37-70. Gordon and Breach, New York.

Le Douarin, N. M. (1975). An experimental analysis of liver development. *Med Biol* **53**, 427-55.

Li, J., Ning, G., and Duncan, S.A. (2000). Mammalian hepatocyte differentiation requires the transcription factor HNF-4α. *Genes Dev* **15**, 464-74.

Liao, W., Bisgrove, B. W., Sawyer, H., Hug, B., Bell, B., Peters, K., Grunwald, D. J. and Stainier, D. Y. (1997). The zebrafish gene *cloche* acts upstream of a *Flk-1* homologue to regulate endothelial cell differentiation. *Development* **124**, 381-9.

Matsumoto, K., Yoshitomi, H., Rossant, J. and Zaret, K. S. (2001). Liver organogenesis promoted by endothelial cells prior to vascular function. *Science* **294**, 559-63.

Motoike, T., Loughna, S., Perens, E., Roman, B. L., Liao, W., Chau, T. C., Richardson, C. D., Kawate, T., Kuno, J., Weinstein, B. M. et al. (2000). Universal GFP reporter for the study of vascular development. *Genesis* **28**, 75-81.

Odenthal, J. and Nüsslein-Volhard, C. (1998). fork head domain genes in zebrafish. *Dev Genes Evol* **208**, 245-58.

Pack, M., Solnica-Krezel, L., Malicki, J., Neuhauss, S. C. F, Schier, A. F., Stemple, D. L., Driever, W., and Fishman, M. C. (1996). Mutations affecting development of zebrafish digestive organs. *Development* **123**, 321-328.

Reimold, A. M., Etkin, A., Clauss, I., Perkins, A., Friend, D. S., Zhang, J., Horton, H. F., Scott, A., Orkin, S. H., Byrne, M. C. et al. (2000). An essential role in liver development for transcription factor XBP-1. *Genes Dev* **14**, 152-7.

Rossi, J. M., Dunn, N. R., Hogan, B. L. and Zaret, K. S. (2001). Distinct mesodermal signals, including BMPs from the septum transversum mesenchyme, are required in combination for hepatogenesis from the endoderm. *Genes Dev* **15**, 1998-2009.

Schilling, T. F., Concordet, J. and Ingham, P. W. (1999). Regulation of left-right asymmetries in the zebrafish by *Shh* and *BMP4*. *Dev Biol* **210**, 277-87.

Slack, J. M. (1995). Developmental biology of the pancreas. *Development* **121**, 1569-80.

Sosa-Pineda, B., Wigle, J. T. and Oliver, G. (2000). Hepatocyte migration during liver development requires Prox1. *Nat Genet* **25**, 254-5.

Stainier, D. Y., Weinstein, B. M., Detrich, H. W., 3rd, Zon, L. I. and Fishman, M. C. (1995). *cloche*, an early acting zebrafish gene, is required by both the endothelial and hematopoietic lineages. *Development* **121**, 3141-50.

Stainier, D. Y. (2001). Zebrafish genetics and vertebrate heart formation. *Nat Rev Genet* **2**, 39-48.

Thisse, C. and Zon, L. I. (2002). Organogenesis--Heart and Blood Formation from the Zebrafish Point of View. *Science* **295**, 457-462.

Thompson, M. A., Ransom, D. G., Pratt, S. J., MacLennan, H., Kieran, M. W., Detrich, H. W., 3rd, Vail, B., Huber, T. L., Paw, B., Brownlie, A. J. et al. (1998). The *cloche* and *spadetail* genes differentially affect hematopoiesis and vasculogenesis. *Dev Biol* **197**, 248-69.

Westerfield, M. (1995). The zebrafish book : a guide for the laboratory use of zebrafish (Danio rerio). Eugene, OR: M. Westerfield.

Wigle, J. T., Chowdhury, K., Gruss, P. and Oliver, G. (1999). *Prox1* function is crucial for mouse lens-fibre elongation. *Nat Genet* **21**, 318-22.

Zaret, K. S. (2002). Regulatory phases of early liver development: paradigms of organogenesis. *Nat Rev Genet* **3**, 499-512.

Zorn, A. M. and Mason, J. (2001). Gene expression in the embryonic *Xenopus* liver. *Mech Dev* **103**, 153-157.

FIGURE LEGENDS

Fig. 2.1. The 52 hpf zebrafish digestive system as visualized in the stable transgenic gutGFP line. (A) Two-dimensional projection of a confocal stack, ventral view with anterior to the top. GFP expression occurs in all organs of the digestive system as well as the endodermal lining of the swim bladder. Scale bar, 100 μm. (B) Schematic drawings (ventral and dorsal views, anterior to the top) showing the identity and location of GFP expressing organs at 52 hpf. L, liver; hd, hepatic duct; pd, pancreatic duct; P, pancreas; ib, intestinal bulb; pi, posterior intestine; pp, posterior region of the pharynx; oe, oesophagus; sb, swim bladder.

Fig. 2.2. Time course of liver budding. (A - F) Two-dimensional projections of confocal stacks showing ventral views of the gutGFP line, anterior to the top. Scale bar, 100 μm. Embryos were fixed and imaged at (A) 24 hpf, (B) 28 hpf, (C) 30 hpf, (D) 34 hpf, (E) 36 hpf, and (F) 46 hpf. (A, B) The liver (arrowhead) starts budding from the intestinal rod between 24 and 28 hpf. (C) At 30 hpf, the liver is a smooth thickening on the outer curvature of the intestinal bulb primordium which at this time has a clear leftward bend. (D) A furrow (open arrow) begins to form between the medial anterior edge of the liver and the adjacent oesophagus, and continues to expand posteriorly (E, F) to separate the liver from the intestinal bulb primordium. The pancreas (asterisk), and endodermal lining of the swim bladder (arrow), can also be seen developing from the intestinal bulb primordium over time. (G - I) Transverse sections through the gutGFP line stained with rhodamine-labeled phalloidin to visualize surrounding tissues. The liver is marked by an arrowhead; the intestinal bulb primordium is outlined in white. Dorsal is to the top, and

left is to the right to keep with the orientation of the ventral views. The level of the sections in (G), (H), and (I) is indicated by the yellow dashed lines in (B), (C) and (E) respectively. (G) At 28 hpf, the first aggregation of hepatocytes from the intestinal bulb primordium is slightly to the left of the midline and adjacent to the yolk (y). The tissue that resides between the endoderm and the overlying notochord and somites is the lateral plate mesoderm. (H) At 30 hpf, the budding liver, which is positioned left of the midline, has an extensive connection to the intestinal bulb primordium. Lateral plate mesoderm is present both dorsal and ventral to the intestinal bulb primordium, but not ventral to the liver. (I) By 36 hpf, the connection between the liver and intestinal bulb primordium has started to restrict, and lateral plate mesoderm is present in the resulting space. The liver sits directly on the yolk (y). n, notochord; s, somites, nt, neural tube.

Fig. 2.3. Sketches showing the location of the liver in the context of the embryo at 30 hpf (A), 50 hpf (B), and 4 dpf (C). (A, B) At 30 and 50 hpf, the liver (arrowhead) extends from the duct of Cuvier, anteriorly, to the mid-level of the fin bud, posteriorly. (C) At 4 dpf, the liver can be seen touching the pericardial cavity and resting on top of the remaining yolk. The intestinal bulb has inflated and is pressed against the left side of the embryo. ov, otic vesicle; dc, duct of Cuvier; L, liver; fb, fin bud; y, yolk; ib, intestinal bulb; n, notochord; pc, pericardial cavity.

Fig. 2.4. Gene expression patterns in the developing digestive system. Dorsal views, anterior to the top. The liver is marked with an arrow (A – J) and outlined in yellow (C, E). The pancreas is marked with an asterisk. (A-E) Embryos are 48 hpf. (A) The level of

prox1 expression is high in the liver, slightly lower in the pancreas (asterisk), and even lower throughout the ducts connecting the two organs to the alimentary canal. (B) *hnf4* expression is restricted to the liver and alimentary canal posterior to the hepatic duct. (C) *foxA2* expression is present in the digestive system from the pharynx to the anterior boundary of the posterior intestine. Expression is highest in the pharynx, oesophagus, the endodermal lining of the swim bladder, the pancreas (asterisk) and its duct, and the ductwork of the liver. (D) *sePb* is expressed exclusively in the liver. (E) *sox17* expression is found at a low level throughout the digestive system and at a higher level in a patch of cells (arrowhead) most likely representing the gall bladder precursors. (F-J) *foxA3* expression at 24 hpf (F), 30 hpf (G), 34 hpf (H), 40 hpf (I), and 48 hpf (J); it reveals structures corresponding to those observed by fluorescence in the gutGFP line, namely the digestive system and the endodermal lining of the swim bladder. (K) Timeline showing the onset and duration of transcription factor gene expression in the liver during budding. Approximate periods of the stages of liver budding are represented under the timeline.

Fig. 2.5. The direction of liver budding can be uncoupled from the direction of intestinal bulb looping. (A, B) Ventral views of confocal stacks, anterior to the top, showing wildtype (A) and *ntl* morpholino injected embryos (B) at 52 hpf. (A) The liver (arrowhead) in wildtype embryos is located to the left of the midline, and the intestinal bulb (ib) curves to the left. (B) In *ntl* morpholino injected embryos where the intestinal bulb (ib) curves to the left, a single liver (arrowhead) can be located symmetrically across the midline. (C, D) Transverse sections through the gutGFP line stained with rhodamine-

labeled phalloidin to visualize surrounding tissues. The liver is marked by an arrowhead; the oesophagus is outlined in white. Dorsal is to the top, and left is to the right. The level of the sections in wildtype (C) and *ntl* morpholino-injected embryos (D) is indicated by the yellow dashed lines in (A) and (B) respectively. These figures clearly show that in *ntl* morpholino-injected embryos the liver can reside symmetrically with respect to the midline even when the intestinal bulb loops correctly.

Fig. 2.6. Endothelial cells during liver development. (A, B, C) Transverse sections through Tie2-GFP transgenic embryos stained with anti-Prox1 antibody (red) to visualize hepatocytes. Dorsal is to the top, and left is to the right. (A) At 48 hpf, endothelial cells (green, arrow) line the periphery of the liver (red). (B) By 60 hpf, endothelial cells (arrow) have started to invade the liver, but are restricted to the outer edges of the liver. (C) At 72 hpf, endothelial cells (arrows) are interspersed throughout the liver. (D, E) In situ hybridization for *foxA3* expression at 48 hpf. Dorsal views, anterior to the top. The liver (arrow) of the wildtype sibling (D) and a representative *clo* mutant embryo (E), are indistinguishable. The length of the swim bladder (bracket) is variably shorter in *clo* mutant embryos. (F, G) In situ hybridization for *sePb* expression at 48 hpf. Dorsal views, anterior to the top. *sePb* expression in liver (arrow) is indistinguishable between wildtype sibling (F) and a representative *clo* mutant embryo (G).

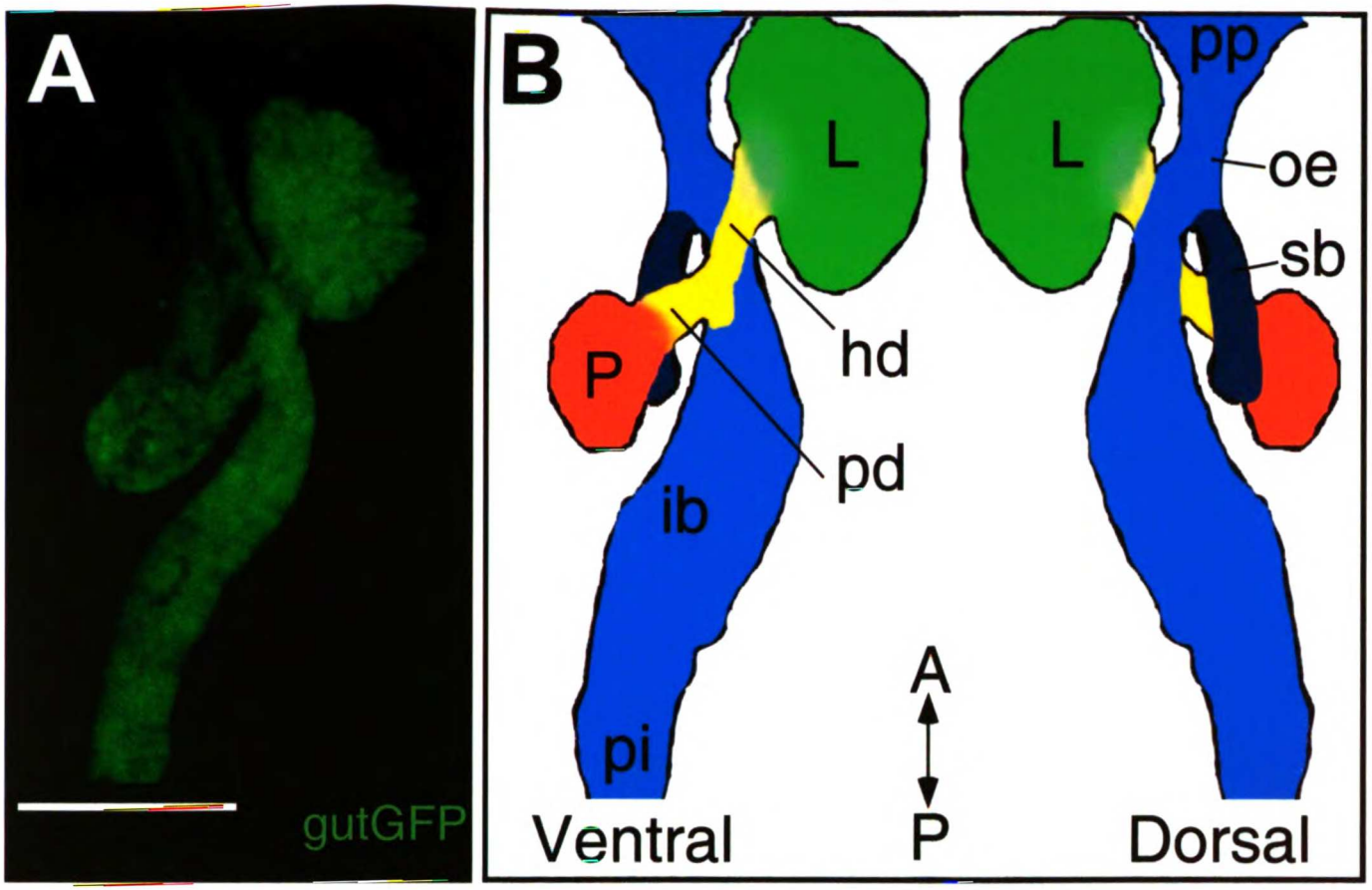

Figure 2.1. The 52 hpf zebrafish digestive system as visualized in the stable transgenic gutGFP line.

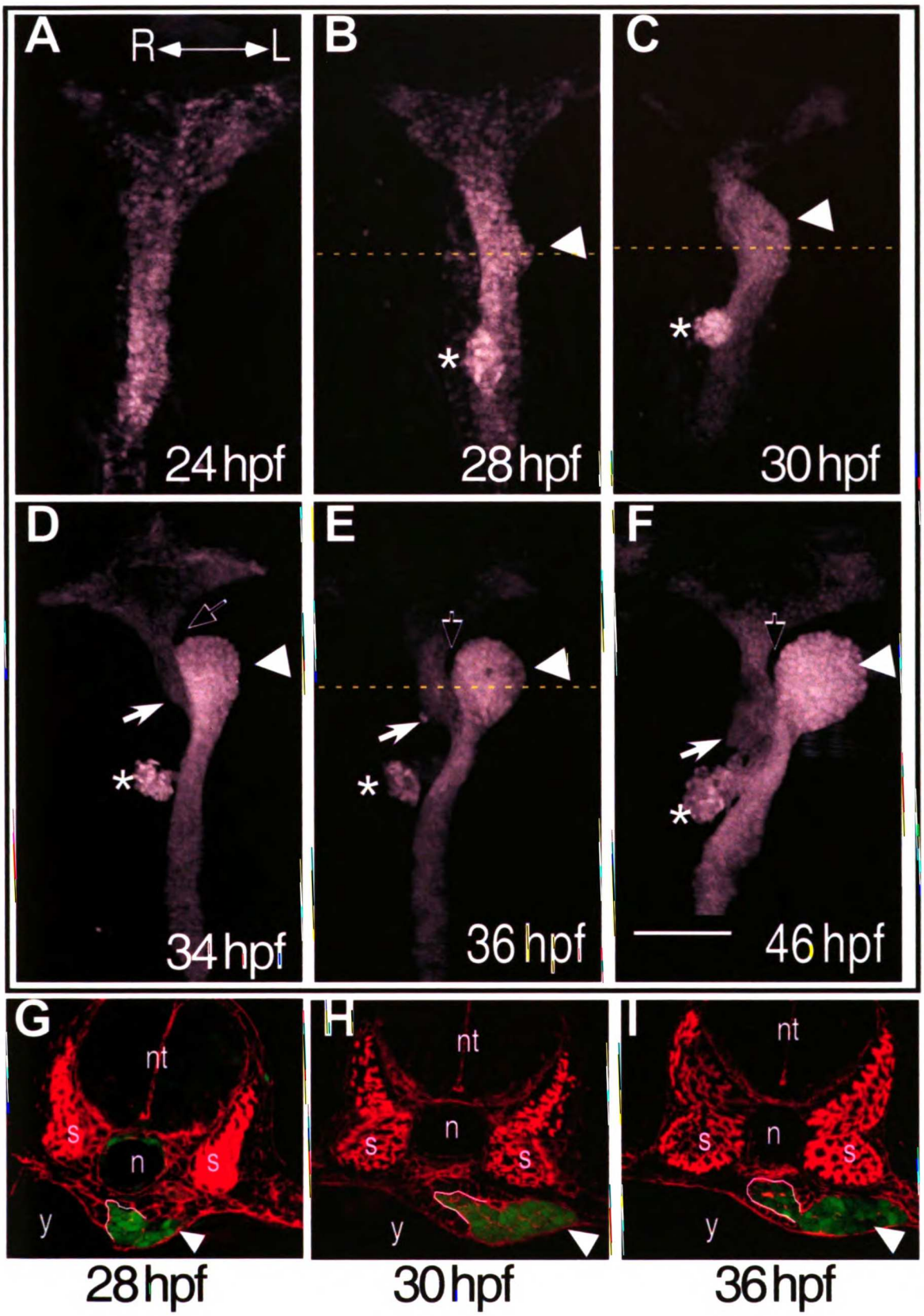

Figure 2.2. Time course of liver budding.

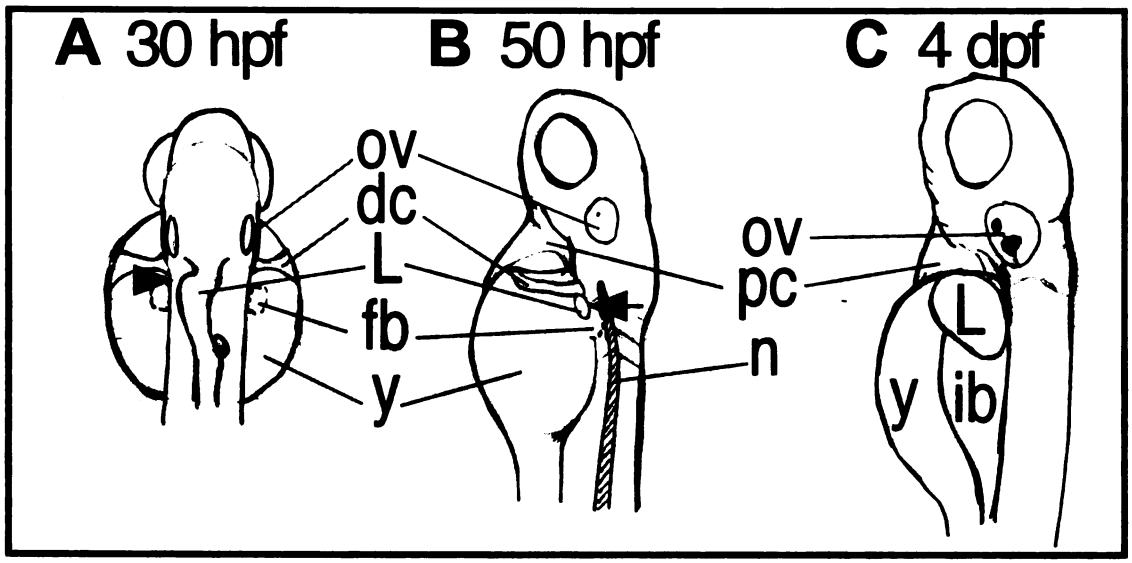

Figure 2.3. Sketches showing the location of the liver in the context of the embryo.

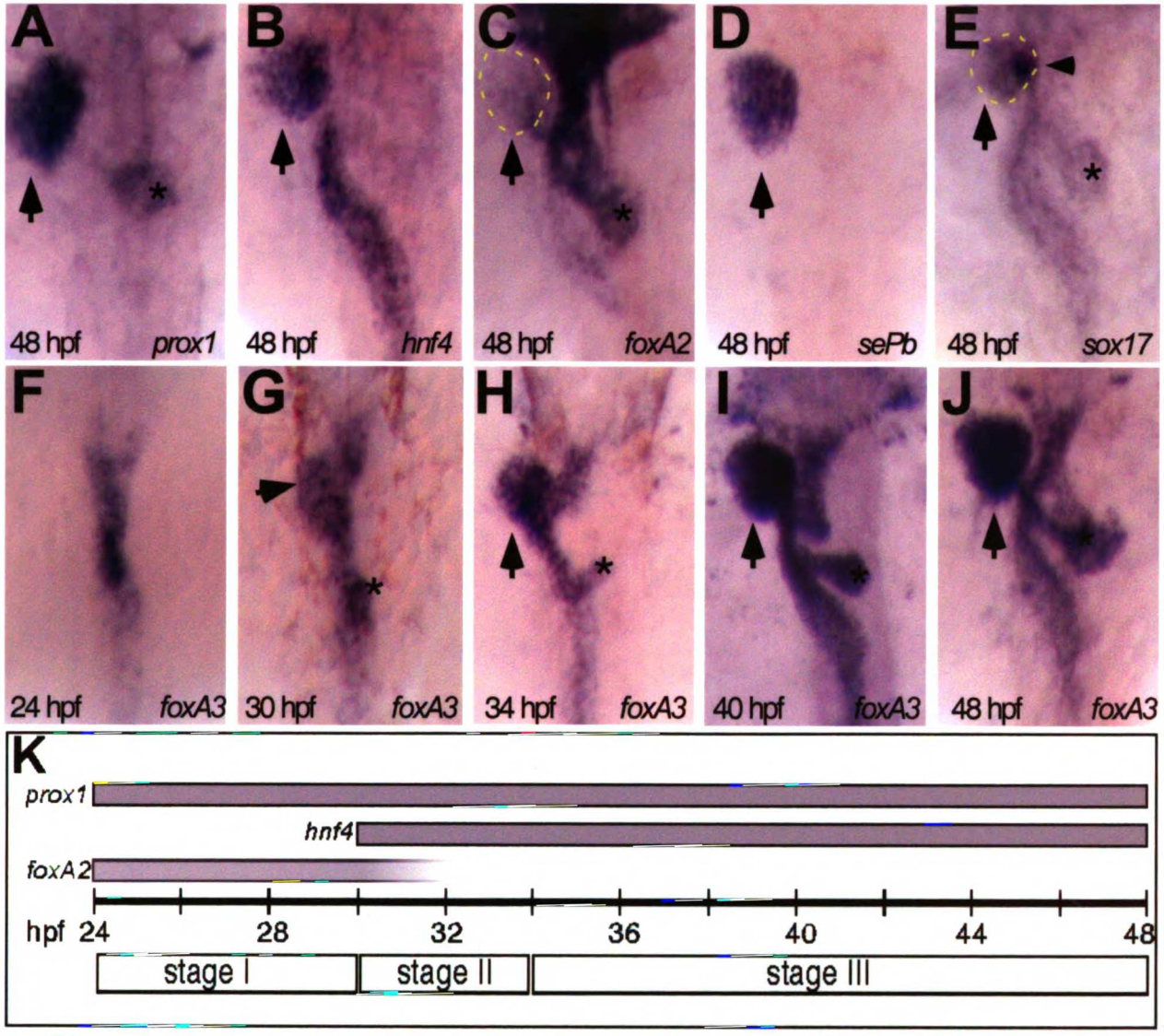

Figure 2.4. Gene expression patterns in the developing digestive system.

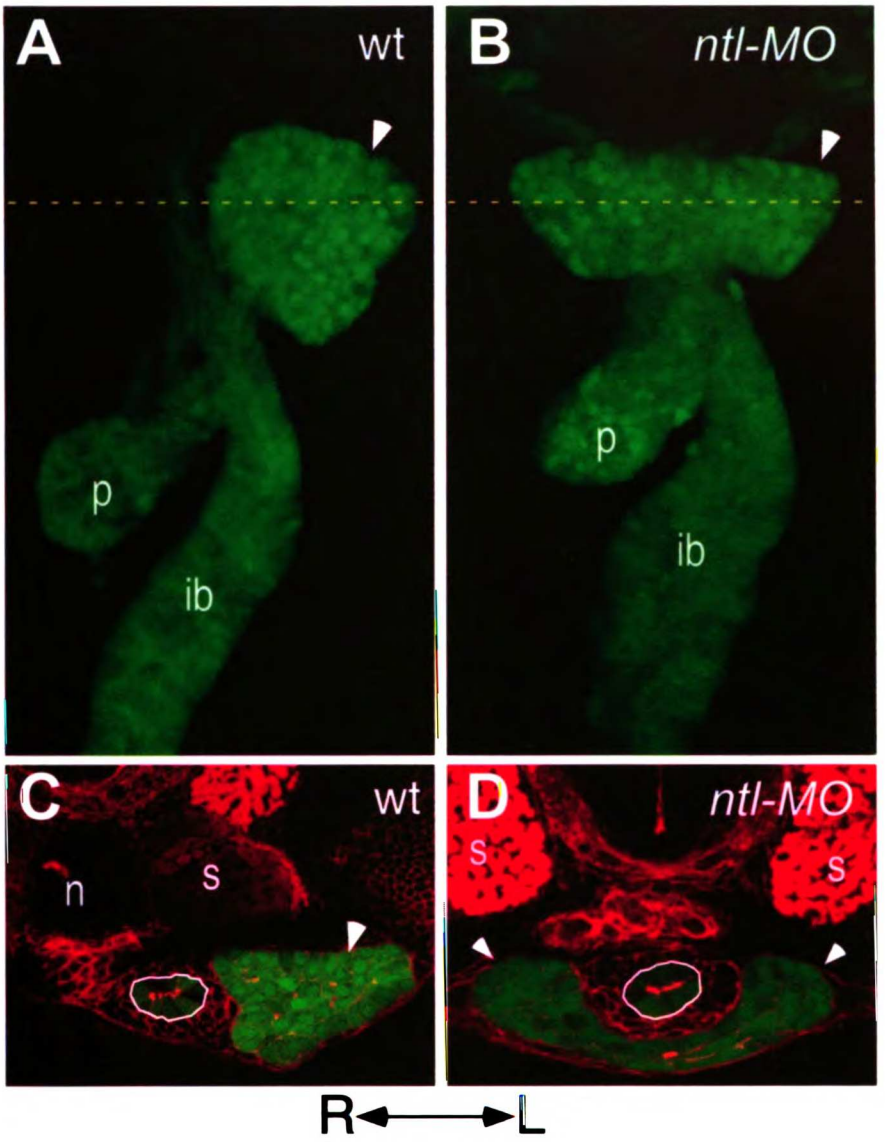

Figure 2.5. The direction of liver budding can be uncoupled from the direction of intestinal bulb looping

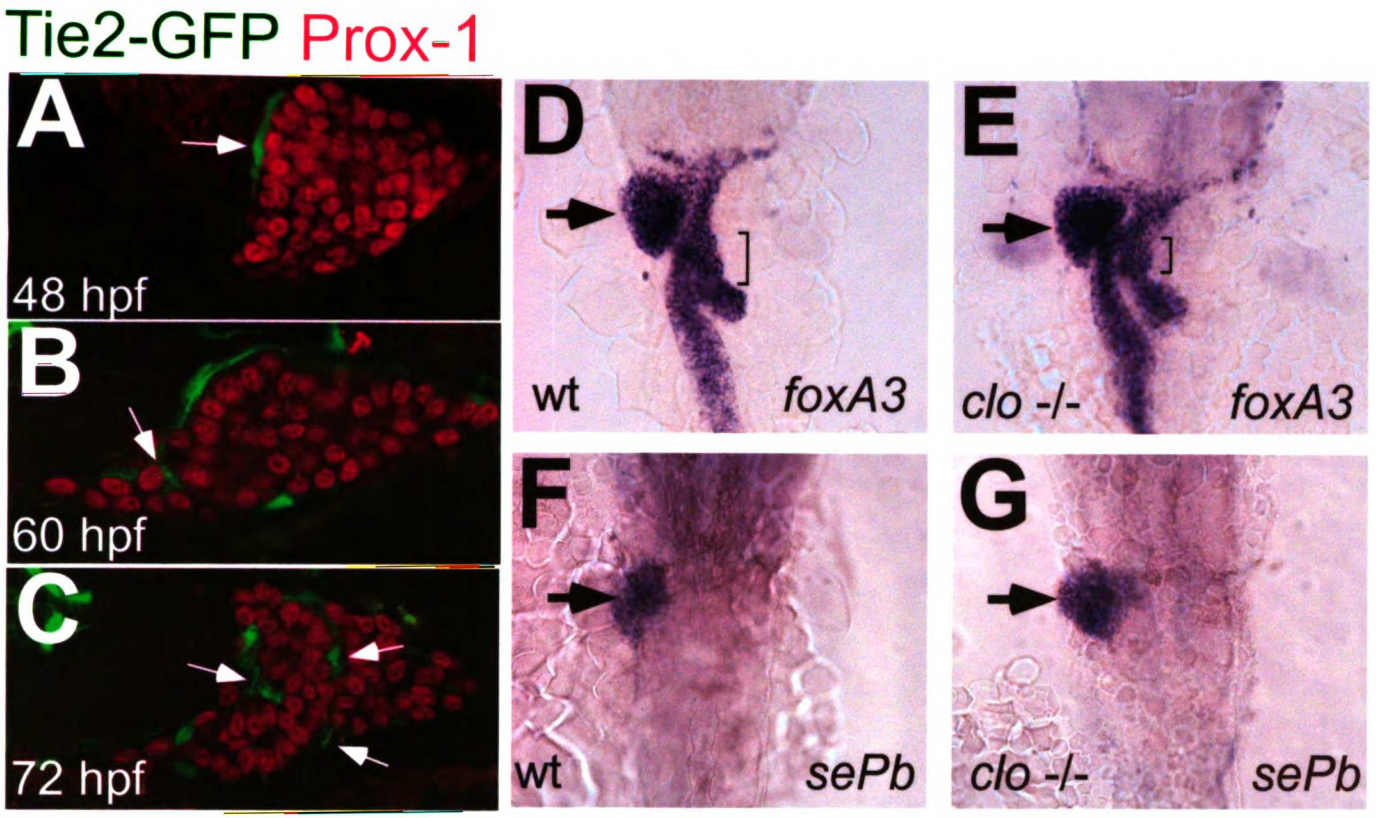

Figure 2.6. Endothelial cells during liver development.

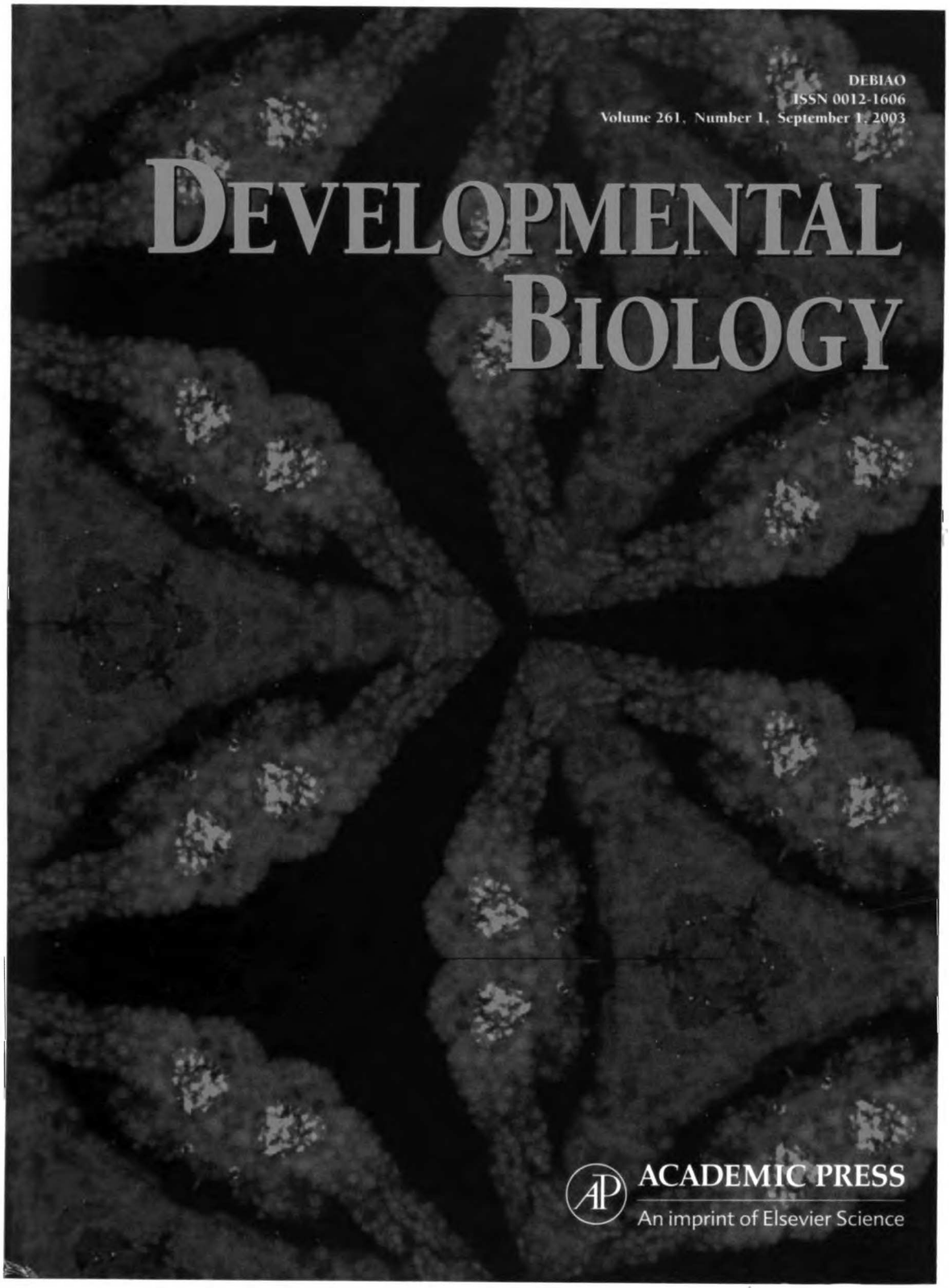
DEBIAO
ISSN 0012-1606
Volume 261, Number 1, September 1, 2003
DEVELOPMENTAL
BIOLOGY
ACADEMIC PRESS
An imprint of Elsevier Science

Chapter 3.

Formation of the Digestive System in Zebrafish:

II. Pancreas Morphogenesis

Holly A. Field, P. D. Si Dong, Dimitris Beis and Didier Y. R. Stainier*

Department of Biochemistry and Biophysics, Programs in Developmental Biology, Genetics and Human Genetics, University of California, San Francisco, San Francisco, California 94143, USA

*Author for correspondence:

Didier Stainier

Dept. of Biochemistry and Biophysics, HSE 1530C

Box 0448

513 Parnassus Ave.

San Francisco, CA 94143-0448

e-mail: didier_stainier@biochem.ucsf.edu

phone: (415) 502-5679

fax: (415) 476-3892

Running title: Two pancreatic anlagen in zebrafish.

ABSTRACT

Recent studies have suggested that the zebrafish pancreas develops from a single pancreatic anlage, located on the dorsal aspect of the developing gut. However, using a transgenic zebrafish line that expresses GFP throughout the endoderm, we report that in fact two pancreatic anlagen join to form the pancreas. One anlage is located on the dorsal aspect of the developing gut and is present by 24 hours post fertilization (hpf), the second anlage is located on the ventral aspect of the developing gut in a position anterior to the dorsal anlage and is present by 40 hpf. These two buds merge by 52 hpf to form the pancreas. Using *heart and soul* mutant embryos, in which the pancreatic anlagen most often do not fuse, we show that the posterior bud generates only endocrine tissue while the anterior bud gives rise to the pancreatic duct and exocrine cells. Interestingly, at later stages the anterior bud also gives rise to a small number of endocrine cells usually present near the pancreatic duct. Altogether, these studies show that the in zebrafish, as in the other model systems analyzed to date, the pancreas arises from multiple buds. To analyze whether other features of pancreas development are conserved and investigate the influence of surrounding tissues on pancreas development, we examined the role of the vasculature in this process. Contrary to reports in other model systems, we find that although vascular endothelium is in contact with the posterior bud throughout pancreas development, its absence in *cloche* mutant embryos does not appear to affect the early morphogenesis or differentiation of the pancreas.

Key words: pancreas, GFP, transgenic, *heart and soul*, *cloche*, vascular endothelium

INTRODUCTION

The pancreas contains two types of glandular tissue that carry out essential physiological functions. The endocrine tissue releases the hormones Insulin, Somatostatin, Pancreatic polypeptide and Glucagon directly into the blood stream, while the exocrine tissue produces digestive enzymes such as Trypsin, Amylase and Carboxypeptidase A that are delivered to the digestive tract through a network of ducts. Morphogenesis of the developing pancreas has been described in a number of organisms. In chick (Kim et al., 1997), *Xenopus laevis* (Kelly and Melton, 2000), and the teleost fish Medaka (Assouline et al., 2002), the pancreas develops from three buds that emerge from the gut tube, two from its ventral aspect, and one from its dorsal aspect. In mouse, although there are initially three buds that arise from the gut tube at the point of contact between the endoderm and the vasculature (Lammert et al., 2001), the pancreas develops from only two of these buds, one dorsal and one ventral (Slack, 1995; Edlund, 2002; Lammert et al., 2003).

So far, all studies have indicated that pancreas development in zebrafish occurs differently than in other vertebrates in that there is a single pancreatic anlage (Argenton et al., 1999; Biemar et al., 2001; Huang et al., 2001). Studies following expression patterns of early pancreatic markers such as *insulin* (*ins*) and *pancreatic duodenal homeobox 1* (*pdx1*) have shown two populations of cells that converge at the midline between the 14- and 18-somite stages to form a single bud of pancreatic tissue at the level of the fourth somite (Biemar et al., 2001). Expression of many endocrine genes has been detected in this midline cluster of cells (Argenton et al., 1999; Biemar et al, 2001).

Few markers of exocrine cell differentiation have been cloned in zebrafish. Of those, the earliest expressed is *trypsin* (*try*) which appears at 48 hpf in the cells surround the single pancreatic islet (Biemar et al., 2001). The lack of earlier expressed exocrine markers has prevented examination of whether there is a single cell population that gives rise to both pancreatic cell types, or whether the exocrine and endocrine cells originate from different locations.

In this study, we use a transgenic zebrafish line in which GFP is expressed throughout the endoderm (Field et al., 2003), together with expression analysis of *ins*, *pdx1* (Milewski et al., 1998), *try* (Biemar et al., 2001), Somatostatin (Sst) and Islet-1 (Isl1) to examine pancreas morphogenesis and the location of several pancreatic cell types within the developing digestive system. We provide evidence for the existence of two distinct pancreatic anlagen – a ventral anterior bud and a dorsal posterior bud – that join to form the definitive pancreas. We further show that the dorsal posterior bud gives rise only to endocrine cells, while the ventral anterior bud gives rise to the exocrine cells, the pancreatic duct and a small but reproducible supply of endocrine cells. In addition, we use *cloche* (*clo*) mutant embryos, which lack endothelial cells from an early stage (Stainier et al., 1995; Liao et al., 1997; Thompson et al., 1998), to investigate the role of the vasculature in zebrafish pancreas development.

Materials and Methods

Embryo culture and zebrafish stocks

Fish and embryos were maintained, collected and staged as described (Westerfield, 1995). Endodermal GFP expression was achieved using embryos homozygous for the gutGFP transgene (Field et al., 2003). Embryos homozygous for the

has^{m567} mutation (Stainier et al., 1996; Horne-Badovinac et al., 2001) and the *clo*^{s5} mutation (Wayne Liao and D.Y.R.S., unpublished) were collected along with wildtype siblings as controls. Embryos homozygous for the *clo*^{m378} mutation (Stainier et al., 1996) and wildtype embryos, either homozygous or heterozygous for the *flk-1*:GFP transgene (Dimitris Beis, Jau-Nian Chen, D.Y.R.S., in preparation) were used in our analyses of the role of vascular endothelium in pancreas development.

Immunofluorescence and RNA in situ localization

Immunofluorescence analysis of protein expression was performed with guinea pig anti-Insulin antibody (no dilution, Biomeda), rabbit anti-Somatostatin antibody (1:100, ICN Biomedicals, Inc.) and mouse anti-Islet antibody (8:100, hybridoma 39.4D5). The anti-Islet antibody, developed by Thomas M. Jessell, was obtained from the Developmental Studies Hybridoma Bank developed under the auspices of the NICHD and maintained by The University of Iowa, Department of Biological Sciences, Iowa City, IA 52242. Embryos were fixed for 2 hours at room temperature with 3.7% formaldehyde in PEM (0.1M Pipes, 1.0mM $MgSO_4$, 2mM EGTA, pH to 7 with NaOH), washed in PBS, manually de-yolked and incubated overnight at 4°C in primary antibody diluted with 0.3% tritonX and 2% sheep serum in PBS. After removal of the primary antibody, embryos were mounted in 4% SeaPlaque agarose (BioWhittaker Molecular Applications) in PBS. Bound antibody was detected on transverse vibratome sections (150 μm thick for transverse and 200 μm thick for ventral views) using Alexa Fluor-647 or Alexa Fluor-594 conjugated to either goat anti-mouse IgG or goat anti-guinea pig IgG antibodies (1:200, Molecular Probes). To visualize actin, transverse vibratome sections were incubated in rhodamine-labeled phalloidin (1:100, Molecular Probes).

Confocal images were acquired using a Leica TCS NT confocal microscope. Image overlays were assembled using Adobe Photoshop 5.0 LE. Two dimensional projections were generated using Scion Image version 4.0.2. Three dimensional rotation movies were generated using Scion Image version 4.0.2 and QuickTime version 5.0.2.

In situ hybridization was performed with digoxigenin-labeled RNA probes for *ins*, *pdx1* (Milewski et al., 1998) and *try* (Biemar et al., 2001). Whole-mount in situ hybridization was performed as described (Field et al., 2003). In situ hybridized embryos were mounted in JB-4 Embedding Medium (Polysciences, Inc.) and 5 μm thick sections obtained by microtome sectioning. Images were acquired using a Zeiss Axioplan, equipped with a Zeiss color Axiocam digital camera running Axiovision 3.0 software.

RESULTS

Two buds contribute to the developing pancreas

While analyzing the gutGFP transgenic line which expresses GFP throughout the endoderm (Field et al., 2003), we noticed a previously undocumented structure originating from the ventral aspect of the intestinal bulb primordium just posterior to the nascent liver. This structure is not apparent in wholemount preparations at 34 hpf (Fig. 3.1A), but by 40 hpf it clearly projects ventrally from the intestinal bulb primordium toward the embryo's right (Fig. 3.1B). It remains a discrete bud for approximately four hours, after which it becomes juxtaposed with a more dorsal posterior aggregation of cells, slightly to the right of the midline (Fig. 3.1C). By 52 hpf, these two buds have fused, and the posterior bud is no longer in direct contact with the intestine (Fig. 3.1D). The anterior bud maintains its connection with the alimentary canal just posterior to the oesophagus, and this connection forms the pancreatic duct. These morphogenetic

changes are presented as three dimensional reconstructions of confocal optical sections (see enclosed CD).

To determine whether this anterior structure has pancreatic identity, we first examined *pdx1* expression at 34, 40, 44 and 52 hpf (Fig. 3.1E-H). *pdx1* expression in the pancreas is well conserved across species (reviewed in Slack, 1995; Edlund, 2002), although it is also expressed in non-pancreatic tissues. We found that *pdx1* is expressed in both the anterior and posterior buds at all stages analyzed, as well as in the intestinal bulb primordium early, and, at 52 hpf, in the oesophagus and intestinal bulb. The fact that the anterior bud expresses *pdx1* together with the morphological data presented above indicate that it contributes to the developing pancreas.

To further characterize the development of this anterior bud, we analyzed its location with respect to surrounding tissues. Transverse sections of the gutGFP line, as well as embryos stained for *pdx1* expression, reveal a ridge along the ventral side of the intestinal bulb primordium at 34 hpf (Fig. 3.2A, B). There are no genes currently known to be specific to the anterior pancreatic bud, so we were unable to confirm the identity of this ridge molecularly. However, the location of this ridge is consistent with that of the anterior pancreatic bud, which at 40 hpf extends to the embryo's right (Fig. 3.2C, D). We used landmarks such as the nephron primordia (Drummond et al., 1998), and the caudal most end of the developing swim bladder to confirm that we were visualizing the gut at the same A/P level. The ventral ridge, and later the anterior pancreatic bud, are directly adjacent to the yolk ventrally, and the lateral plate mesoderm dorsolaterally (Fig. 3.2A-D), with the connection to the intestinal bulb primordium situated approximately at the level of the 3rd somite.

Identity of the two pancreatic buds

Previous analyses have shown that, by 24 hpf, cells of the pancreatic islet are located in a cluster at the level of the fourth somite, and express *pdx1, ins, glucagon* (*glu*), *somatostatin* (*sst*), and *islet-1* (*isl1*) (Biemar et al., 2001; Argenton et al., 1999; Huang et al., 2001). The location and morphology of the dorsal posterior aggregation of cells in the gutGFP transgenic line suggests that this structure corresponds to the previously described pancreatic anlage. Data from protein expression analyses in the gutGFP transgenic line concur with this hypothesis. Sst expression (Fig. 3.2E-H), as well as Ins and Isl1 (data not shown) are located in the posterior bud confirming that the dorsal posterior bud is the previously described pancreatic anlage.

Morphological data combined with gene expression analyses strongly suggest that the newly discovered anterior bud forms part of the mature pancreas, but the identity of the tissues that derive from this bud was not clear. At 52 hpf, *pdx1* expression shows the pancreas as a single structure with a bulbous 'head' attached to the alimentary canal by the pancreatic duct at a position between the oesophagus and the intestinal bulb (Fig. 3.3A). A single cluster of *ins*-expressing cells is located in the head of the pancreas (Fig. 3.3B) surrounded by cells expressing *try* (Fig. 3.3C). The pancreatic duct expresses *pdx1* (Fig. 3.3A), but lacks *try* expression (Fig. 3.3C). Since exocrine gene expression is first detected after the anterior and posterior anlagen have joined, analysis of exocrine gene expression in wildtype embryos is uninformative with respect to the origin of these *try* positive exocrine cells.

To determine which cell types are derived from the anterior pancreatic bud, we analyzed pancreatic gene expression in *has* mutant embryos (Stainier et al., 1996). *has* encodes aPKCλ, a tight junction protein required for the formation and maintenance of a

number of epithelia in the zebrafish embryo (Horne-Badovinac et al., 2001). One of the reported phenotypes of *has* mutant embryos is a pancreas positioned symmetrically with respect to a non-looping gut (Horne-Badovinac et al., 2001). The finding that there are not one but two pancreatic anlagen prompted us to reexamine the *has* mutant pancreatic phenotype. We found that at 52 hpf, the duplicated structures express *pdx1* and attach to the alimentary canal between the oesophagus and intestinal bulb (Fig. 3.3D), while the posterior pancreatic bud, which expresses *pdx1* (Fig. 3.3D) and *ins* (Fig. 3.3E), remains a dorsal midline structure separate from the duplicated anterior structures. Since the duplicated pancreatic structures have a clear pancreatic duct connecting them to the ventral aspect of the alimentary canal, we concluded that they represent a duplication of the anterior pancreatic anlage, while the single posterior bud remains a separate, midline structure. The isolation of the anterior and posterior buds from one another during pancreatic development in *has* mutant embryos provided a system in which to study their respective cellular components.

To identify the location of the exocrine component of the pancreas, we analyzed *try* expression at 52 hpf. In *has* mutant embryos, *try* expression is present in bilateral patches that correspond to the heads of the duplicated anterior buds, but is consistently absent from the midline posterior bud (n=28, Fig. 3.3F). These data show that exocrine cells, as well as the pancreatic duct--identifiable by morphology (data not shown) and by the presence of *pdx1* expression but the absence of *try* expression--are developing from the anterior pancreatic bud. The consistent absence of *try* from the posterior bud suggests that it gives rise only to the pancreatic islet.

Gene expression studies conducted at 76 hpf showed essentially the same results as those described above: the duplicated anterior buds contain *try*-expressing pancreatic exocrine cells, and the posterior bud remains a separate midline structure absent of any *try* expression (data not shown). However, there was one striking difference: At 52 hpf *ins* expression is consistently found only in the posterior bud in *has* mutant embryos (n=22) (Fig. 3.3E), but at 76 hpf, 84% of *has* mutant embryos (n=32) possessed *ins*-expressing cells outside the islet (Fig. 3.4B). In all instances, these *ins*-expressing cells were at the level of, or anterior to, the islet. This observation was not specific to the *has* mutant as 83% of wildtype embryos (n=24) also showed *ins*-expressing cells outside of the islet (Fig. 3.4A). To determine the location of these stray *ins*-expressing cells, we analyzed Ins expression in the gutGFP line at 76 hpf. We found that, at this stage, Ins positive cells found outside the islet are usually located in or near the pancreatic duct in both wildtype and *has* mutant embryos (Fig. 3.4C, D). Cells expressing Isl1 and Glu or Sst are also found in this region of the pancreas (data not shown).

The role of vascular endothelium in pancreas development

Studies carried out in mouse and *Xenopus* have shown that in the absence of vascular endothelial cells, *pdx1* positive endoderm fails to differentiate into *ins* producing endocrine cells (Lammert et al., 2001). To assess the role of vascular endothelium in zebrafish pancreas development, we first analyzed the location of vascular endothelium with respect to the anterior and posterior pancreatic buds by using a transgenic line expressing GFP under the control of the zebrafish *flk1* promoter (D. B., Jau-Nian Chen and D.Y.R.S., in preparation). We started our analysis at the 18-somite stage at which time *flk1* positive vascular endothelial cells are already in close association with the

posterior bud (Fig. 3.5A). Between 24 and 40 hpf, the posterior bud maintains contact with the dorsal aorta and posterior cardinal veins (Fig. 3.5B-D), while the anterior bud does not appear to be in contact with any endothelial cells (Fig. 3.5E). Endothelial cells are also seen extensively throughout the pancreatic islet by approximately 52 hpf (Fig 3.5F).

To study pancreas development in the absence of vascular endothelial cells, we examined the pancreas of *clo* mutant embryos, which appear to lack most endothelial cells (Stainier et al., 1995; Liao et al., 1997; Thompson et al., 1998). General pancreas morphology was assessed by examining *pdx1* expression at 52 hpf. *clo* mutant embryos were identified based on their severe heart phenotype at this stage. In *clo* mutant embryos, although the level of *pdx1* expression in the intestinal bulb is reduced compared to wildtype, pancreatic *pdx1* expression appears mostly unaffected (Fig. 3.6A, B). In some *clo* mutant embryos the morphology of the pancreas is abnormal which could be due to the severe edema. To assess the differentiation of pancreatic tissues in the absence of vascular endothelium, we examined the expression of the endocrine gene *ins* and exocrine gene *try*. Both *ins* and *try* are expressed in 52 hpf *clo* mutant embryos in a pattern expected from the morphological analysis with *pdx1* (Fig. 3.6C-F), and at a level comparable to wildtype.

Since it was formally possible that the *ins* positive cells seen in *clo* mutant embryos at 52 hpf originated from the anterior bud which, unlike the posterior bud, is not normally in contact with vascular endothelium, we analyzed the posterior bud of *clo* mutant embryos for the presence of differentiated endocrine cells at 24 hpf. On the basis of *flk-1*:GFP expression, we sorted *clo* mutant embryos and their wildtype siblings at 24

hpf and examined transverse sections. Surprisingly, we saw no difference in the number or position of Isl1 or Ins positive cells in *clo* mutant embryos, despite the apparent absence of endothelial cells in this region (Fig. 3.6G, H).

DISCUSSION

Spatiotemporal development of the zebrafish pancreas

In all vertebrates where it has been examined in detail, the pancreas develops from two or three endodermal anlagen that bud independently from the intestine and join to form the definitive pancreas (Slack, 1995; Kim et al., 1997; Kelly and Melton, 2000; Assouline et al., 2002; Edlund, 2002; Lammert et al., 2003). However, in zebrafish, previous studies have suggested that the pancreas develops from a single structure arising dorsally on the developing intestine (Argenton et al., 1999; Biemar et al., 2001; Huang et al., 2001). Using the gutGFP line to observe endoderm morphogenesis, we have identified a second pancreatic anlage which is located ventrally and anterior to the previously described dorsal pancreatic bud.

Previous analyses of endocrine specific gene expression have described zebrafish pancreas development starting at the 10-somite stage, the time when *pdx1* positive cells are first detected (Biemar et al., 2001). Two bilateral populations of *pdx1*-expressing cells converge to the midline by the 18-somite stage by which time a subset of these cells express *ins*, *isl1*, *sst* and *pax6.2*. Based on the location and movements of the endoderm between the 10- and 18-somite stages (Ober et al., 2003), we propose that the two patches that converge at the midline do not represent a more ancestral form of two mammalian buds, as has been suggested (Biemar et al., 2001), but rather that these cells take on a pancreatic identity before the endoderm has coalesced at the midline. In this model, the

movement of these patches to the midline is not specific to pancreas morphogenesis but generally reflective of early endoderm morphogenesis. Once at the midline, the subsets of *pdx1*-expressing cells that also expresses *ins*, *sst* and *glu* undergo morphogenesis as a single dorsal anlage (Biemar et al., 2001). The condensation of this pancreatic bud likely represents the initial step in pancreas morphogenesis. It should be noted that although we refer to this pancreatic anlage as a pancreatic bud, there are no data to date showing whether these cells are integrated into the developing intestine and subsequently bud out to form a separate structure, or whether they remain separate from the rod of endoderm, sitting dorsal and adjacent to, but not incorporated within, the intestinal primordium.

Data presented here describe a subsequent morphogenetic event in pancreas organogenesis, the budding of a ventral anterior pancreatic anlage by 40 hpf. Before this structure is apparent, the lateral plate mesoderm lies alongside the intestinal bulb primordium at the level where the anterior pancreatic bud develops, making the lateral plate mesoderm a potential source for signaling molecules to stimulate morphogenesis, and possibly help establish the exocrine identity of the anterior pancreatic bud. In addition to its close proximity to the lateral plate mesoderm, the area of the intestinal bulb primordium that gives rise to the anterior pancreatic bud is also adjacent to the yolk cell. Therefore, the yolk syncytial layer must also be considered as a candidate source for signals regulating the development of the anterior pancreatic bud. Like in mouse, the cells contributing to the anterior pancreatic bud lie close to the liver, although in zebrafish, liver morphogenesis begins several hours before the initiation of the anterior pancreatic bud. Also, in mouse the ventral pancreatic buds appear where the vitelline veins contact the endoderm (Lammert et al., 2001), while in zebrafish there does not

appear to be any association of the vascular endothelium with the anterior pancreatic bud. It will be interesting to identify the signals regulating the development of the anterior pancreatic bud and determine whether retinoic acid and Hedgehog signaling, which have been indicated in the development of the posterior pancreatic bud (Roy et al., 2001; dilorio et al, 2002; Stafford and Prince, 2002), are also involved in the development of the anterior pancreatic bud.

The two zebrafish pancreatic anlagen appear to contain distinct cell types

In mouse and chick, the dorsal and ventral pancreatic anlagen each gives rise to both endocrine and exocrine cells (Kim and Hebrok, 2001). An independent origin of endocrine and exocrine populations has been suggested in both Medaka and *Xenopus laevis*, in which the dorsal pancreatic bud appears to give rise exclusively to the islet (Kelly and Melton, 2000; Assouline et al., 2002; Horb and Slack, 2002).

Using available markers, exocrine gene expression can not be detected in zebrafish until after the anterior and posterior buds have fused, thus it is not possible to determine which anlage gives rise to which cell type in wildtype embryos. To answer this question, we analyzed pancreatic gene expression in *has* mutant embryos in which the anterior and posterior pancreatic anlagen remain separated. Based on the spatially distinct regions of endocrine and exocrine gene expression in *has* mutant embryos, we propose that the anterior bud forms the pancreatic duct and the exocrine tissue, while the posterior bud forms the islet. With the tools currently available, we can not rule out the possibility that contact of the two buds might induce exocrine cell differentiation in posterior bud-derived tissues as well. However, since these pancreatic anlagen can

express differentiation markers while remaining separate, we conclude that endocrine and exocrine cells can at least partly differentiate independently of each other.

We observed that at 76 hpf, both wildtype and *has* mutant embryos exhibit additional Ins-expressing cells within the pancreas but outside the islet. The location of these Ins-expressing cells suggests that there is a population of cells within the anterior pancreatic bud which has the ability to give rise to endocrine cells, and that contact with the posterior bud is not necessary to induce their differentiation. These cells may arise from within the pancreatic duct, as is suspected to occur in mouse (Gu et al., 2003) or from within the exocrine component which would suggest the presence of bi-potential precursors. This latter explanation is consistent with data in zebrafish transiently lacking functional Pdx1: such embryos have reduced endocrine and exocrine cell populations at 48 hpf, but the pancreas recovers by 5 days post fertilization (Yee et al., 2001). The cell proliferation leading to the recovery of both endocrine and exocrine cells occurs only in the exocrine component of the pancreas (Yee et al., 2001). This observation is consistent with the existence of precursor cells contained within the exocrine component, and thus presumably derived from the anterior bud, that can give rise to both endocrine and exocrine cells. Although we have not ruled out the possibility that these Ins-expressing cells could migrate from the islet into the anterior pancreatic bud, the fact that the pancreatic anlagen in *has* mutant embryos do not usually come in contact makes this explanation unlikely. We therefore suggest that in zebrafish there are two populations of endocrine cells based on their developmental origin: one that arises from the posterior pancreatic bud, and the other from the anterior pancreatic bud, presumably from a multipotential cell. It will be interesting to better characterize this latter population of

endocrine cells by determining whether they arise directly from the pancreatic duct or through a bi-potential precursor in the exocrine tissue, as well as analyze what regulates their emergence.

Vascular endothelium does not appear to be necessary for zebrafish pancreas development

Work by Lammert et al. (2001) has shown that the initiation of pancreas development in mouse is coincident with vascular endothelial cells contacting specified endoderm. In addition, isolated competent prepancreatic endoderm expresses the pancreatic endocrine marker *ins* in the presence, but not absence, of dorsal aorta. Furthermore, removal of the dorsal aorta in *Xenopus* embryos blocks endocrine cell differentiation. These data indicate that signals from vascular endothelial cells are necessary for pancreatic endocrine differentiation. We have shown that zebrafish pancreas morphogenesis, as well as endocrine and exocrine differentiation, occur relatively normally in *clo* mutant embryos which lack most endothelial cells (Stainier et al., 1995; Liao et al., 1997; Thompson et al., 1998). *flk-1*-expressing cells are found in *clo* mutant embryos, although they are mostly located in the posterior region of the embryo and the ectodermal region of the hindbrain (Liao et al., 1997), thus physically far from the pancreas. There are a few plausible explanations for the apparent lack of conservation between this aspect of pancreas development in zebrafish and other vertebrates. The vascular endothelial cells may be signaling to the posterior pancreatic bud in zebrafish but are not the only inducers of endocrine differentiation and other tissues are compensating in their absence. It is also possible that signals provided by endothelial cells in mouse and *Xenopus* are produced by a different cell type in zebrafish.

A new model of zebrafish pancreas development

Based on the results presented here, we would like to propose a new model of zebrafish pancreas development which incorporates both the ventral anterior and dorsal posterior pancreatic anlagen (Fig. 3.7). At 34 hpf, the posterior pancreatic bud is already present as a cluster of cells dorsal, and slightly medial, to the developing intestine. Endocrine gene expression is present in this posterior bud. The anterior pancreatic bud begins as a ridge on the ventral side of the intestinal bulb primordium at 34 hpf contiguous with the developing liver, and by 40 hpf it has extended ventrally and to the right beyond the developing intestine. The anterior pancreatic bud maintains a connection to the intestinal bulb primordium and grows out toward the posterior pancreatic bud. By 44 hpf, the two anlagen have come into contact, with the anterior pancreatic bud ventral to the posterior bud, and by 52 hpf the two buds have fused. The connection of the anterior bud to the alimentary canal forms the pancreatic duct while the posterior bud, which progressively becomes surrounded by exocrine cells from the anterior bud, forms the islet. Presumably, proliferation of cells derived from the anterior pancreatic bud leads to the formation of the exocrine pancreas tail, which can be seen at 76 hpf, and total engulfment of the islet by exocrine tissue ,which is clearly seen by 5.5 days of development (Biemar et al., 2001; data not shown).

The identification of two spatially distinct pancreatic anlagen, as well as two spatially distinct origins for endocrine cells in zebrafish, has important implications on the study of pancreas development and cell differentiation. Since the posterior pancreatic bud gives rise only to endocrine tissue, the zebrafish provides a model system in which the developmental program of these cells can be studied in isolation from that of exocrine

pancreas or bi-potential precursor cells. In addition, the understanding of anterior pancreatic bud development will help shed light on the nature of phenotypes such as that caused by the *slim jim* mutation (Pack et al., 1996), which results in the absence of exocrine but not endocrine cells.

ACKNOWLEDGEMENTS

We thank Steve Waldron for expert maintenance of the zebrafish stocks; Suk-Won Jin for assistance with vascular identity; Juan Engel for assistance on the confocal microscope; Peter Chien, Matthias Hebrok, Sally Horne and members of the Stainier lab for support, valuable discussions, and feedback on the manuscript. This work was supported in part by the UCSF Liver Center (P30 DK26743), the Human Frontier Science Program (long-term fellowship to D. B.) and the NIH (T32 CA09270 to P. D. S. D. and DK61245 to D.Y.R.S.).

REFERENCES

Argenton, F., Zecchin, E., and Bortolussi, M. (1999). Early appearance of pancreatic hormone-expressing cells in the zebrafish embryo. *Mech Dev* **87**, 217-21.

Assouline, B., Nguyen, V., Mahe, S., Bourrat, F., and Scharfmann, R. (2002). Development of the pancreas in medaka. *Mech Dev* **117**, 299.

Biemar, F., Argenton, F., Schmidtke, R., Epperlein, S., Peers, B., and Driever, W. (2001). Pancreas development in zebrafish: early dispersed appearance of endocrine hormone-expressing cells and their convergence to form the definitive islet. *Dev Biol* **230**, 189-203.

diIorio, P. J., Moss, J. B., Sbrogna, J. L., Karlstrom, R. O., and Moss, L. G. (2002). Sonic hedgehog is required early in pancreatic islet development. *Dev Biol* **244**, 75-84.

Drummond, I. A., Majumdar, A., Hentschel, H., Elger, M., Solnica-Krezel, L., Schier, A. F., Neuhauss, S. C., Stemple, D. L., Zwartkruis, F., Rangini, Z., Driever, W., and Fishman, M. C. (1998). Early development of the zebrafish pronephros and analysis of mutations affecting pronephric function. *Development* **125**, 4655-67.

Edlund, H. (2002). Pancreatic organogenesis--developmental mechanisms and implications for therapy. *Nat Rev Genet* **3**, 524-32.

Field HA, Ober EA, Roeser T, Stainier D. Y. R. (2003). Formation of the digestive system in zebrafish: I. Liver morphogenesis. *Dev Biol* **253**, 279-290.

Gu, G., Brown, J. R., Melton, D. A. (2003). Direct lineage tracing reveals the ontogeny of pancreatic cell fates during mouse embryogenesis. *Mech Dev* **120**, 35-43.

Horb, M. E., and Slack, J. M. (2002). Expression of amylase and other pancreatic genes in Xenopus. *Mech Dev* **113**, 153-7.

Horne-Badovinac, S., Lin, D., Waldron, S., Schwarz, M., Mbamalu, G., Pawson, T., Jan, Y., Stainier, D. Y., and Abdelilah-Seyfried, S. (2001). Positional cloning of *heart and soul* reveals multiple roles for PKC lambda in zebrafish organogenesis. *Curr Biol* **11**, 1492-502.

Huang, H., Vogel, S. S., Liu, N., Melton, D. A., and Lin, S. (2001). Analysis of pancreatic development in living transgenic zebrafish embryos. *Mol Cell Endocrinol* **177**, 117-24.

Kelly, O. G., and Melton, D. A. (2000). Development of the pancreas in *Xenopus laevis*. *Dev Dyn* **218**, 615-27.

Kim, S. K., Hebrok, M., and Melton, D. A. (1997). Pancreas Development in the Chick Embryo. *Cold Spring Harb Symp Quant Biol* **62**, 377-83.

Kim, S. K., and Hebrok, M. (2001). Intercellular signals regulating pancreas development and function. *Genes Dev* **15**, 111-27.

Lammert, E., Cleaver, O., and Melton, D. (2001). Induction of pancreatic differentiation by signals from blood vessels. *Science* **294**, 564-7.

Lammert, E., Cleaver, O., and Melton, D. (2003). Role of endothelial cells in early pancreas and liver development. *Mech Dev* **120**, 59-64.

Liao, W., Bisgrove, B. W., Sawyer, H., Hug, B., Bell, B., Peters, K., Grunwald, D. J. and Stainier, D. Y. (1997). The zebrafish gene *cloche* acts upstream of a *Flk-1* homologue to regulate endothelial cell differentiation. *Development* **124**, 381-9.

Milewski, W. M., Duguay, S. J., Chan, S. J., and Steiner, D. F. (1998). Conservation of PDX-1 structure, function, and expression in zebrafish. *Endocrinology* **139**, 1440-9.

Ober, E. A., Field, H. A., and Stainier, D. Y. R. (2003). From endoderm formation to liver and pancreas development in zebrafish. *Mech Dev* **120**, 5-18.

Pack, M., Solnica-Krezel, L., Malicki, J., Neuhauss, S. C., Schier, A. F., Stemple, D. L., Driever, W., and Fishman, M. C. (1996). Mutations affecting development of zebrafish digestive organs. *Development* **123**, 321-8.

Roy, S., Qiao, T., Wolff, C., and Ingham, P. W. (2001). Hedgehog signaling pathway is essential for pancreas specification in the zebrafish embryo. *Curr Biol* **11**, 1358-63.

Slack, J. M. (1995). Developmental biology of the pancreas. *Development* **121**, 1569-80.

Stafford, D., and Prince, V. (2002). Retinoic Acid signaling is required for a critical early step in zebrafish pancreatic development. *Curr Biol* **12**, 1215.

Stainier, D. Y., Weinstein, B. M., Detrich, H. W., 3rd, Zon, L. I. and Fishman, M. C. (1995). *cloche*, an early acting zebrafish gene, is required by both the endothelial and hematopoietic lineages. *Development* **121**, 3141-50.

Stainier, D. Y., Fouquet, B., Chen, J. N., Warren, K. S., Weinstein, B. M., Meiler, S. E., Mohideen, M. A., Neuhauss, S. C., Solnica-Krezel, L., Schier, A. F., Zwartkruis, F., Stemple, D. L., Malicki, J., Driever, W., and Fishman, M. C. (1996). Mutations affecting the formation and function of the cardiovascular system in the zebrafish embryo. *Development* **123**, 285-92.

Thompson, M. A., Ransom, D. G., Pratt, S. J., MacLennan, H., Kieran, M. W., Detrich, H. W., 3rd, Vail, B., Huber, T. L., Paw, B., Brownlie, A. J. et al. (1998). The *cloche* and *spadetail* genes differentially affect hematopoiesis and vasculogenesis. *Dev Biol* 197, 248-69.

Westerfield, M. (1995). "The zebrafish book : a guide for the laboratory use of zebrafish (Danio rerio)." M. Westerfield, Eugene, OR.

Yee, N. S., Yusuff, S., and Pack, M. (2001). Zebrafish pdx1 morphant displays defects in pancreas development and digestive organ chirality, and potentially identifies a multipotent pancreas progenitor cell. *Genesis* **30**, 137-40.

FIGURE LEGENDS

Fig. 3.1. Two anlagen make up the pancreas. (A-D) Two dimensional projections of confocal stacks. (E-H) Whole-mount in situ hybridization with *pdx1*. Ventral views, anterior to the top. The posterior anlage (arrowhead) is clearly visible at 34 hpf (A), and 40 hpf (B), but is obscured by the anterior bud (arrow) at 44 hpf (C) and 52 hpf (D). *pdx1* expression is found in both structures before (E-F) and after (G, H) they come into contact. At 52 hpf, (D, G) the pancreas appears as a single structure. L, liver. Scale bar, 50 μm.

Fig. 3.2. Morphogenesis of the anterior and posterior buds. [In all sections, dorsal is to the top, and right is to the reader's left to maintain orientation with the ventral views shown throughout the paper.] (A-D) The anterior pancreatic bud initiates morphogenesis adjacent to the lateral plate mesoderm and the yolk cell. Transverse sections of wildtype gutGFP embryos showing *pdx1* expression in purple (A, C), endodermal GFP expression (green) and actin staining (red) (B, D). The A/P level of the these sections was determined using landmarks such as the nephron primordia (outlined by solid yellow lines) and the posterior end of the developing swim bladder. The first sign of anterior bud morphogenesis occurs by 34 hpf (A, B) as a ridge (arrow) of tissue on the ventral right side of the intestinal bulb primordium (i). (C, D) At the same A/P level at 38 hpf, the anterior pancreatic bud has stretched to the embryo's right (toward the embryonic midline) and is still in contact ventrally with the yolk cell. The lateral and dorsal edges of the anterior pancreatic bud are in contact with the surrounding mesodermal cells, outlined by red actin staining. (E-H) The posterior bud is the pancreatic islet. Transverse sections

through wildtype gutGFP embryos at 24 hpf. Endodermal GFP expression shown in green (E), Sst in red (F), and actin in blue (G). (H) Overlay. The posterior structure (arrow) contains Sst positive cells clustered on the dorsal side of the endodermal rod (e). The hypochord and endothelial cells (Fig. 3.5) separate the pancreatic islet from the notochord (*, outlined by a dashed yellow line) at this stage. s, somite; nt, neural tube; e, endodermal rod; *, notochord; ib, intestinal bulb primordium; y, yolk. Scale bars, 25 μm.

Fig. 3.3. Pancreatic duct and exocrine tissue develop from the anterior bud. (A-F) Whole-mount in situ hybridization of wildtype (A-C) and *has* mutant embryos (D-F) at 52 hpf. Ventral views, anterior to the top. (A) In wildtype embryos, *pdx1* expression is found throughout the entire pancreas, including the pancreatic duct (bracket), as well as in the oesophagus (o) and intestinal bulb (ib). (B) *ins* expression is found in a cluster of cells sitting at the center of the *try* expression domain (C). (D) In *has* mutant embryos, the anterior pancreatic bud is duplicated, as seen with *pdx1* expression. The islet (outlined in yellow) remains separate from the anterior structures. (E) Examination of *ins* expression reveals that only the posterior islet contains *ins* positive cells at this time. (F) *try* expression is found only in the duplicated anterior structures. o, oesophagus; ib, intestinal bulb.

Fig. 3.4. Insulin positive cells arise within the anterior pancreatic bud. (A, B) Whole-mount in situ hybridization at 76 hpf. (C-E) Two dimensional projections of confocal stacks showing Ins (red) expression and GFP expression in the endoderm. Ventral views, anterior to the top. At 76 hpf, both wildtype (A) and *has* mutant embryos (B) exhibit *ins*-

expressing cells (arrowheads) outside of the major islet structure (circled). Ins staining in the gutGFP line shows these Ins positive cells situated near the pancreatic duct in both wildtype (C) and *has* mutant embryos (D) [areas outlined in (C, D) are cropped and enlarged in (E, F)]. e, eyes; L, liver; gb, gall bladder; pd, pancreatic duct; ib, intestinal bulb.

Fig. 3.5. Vascular endothelium and pancreas development. (A-F) Transverse sections showing GFP expression in endothelial cells (green), Islet-1 (blue), and actin staining (red) in wildtype embryos at the 18-somite stage (A), 24 hpf (B), 30 hpf (C), 34 hpf (D), 40 hpf (E) and 52 hpf (F). [Dorsal is to the top, and right is to the reader's left to maintain orientation with the ventral views shown throughout the paper.] As early as the 18-somite stage (A) vascular endothelial cells (green) of the fusing dorsal aorta (arrowheads) are in contact with the developing pancreatic islet (blue). By 24 hpf and throughout the rest of pancreas morphogenesis, the islet is in close association with the dorsal aorta (arrowhead) and the posterior cardinal veins (grey arrows) (B-D). At 40 hpf (E), the developing anterior bud (outlined in yellow) does not appear to be in direct contact with vascular endothelium. The identity of the anterior bud was determined based on tissue morphology and A/P location within the embryo, using landmarks such as the nephron primordia (n) and the posterior end of the developing swim bladder. At 52 hpf (F) vascular endothelial cells are found within the islet. n, pronephric nephron; *, notochord; ib, intestinal bulb primordium (E) and intestinal bulb (F). Scale bar, 50 μm.

Fig. 3.6. Vascular endothelium does not appear to be necessary for pancreas development. (A-F) Whole-mount in situ hybridization of wildtype (A, C, E) and *clo* mutant embryos (B, D, F) at 52 hpf. Ventral views, anterior to the top. Although the level of *pdx1* expression in the intestinal bulb (ib) appears reduced in *clo* mutant embryos (B), the morphogenesis of the pancreas (arrow) has occurred normally. At 52 hpf, both endocrine and exocrine tissues have differentiated normally in *clo* mutant embryos, as assessed by *ins* (D) and *try* (F) expression respectively. (G, H) Transverse sections at 24 hpf showing GFP expression in endothelial cells (green), Isl-1 (red), and Ins (blue). (G) In wildtype embryos, cells of the posterior pancreatic bud express Isl-1 (red). Ins is restricted to the cytoplasm [appears purple due to the overlay with red Isl-1]. The posterior bud contacts the dorsal aorta (arrowhead) and the posterior cardinal veins (grey arrows). (H) The posterior pancreatic bud of *clo* mutant embryos, which lack endothelial cells (as shown by the absence of *flk-1*:GFP expressing cells), contains a wildtype-like number of Isl-1 and Ins positive cells. Non-specific Ins staining can be seen ventral to the islet in both *clo* mutant embryos and their wildtype siblings. o, oesophagus; ib, intestinal bulb.

Fig. 3.7. A new model of zebrafish pancreas development. Sketches showing the anterior (arrow) and the posterior (arrowhead) pancreatic buds. All sketches represent ventral views of the endoderm, anterior to the top. At 34 hpf, a ridge on the ventral side of the intestinal bulb primordium, contiguous with the developing hepatic region (L), is the first sign of anterior pancreatic bud morphogenesis. At this time, the posterior pancreatic bud is a single cluster of cells dorsal and adjacent to the developing intestine.

By 40 hpf, the anterior bud has grown ventrally and to the right, extending beyond the edge of the intestinal bulb primordium. At 44 hpf, the two pancreatic anlagen are in contact, the anterior pancreatic bud sitting ventral to the posterior bud. The connection of the anterior bud to the intestine gives rise to the pancreatic duct. At 52 hpf, cells from the anterior bud have merged with the posterior bud which is no longer in contact with the intestinal bulb. By this time, endothelial cells are present in the pancreas. It is also around 52 hpf that exocrine specific genes are first expressed. By 76 hpf, exocrine tissue from the anterior bud completely surrounds the islet and extends caudally to form the pancreatic tail. The swim bladder develops dorsal to, but does not have direct contact with, the pancreas. s, swim bladder; gb, gall bladder; L, liver.

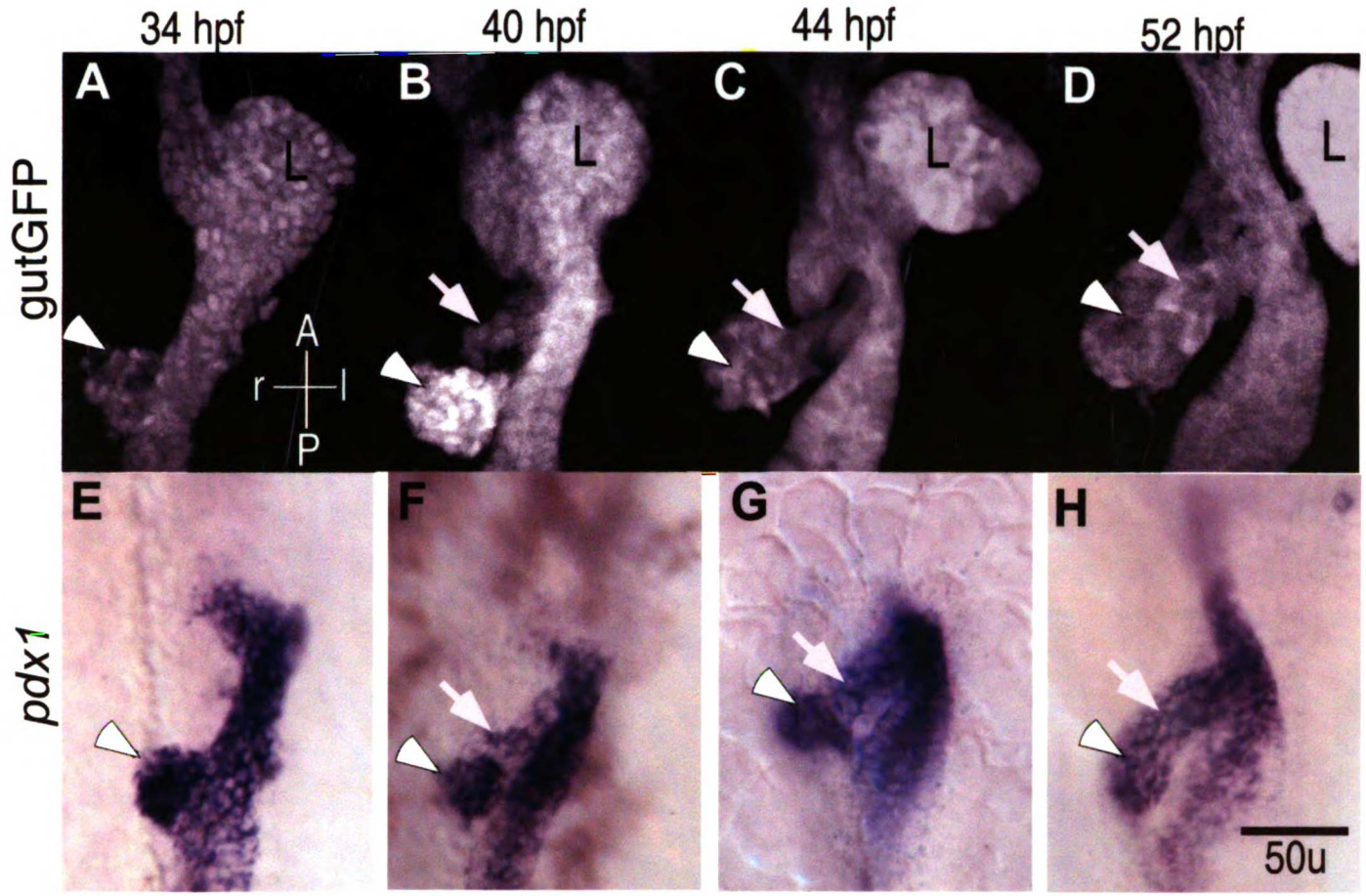

Figure 3.1. Two anlagen make up the pancreas.

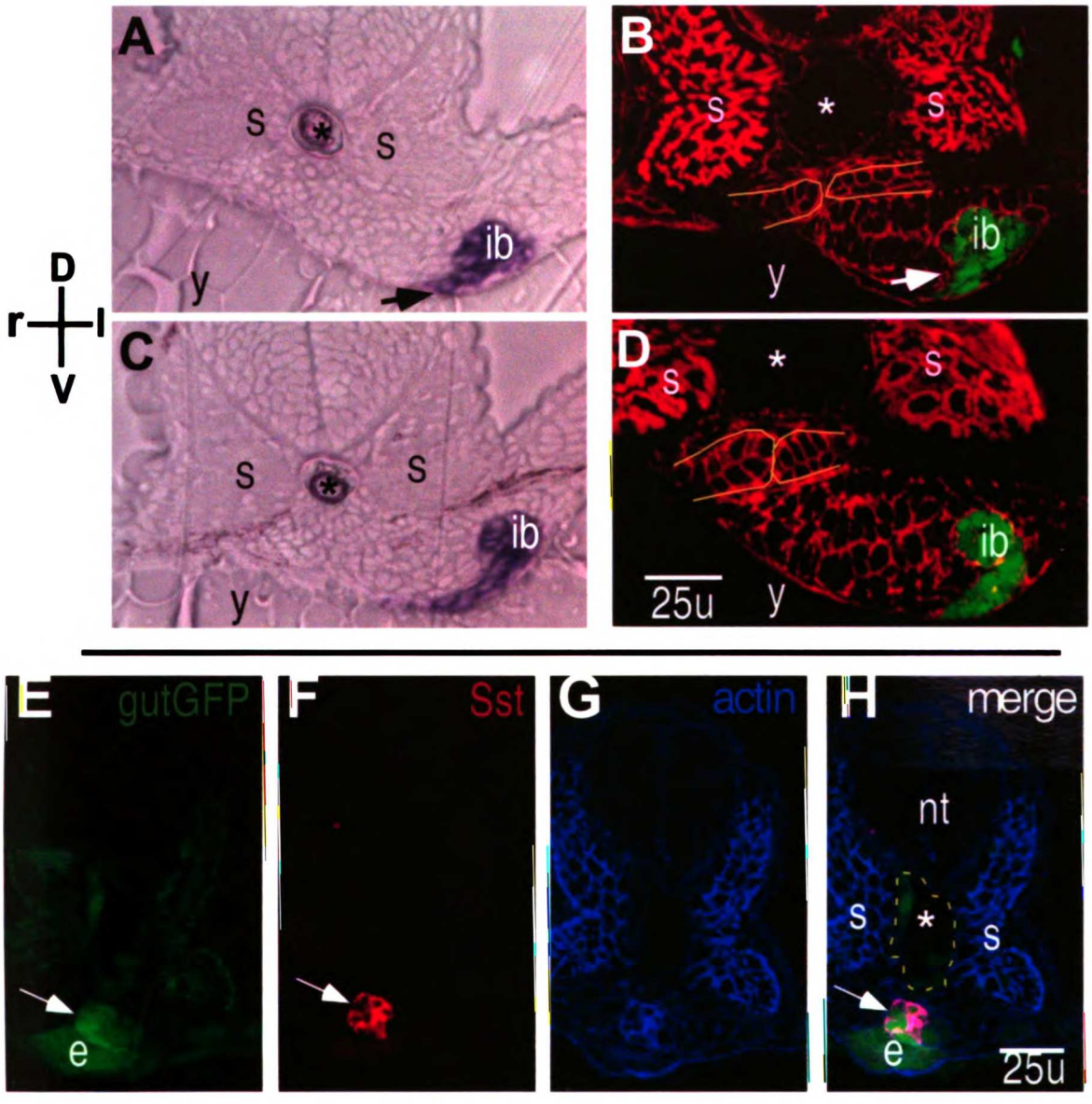

Figure 3.2. Morphogenesis of the anterior and posterior buds.

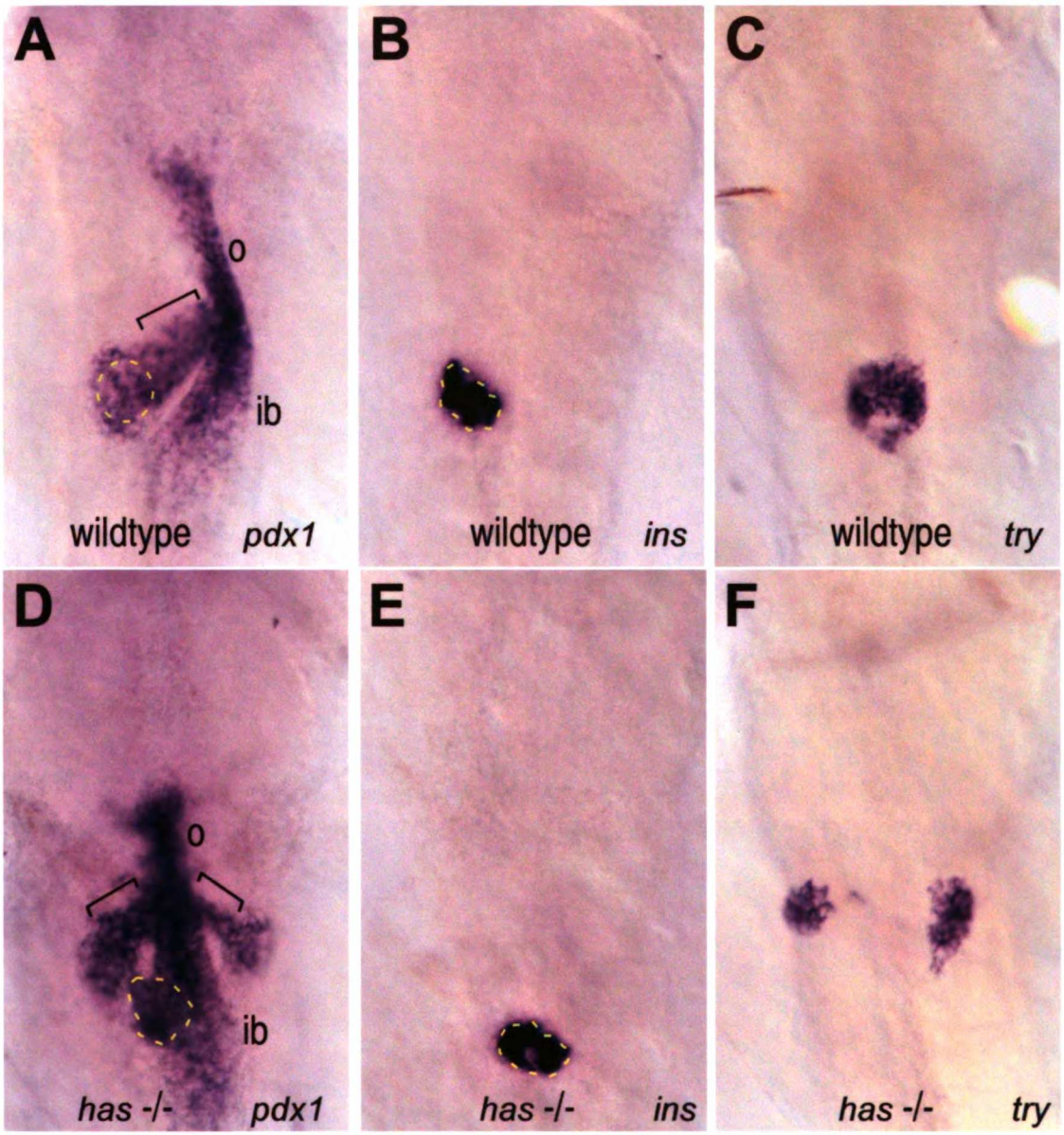

Figure 3.3. Pancreatic duct and exocrine tissue develop from the anterior bud.

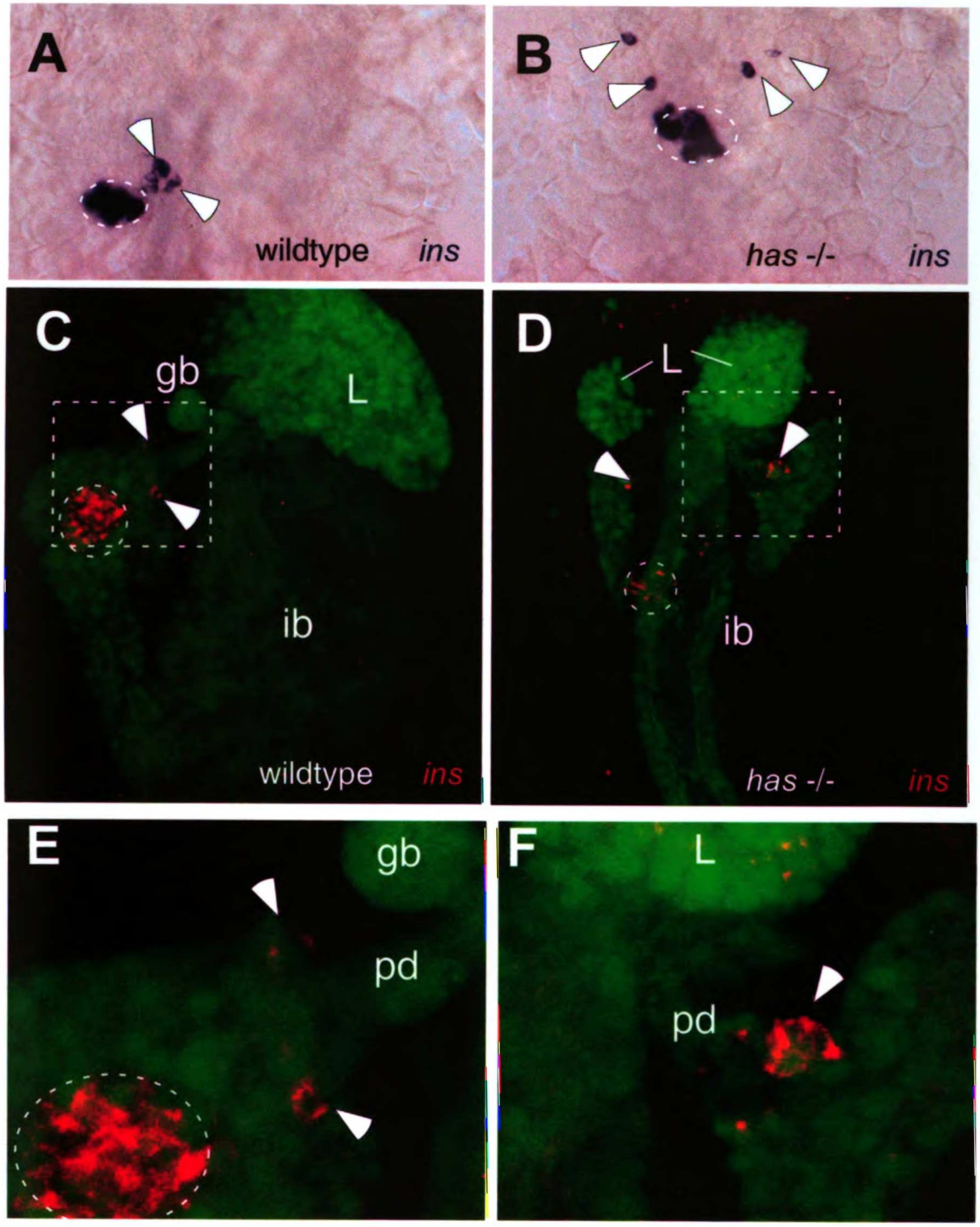

Figure 3.4. Insulin positive cells arise within the anterior pancreatic bud.

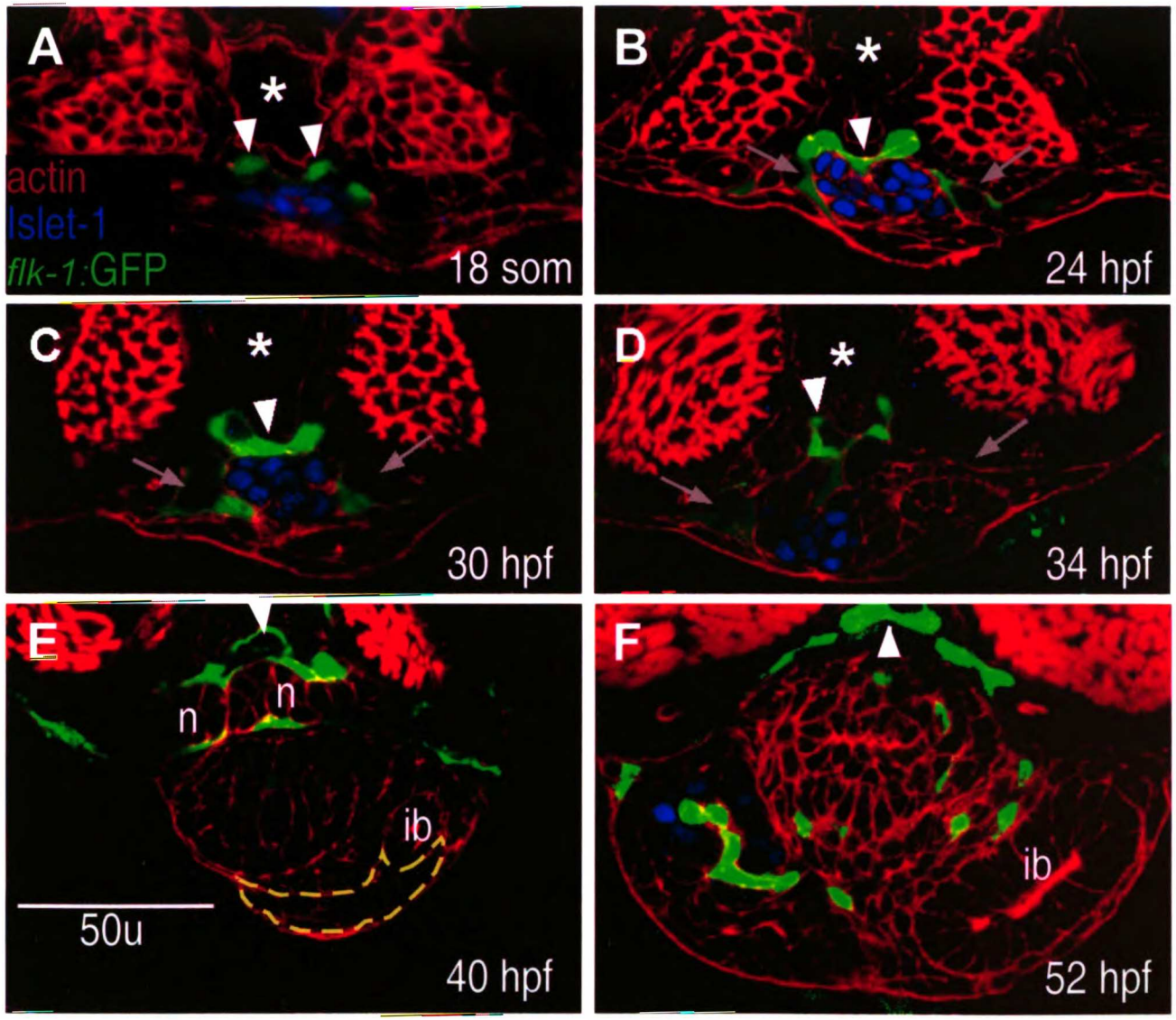

Figure 3.5. Vascular endothelium and pancreas development.

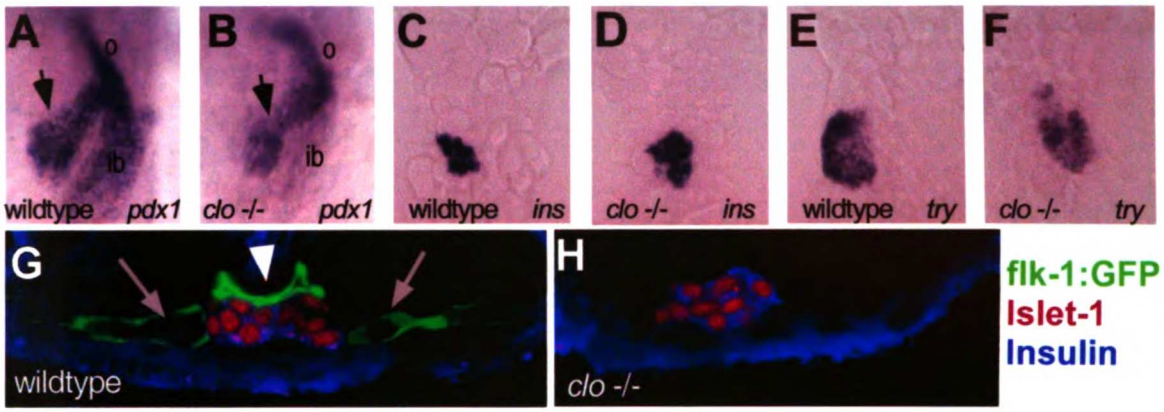

Figure 3.6. Vascular endothelium does not appear to be necessary for pancreas development.

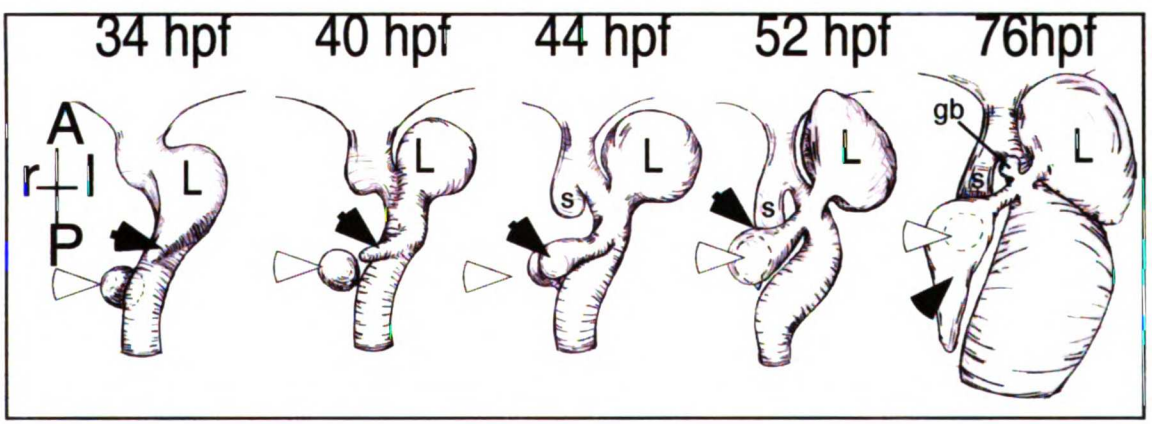

Figure 3.7. A new model of zebrafish pancreas development.

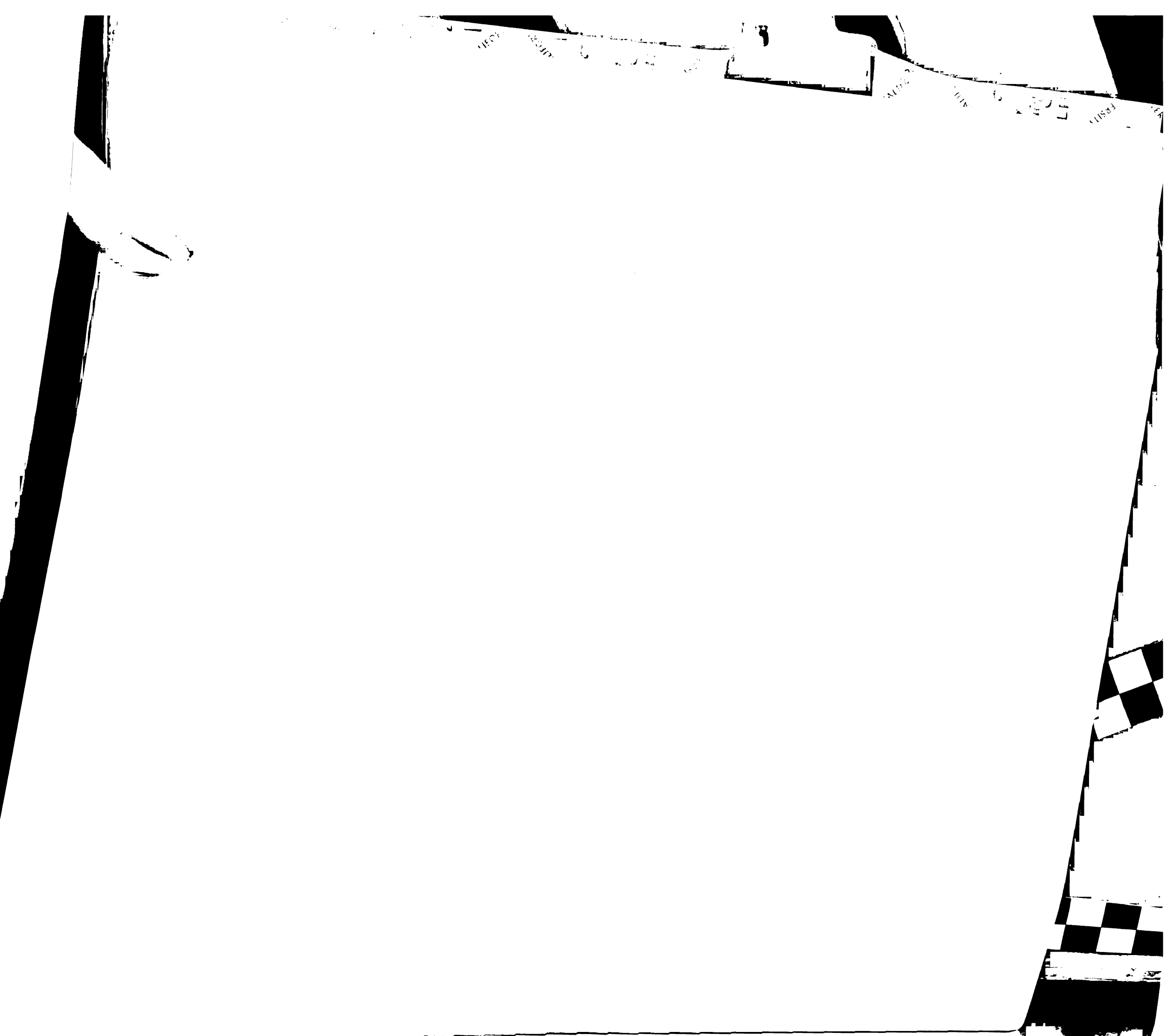

Appendix 1.

Future directions for wildtype liver development studies: formation of the bile drainage system

INTRODUCTION

Human bile consists of a number of compounds: bile salts formed primarily from cholic acid and chenodeoxycholic acid, bilirubin (bile pigment), lecithin and other phosopholipids, cholesterol and inorganic ions such as sodium, potassium, chloride and bicarbonate (Fox, 1996). Bile salts are amphipathic derivatives of cholesterol which form micelles in aqueous solution. Once secreted into the duodenum, these micelles assist in dissolving lipids to aid in digestion and absorption of fats. Bilirubin is a breakdown product of hemoglobin. Alone it is not very water soluble so it is carried in the blood bound to albumin. The liver has the capacity to extract free bilirubin from the blood and conjugate it with glucuronic acid, making it water soluble so it may be excreted through bile (Fox, 1996). Because bilirubin can not be filtered from the blood by the kidneys, if the liver is not functioning properly to remove it the bilirubin can accumulate in the blood causing jaundice (Fox, 1996).

The bile drainage system is made up of a hierarchy of channels through which bile flows and the gallbladder, an organ where bile is stored. Hepatocytes secrete the components of bile into bile canaliculi. Hepatocytes connected by tight junctions and desmosomes line the bile canaliculi and project microvilli into the small lumen. Canaliculi drain into slightly larger channels called choleangiols or bile ductules (Wilson et al., 1963). These small ducts in turn drain into intrahepatic bile ducts which follow the same tracks through the liver as branches of the portal vein. Intrahepatic bile ducts are

surrounded by connective tissue and a basement membrane (Wilson et al., 1963) which distinguishes them from ductules (small ducts) which appear epithelial in morphology but lack a basal lamina (Rocha et al., 1994). Bile exits the liver and is carried through the extrahepatic bile ducts to the gallbladder for storage. When a fatty meal is eaten, the small intestine releases the hormone Cholecystokinin (CCK) which stimulates contraction of the muscles around the gallbladder and release of bile into the alimentary canal via the sphincter of Oddi.

In mammals, all endodermally derived liver cells express cytokeratins no. 8 and no. 18, with heightened expression of no. 8 along the canalicular membrane (Van Eyken et al., 1988). In humans, bile duct cells express cytokeratins no. 7 and no. 19 in addition to no. 8 and no. 18, making them molecularly distinct from the hepatic parenchyme (Van Eyken et al., 1988). Another molecular difference between hepatocytes and bile duct cells is that the bilary epithelial cells express γ-glutamyl transpeptidase but lack glucose-6-phosphate activity (Arias et al., 1988).

There are multiple hypotheses in the literature concerning the origin of intrahepatic bile drainage system. One hypothesis is that the epithelial cells that form the intrahepatic bile ducts differentiate from hepatocytes (Van Eyken et al., 1988). This model is based on a time course of antibody staining against different cytokeratins on fixed sections. A subset of hepatocytes, all of which were observed to express cytokeratin no. 8, showed a gradual accumulation of bile duct cytokeratins (Van Eyken et al., 1988). These studies did not make any claims to the degree of hepatocyte differentiation at the time they started to acquire bilary epithelial identity, but simply stated that from a population of what appear to be homogenous cells all expressing

cytokeratin no.8, a subset of these gradually acquire additional cytokeratins, and only bile duct epithelium is observed later to express those additional cytokeratins.

An alternative hypothesis is that the intrahepatic bile ducts develop as a result of the morphogenesis of the developing hepatocytes: the hepatocytes migrate away from the developing intestine in tubes or 'cords', the lumen of which is the lumen of the intrahepatic bile duct (Vassy and Kraemer, 1993). Yet another speculation is that extrahepatic bile ducts, which have been suggested to develop from a different portion of the hepatic diverticulum than the rest of the endodermal liver components (Arias et al., 1988; Vassy and Kraemer, 1993), invade the liver parenchyme to form intrahepatic bile ducts. This is supported by the observation that differentiated intrahepatic bile ducts are first observed at the base of the liver, near where it connects to the extrahepatic bile duct, and over time appear in the liver as though radiating from this original location of invasion.

Understanding the relationship between hepatocytes and bile duct epithelium will be quite interesting. If hepatocytes, or perhaps a precursor cell, can give rise to bile duct cells, what are the stimuli controlling this transformation? Do hepatocytes generate more bile duct cells, or vice versa, during liver regeneration? If intrahepatic bile ducts are not derived from hepatocytes but are instead an outgrowth of extrahepatic bile ducts, what guides their pattern of invasion throughout the liver? Studies on the general development of the zebrafish liver have provided information, tools and techniques which will serve as a basis for studies in the zebrafish to address these questions.

Little has be done to study the development of bile ducts in fishes. Generally their presence has simply been noted (Gromon, 1982; Pack et al., 1996), although for

some species like the brown trout, *Salmo trutta fario*, there is a thorough description of the bilary tree in the adult (Rocha et al., 1994). In this study Rocha et al. observed the same levels of arborization in the biliary tree of the brown trout as it had been described in mammals. One major difference was the absence of microvilli in the smallest canaliculi of the trout liver. In the sea bream, *Sparus aurata*, bile canaliculi are thought to develop when hepatoblasts polarize and their apical sides converge at a single point. Vesicles are seen in the cytoplasm near this convergence point, and a day later. A small amount of information about the zebrafish liver can be gleaned from the transverse liver sections acquired in the Stainier Lab. Areas of heightened actin accumulation appear to be around a duct in the gutGFP line at 54 hpf (data not shown). However, the cells contributing to this organized actin accumulation do not have the pyramidal shape of cells developing into intrahepatic bile duct cells as described by Guyot et al. (Guyot et al., 1995), nor is there a lumen into which bile could drain. Perhaps these are the beginnings of bile canaliculi, or simply the first stage in intrahepatic bile duct formation.

FUTURE DIRECTIONS

In order to make any progress on developmental studies of bile ducts in the zebrafish, one would first need to establish a reliable molecular marker to distinguish differentiated duct cells from the other cells making up the liver. The obvious choice would be cytokeratins. To date, an acidic cytokeratin, type I, (zfCKI) and a basic cytokeratin, type II, (zfCKII) have been cloned from the zebrafish (Chua and Lim, 2000). Although cytokeratins no. 8 and no. 18, type II and type I cytokeratins respectively, have been detected in all endodermally derived liver cells (Van Eyken et al., 1988), it is unclear whether zfCKI and zfCKII will be broadly expressed throughout the liver or

restricted to a specific differentiated cell type. A number of antibodies are available against various mouse cytokeratins, however there is no published record of any being used successfully against a zebrafish antigen.

Once sufficient markers of biliary cells is established, the developmental timing of bile duct development would need to be established. The location of intrahepatic bile ducts with relation to the liver's vasculature would also be interesting to characterize as in most species studied, the bile ducts are seen to be associated with the location of blood vessels in the liver. Depending on timing, the endothelial cells may be following the bile duct system as they invade the liver, or perhaps intrahepatic bile ducts form after vascularization of the liver. Third, a study of the bile drainage system in zebrafish could look at the relationship between bile flow and differentiation or maintenance of the biliary epithelium.

The medical relevance of such studies is clear. For example, infants with biliary atresia exhibit obstruction and inflammation of the bile ducts leading to bile backing up into the liver and eventually to cirrhosis. Currently the cause of this disease is unknown and the only treatment of the disease is surgery (http://www.liverfoundation.org). Alagille syndrome is another disease characterized by a progressive loss of intrahepatic bile ducts in infants and subsequent shrinking of extrahepatic bile ducts (http://www.liverfoundation.org). Having a clear understanding bile duct differentiation and maintenance will shed light on the progression of these debilitating diseases. In addition, such studies will be generally relevant to the development and diseases of other ductal systems like those present in the pancreas, kidney and the reproductive tract.

REFERENCES

Arias, I. M., Jakoby, W. B., Popper, H., Schachter, D., and Shafritz, D. A. (1988). The Liver: Biology and Pathobiology. Raven Press, New York.

Chua, K. L., and Lim, T. M. (2000). Type I and type II cytokeratin cDNAs from the zebrafish (Danio rerio) and expression patterns during early development. *Differentiation* **66,** 31-41.

Fox, S. I. (1996). "Human Physiology." Times Mirror Higher Education Group, Inc., Dubuque, IA.

Gromon, D. B. (1982). "Histology of the Striped Bass."

Guyot, E., Diaz, J. P., and Connes, R. (1995). Organogenesis of the liver in sea bream. *The Fisheries Society of the British Isles* **47,** 427-37.

Pack, M., Solnica-Krezel, L., Malicki, J., Neuhauss, S. C., Schier, A. F., Stemple, D. L., Driever, W., and Fishman, M. C. (1996). Mutations affecting development of zebrafish digestive organs. *Development* **123,** 321-8.

Rocha, E., Monteiro, R. A. F., and Pereira, C. A. (1994). The liver of the brown trout, *Salmo trutta fario*: a light and electron microscope study. *J Anat* **185,** 241 - 249.

Van Eyken, P., Sciot, R., and Desmet, V. (1988). Intrahepatic bile duct development in the rat: a cytokeratin-immunohistochemical study. *Lab Invest* **59,** 52-9.

Vassy, J., and Kraemer, M. (1993). Fetal and Postnatal Growth. *In* "Molecular and Cell Biology of the Liver" (A. V. LeBouton, Ed.), pp. 265 - 307. CRC Press, Boca Raton, Florida.

Wilson, J. W., Groat, C. S., and Leduc, E. H. (1963). Histogenesis of the Liver. *Ann N Y Acad Sci* **111,** 8-24.

Appendix 2.

Initial observations of mutations affecting liver development

hhex

Introduction

Hex, also called *Prh*, is a divergent (ie. not clustered like Hox genes) homeobox gene. It was first isolated from hematopoietic tissue, which inspired its name (*h*ematopoietically *e*xpressed homeobo*x*). The expression of *Hex* homologues has been detected in a number of organisms including human, chicken, rat, mouse, Xenopus and zebrafish. Expression domains in mouse include expression in the anterior visceral endoderm (AVE), early angioblasts and endothelial cells (Thomas et al., 1998) as well as later expression in the thymus, pancreas, gallbladder, and bile duct (Bogue et al., 2000). Additionally, early expression in the AVE and later expression in the liver, thyroid and vasculature are controlled by distinct enhancer elements (Rodriguez et al., 2001). On the basis of these timing, location and control of these expression patterns, it was believed that *Hex* played a role in endodermal organ development.

A transgenic mouse mutant for the *Hex* gene was generated by replacing 1.3 kb of DNA – including the translational and transcriptional start sites, exon 1 and part of the first intron – with a neomycin cassette (Keng et al., 2000). Knocking out this gene lead to embryonic lethality by E12.5. At E8.5 the ventral foregut endoderm of *Hex* -/- embryos displayed no histological difference from wildtype siblings. However at E9.5, when liver bud formation was detected in wildtype siblings, Keng et al. detected only a "liver-like capsule structure" in *Hex* -/- embryos (Keng et al., 2000). This liver-like

structure was reduced in size compared to similarly aged siblings from E9.5 through E11.5, and normal perenchymal hepatocytes were not detected. The absence of apoptotic cells in the liver-like structure of *Hex* mutant mice indicates that the reduced size and apparent absence of hepatocytes is not due to cell death (Keng et al., 2000). In that same study, the absence of the hepatocyte marker *Albumin* by RT-PCR analysis at E8.5 lead to the conclusion that *Hex* is necessary for hepatocyte differentiation.

The zebrafish homologue of mouse Hex is Hhex. RNA expression domains in zebrafish are similar to those described for mouse. Initially *hhex* is expressed in the dorsal portion of the yolk syncytial layer (YSL) (Ho et al., 1999). Later in development, *hhex* expression is present in a number of organs including the liver, pancreas, thyroid, endothelial and blood lineages (Fig. A2.1) (Liao et al., 2000).

The zebrafish cyc^{b16} mutation is a deletion on the lower half of linkage group 12 that covers the *hhex* locus (Liao et al., 2000). Therefore, this deletion mutation can be used as a tool for investigating the role of Hhex in liver development.

Results and discussion

Crossing the cyc^{b16} mutation into the gutGFP transgenic background facilitated observations of endodermal morphology in the absence of *hhex*. Initial observations of the endoderm in embryos approximately 52 hours post fertilization (hpf) reveals a randomly looped dismorphic gut with a small liver that fails to complete budding from the developing intestine and does not appear to develop an extrahepatic bile duct (Fig. A2.2B). Anterior pancreatic bud development is also perturbed in these mutant embryos (Fig. A2.2B).

To insure that this endodermal phenotype was not due to the absence of functional Cyc, I also crossed the *cyc*^{m294} mutation into the gutGFP background for observation of the endoderm. The *m294* allele of *cyc* is a small ENU-induced mutation in the *cyc* gene which leads to cyclopia (Talbot et al., 1998). Embryos homozygous for the *cyc*^{m294} mutation were collected based on their cyclopic phenotype. The endoderm in these embryos, visualized using fluorescent microscopy, was indistinguishable from their wildtype siblings (Fig. A2.2C) indicating that the phenotype seen in embryos homozygous for the *cyc*^{b16} mutation is not due to the lack of Cyc.

To further support the supposition that the endodermal phenotype observed in embryos homozygous for the *cyc*^{b16} mutation is due to the absence of *hhex*, I injected a morpholino oligo (MO) against the translational start site of *hhex* mRNA into wildtype gutGFP embryos to specifically knock-down Hhex (for details on the morpholino, see Table A2.1). 0.5 ng of Hhex-MO injected at the one-cell stage lead to a phenocopy of the endodermal morphology observed in *cyc*^{b16} mutant embryos (Fig. A2.3). Upon injecting more than 0.5 ng per embryo, non-specific phenotypes were observed (data not shown).

As mentioned above, *hhex* is present at various locations in multiple developmental stages, including an early domain of expression in the YSL (Ho et al., 1999). Due to the close apposition of the YSL and the developing liver (Field et al., 2003) it is possible that Hhex in the YSL regulates a non-autonomous influence on liver development. Wallace et al. reported that when Hhex-MO is injected specifically into the YSL liver development is normal although gut looping becomes randomized (Wallace et al., 2001). These data in conjunction with expression patterns strongly suggest that *hhex* is acting autonomously in hepatocytes to direct liver morphogenesis.

Liver size in embryos lacking Hhex is noticeably smaller. In an attempt to quantitate the liver size difference observed between embryos lacking Hhex and their wildtype siblings, I calculated the size of Hhex-MO injected and wildtype livers at different developmental stages. This was achieved by photographing the endoderm of gutGFP wildtype embryos and siblings injected at the one-cell stage with 0.5 ng of Hhex-MO. The area of the livers in the resulting two-dimensional images was calculated by selecting all pixels that represent the liver, determining the conversion between a pixel and micrometers using a scale bar, then calculating the area of the liver by simple multiplication. This analysis shows that the liver in embryos lacking Hhex is significantly smaller than wildtype siblings of the same age (Fig. A2.4).

Based on observations of whole-mount embryos lacking Hhex outlined above, cells are present in the correct location to be hepatocytes, and liver budding morphogenesis appears to initiate but arrest. To determine the molecular identity of these Hhex -/- hepatocytes, I performed in situ hybridization on two genes known to be expressed in developing hepatocytes: *ceruloplasmin* (*cp*) and *prox1*. *cp* expression is clearly visible in wildtype siblings (Fig. A2.5A) while embryos homozygous for the cyc^{b16} mutation (identified by the presence of cyclopia, Fig. A2.5B) as well as embryos injected with Hhex-MO (data not shown) lack detectable expression in the liver. In contrast, *prox1* expression is present in both Hhex-MO injected embryos and wildtype siblings (Fig. A2.5C, D). Although preliminary, these data suggest that either Hhex is directly involved in the progression of hepatocyte differentiation, or Hhex is controlling genes necessary for normal liver morphogenesis in the absence of which hepatocytes do not receive the proper cues to continue differentiating.

In wildtype livers, laminin is deposited around the developing intestine but is absent from the perimeter of the liver when viewed in transverse section (Fig. A2.6A). Preliminary experiments were inconclusive in determining whether laminin was present or absent from the perimeter of the liver in embryos homozygous for the *cyc*^{b16} mutation (Fig. A2.6B). Laminin deposition was detected in embryos fixed overnight at 4oC with 4% PFA using a rabbit anti-laminin antibody (Sigma) diluted 1:25 in PBS with 0.1% TritonX and 2% sheep serum. Embryos were sectioned and visualized as described (Field et al., 2003).

Future directions

The primary role of Hhex in the liver is still unclear. Embryos lacking Hhex show small, dismorphic livers with at least some defect in normal hepatocyte gene expression. This suggest three avenues for investigation to identify the primary defect in Hhex-deficient livers: proliferation, morphogenesis and differentiation.

The first direction of study should be to compare the level of proliferation present in wildtype livers to that in the livers of embryos lacking Hhex. An rabbit antibody against phospho-Histone H3 (Upstate biotechnology) detects cells in mitosis. Used at a dilution of 1:1000 in PBS with 0.1% TritonX and 2% sheep serum, this antibody recognizes cells in whole-mount or sectioned zebrafish embryos fixed overnight at 4oC in 4% PFA. Since this antibody only recognizes cells actively in mitosis, BrdU incorporation may be a more effective way to detect proliferating cells in the liver. My attempts at BrdU incorporation and detection in the endoderm of embryos on ice at one to two days post fertilization were unsuccessful. However, optimization of the protocol is necessary before the success or failure of this method can be decided.

The second possible role of Hhex in liver development is morphogenesis. Based on new observations of the interactions between the lateral plate mesoderm and the budding liver (Horne-Badovinac, 2003), the most informative analysis of liver morphogenesis in embryos lacking Hhex would be a visual assessment of the interactions between the LPM and developing hepatocytes at different stages of liver budding.

To address Hhex's role in the third possibility, differentiation, a complete analysis of gene expression in embryos lacking Hhex should be performed. Preliminary results above show the presence of *prox1* expression and the absence of *cp* expression at single time-points in development. More genes expressed in the liver are currently available for *in situ* hybridization analysis in the zebrafish (see Table A2.1). These markers should also be analyzed to determine if Hhex is specifically involved in the expression of *cp*, or if Hhex has a broader role in hepatocyte development. Since Hhex-deficient livers appear similar to the size and morphology of wildtype livers at 30 hpf, it is possible that development up to that embryonic stage is normal, but without Hhex further development is arrested and hepatocytes may even begin to lose their molecular identity. For this reason, I suggest *in situ* analysis of liver-specific gene expression both before and after 30 hpf.

logelei^{s400}

A forward genetic screen performed in the Stainier lab resulted in a number of zebrafish lines containing interesting endodermal phenotypes. One of these lines, given the allele designation of s400, has an endodermal phenotype similar to that seen in embryos lacking Hhex (Fig. A2.7). Complementation testing between the *hhex* deletion

in the *cycb16* mutation and s400 showed that s400 is not an allele of *hhex*. Further complementation tests by Suk-Won Jin showed s400 was an allele of *logelei*. Initial mapping efforts using 141 embryos collected from the original pair isolated from the screen found s400 to be located between z24844 and z67731 on linkage group 9 (Fig. A2.8).

REFERENCES

Bogue, C. W., Ganea, G. R., Sturm, E., Ianucci, R., and Jacobs, H. C. (2000). Hex expression suggests a role in the development and function of organs derived from foregut endoderm. *Dev Dyn* **219,** 84-9.

Field, H. A., Ober, E. A., Roeser, T., and Stainier, D. Y. R. (2003). Formation of the digestive system in zebrafish. I. liver morphogenesis. *Developmental Biology* **253,** 279-290.

Ho, C. Y., Houart, C., Wilson, S. W., and Stainier, D. Y. (1999). A role for the extraembryonic yolk syncytial layer in patterning the zebrafish embryo suggested by properties of the hex gene. *Curr Biol* **9,** 1131-4.

Horne-Badovinac, S. (2003). Asymmetric LPM morphogenesis: the *heart and soul* of organ laterality in zebrafish. *In* "Department of Biochemistry and Biophysics", pp. 150. University of California, San Francisco, San Francisco.

Keng, V. W., Yagi, H., Ikawa, M., Nagano, T., Myint, Z., Yamada, K., Tanaka, T., Sato, A., Muramatsu, I., Okabe, M., Sato, M., and Noguchi, T. (2000). Homeobox gene Hex is essential for onset of mouse embryonic liver development and differentiation of the monocyte lineage. *Biochem Biophys Res Commun* **276,** 1155-61.

Liao, W., Ho, C. Y., Yan, Y. L., Postlethwait, J., and Stainier, D. Y. (2000). Hhex and scl function in parallel to regulate early endothelial and blood differentiation in zebrafish. *Development* **127,** 4303-13.

Rodriguez, T. A., Casey, E. S., Harland, R. M., Smith, J. C., and Beddington, R. S. (2001). Distinct enhancer elements control hex expression during gastrulation and early organogenesis. *Dev Biol* **234,** 304-16.

Talbot, W. S., Egan, E. S., Gates, M. A., Walker, C., Ullmann, B., Neuhauss, S. C., Kimmel, C. B., and Postlethwait, J. H. (1998). Genetic analysis of chromosomal rearrangements in the cyclops region of the zebrafish genome. *Genetics* **148,** 373-80.

Thomas, P. Q., Brown, A., and Beddington, R. S. (1998). Hex: a homeobox gene revealing peri-implantation asymmetry in the mouse embryo and an early transient marker of endothelial cell precursors. *Development* **125,** 85-94.

Wallace, K. N., Yusuff, S., Sonntag, J. M., Chin, A. J., and Pack, M. (2001). Zebrafish hhex regulates liver development and digestive organ chirality. *Genesis* **30,** 141-3.

FIGURE LEGENDS

Fig. A2.1. *hhex* expression in wildtype embryos. At the 18 somite stage (A) and at the 27 somite stage (B), it is difficult to distinguish the identity of the cells expressing *hhex* as endodermal or endothelial without additional cell identity markers. By 24 hpf (C) and at 30 hpf (D), *hhex* expression is clearly present in the endoderm that giving rise to the liver (arrow) and the posterior pancreatic bud (asterisk). (E) By 48 hpf, *hhex* expression is present in a subset of pancreatic cells (asterisk). Liver expression starts to heighten at the posterior end liver (arrow). (F) At 52 hpf, the liver (arrow) and pancreas (asterisk) maintain a low level of *hhex* expression, while what appears to be the bile duct and cells that will give rise to the gallbladder have a heightened level of expression.

Fig. A2.2. A defect in *cyc* is not responsible for the endodermal phenotype in *cycb16* mutant embryos. The cyc^{b16} mutation is a deletion that covers the *hhex* locus. Compared to their wildtype siblings (A), embryos homozygous for the cyc^{b16} mutation (B) show defects in gut looping and liver budding (arrow). (C) Embryos homozygous for the *m294* allele of *cyc* do not show the same endodermal phenotypes as seen in embryos homozygous for the cyc^{b16} mutation, indicating that the endodermal phenotype is not due to a lack of functional Cyc.

Fig. A2.3. Hhex-MO injection phenocopies the endodermal defect seen in cyc^{b16} mutant embryos. Embryos injected with 0.5 ng of Hhex-MO at the one cell stage (C) have a small liver (arrow) that fails to complete budding. The phenotype observed in these

embryos falls within the normal variation of phenotypes observed in embryos homozygous for the *cyc*^{b16} mutation (B).

Fig. A2.4. Quantitation of liver size defect in Hhex-MO injected embryos. Wildtype embryos aged 32 hpf have a normal liver size of approximately 6,000 μm^2. Liver size in wildtype embryos does not vary significantly between 32 hpf and 36 hpf. By 50 hpf, wildtype liver size has increased to approximately 12,500 μm^2. At 36 hpf, embryos injected with 0.5 ng of Hhex-MO have livers that measure approximately 3,000 μm^2, significantly smaller than their wildtype siblings of the same age. The liver size in embryos injected with Hhex-MO does not change significantly from 36 hpf to 50 hpf as did their wildtype siblings.

Fig. A2.5. *in situ* hybridization of *cp* (A and B) and *prox1* (C and D) in embryos lacking Hhex and their wildtype siblings. (A, B) At 36 hpf, *cp* expression in the liver is strong in wildtype embryos (A, arrow) but absent from the same region in embryos homozygous for the *cyc*^{b16} mutation (B). (C, D) Although the domain of *prox1* expression at 40 hpf is smaller in Hhex-MO injected embryos (D, arrow) than in their wildtype siblings (C, arrow), the level of expression is comparable.

Fig. A2.6. The presence of laminin around the liver perimeter of embryos lacking Hhex is debatable. (A) In transverse sections of wildtype embryos at 40 hpf, laminin (red) encases the developing intestine (i) but is absent from the perimeter of the liver (L). (B) Embryos homozygous for the *cyc*^{b16} mutation and thus lacking Hhex, may have laminin

around the perimeter of the liver (arrows). There is not as much laminin around the liver as is present around the developing intestine (i), but there does appear to be some laminin around the liver in these embryos. s, somite; nt, neural tube. Dorsal is to the top and left is to the reader's right.

Fig. A2.7. Morphology of endoderm in embryos homozygous for the s400 mutation resembles that in embryos lacking Hhex. At 52 hpf, the endodermal phenotype of embryos homozygous for the s400 mutation isolated in the "Liver plus" screen (B) is very similar to that seen in embryos homozygous for the *cyc*^{b16} mutation.

Fig. A2.8. s400 maps between z24844 and z67731 on LG9; approximately 1.06cM distal to z24844 and 12.8cM proximal to z67731. (A) Initial efforts to positionally clone the s400 mutation used DNA from 141 embryos. These embryos were collected from the pair of adults isolated from F2 families used in the "Liver plus" screen as carriers of the s400 mutation. Both mutant and wildtype embryos were collected and analyzed for the presence of linked polymorphic alleles of various z-markers. (B) Initial linkage was found to a size polymorphism at z1273 on LG9, where all but 6 mutant embryos tested were homozygous for the linked allele. Of the 6 embryos that were heterozygous for this z-marker polymorphism, three reverted to homozygous linked at z24844, leaving only 3 mutant embryos heterozygous for this z-marker polymorphism. This calculates to a rough distance of 1.06cM between z24844 and the s400 mutation. All three of these embryos became homozygous for the linked allele at z67731. 30 mutant embryos, different from those discussed above, were heterozygous for the z67731 polymorphism,

and 3 additional mutant embryos were homozygous for the unlinked allele. All 33 of these embryos were homozygous for the linked allele at z1273. This places the s400 mutation between z24844 and z67731 on LG9.

Table A2.1. Reagents useful in the study of Hhex and its role in liver development.

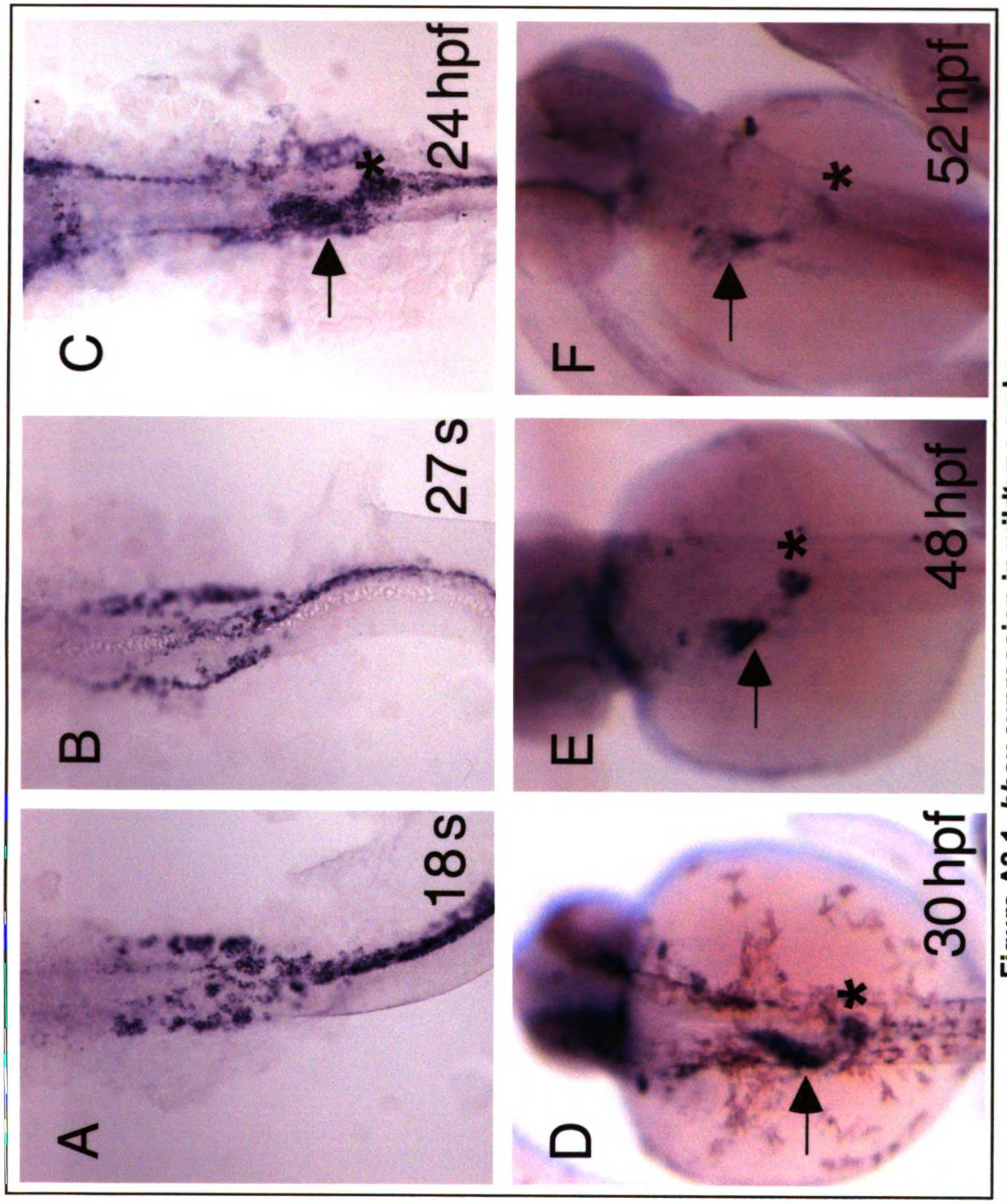

Figure A2.1. *hhex* expression in wildtype embryos.

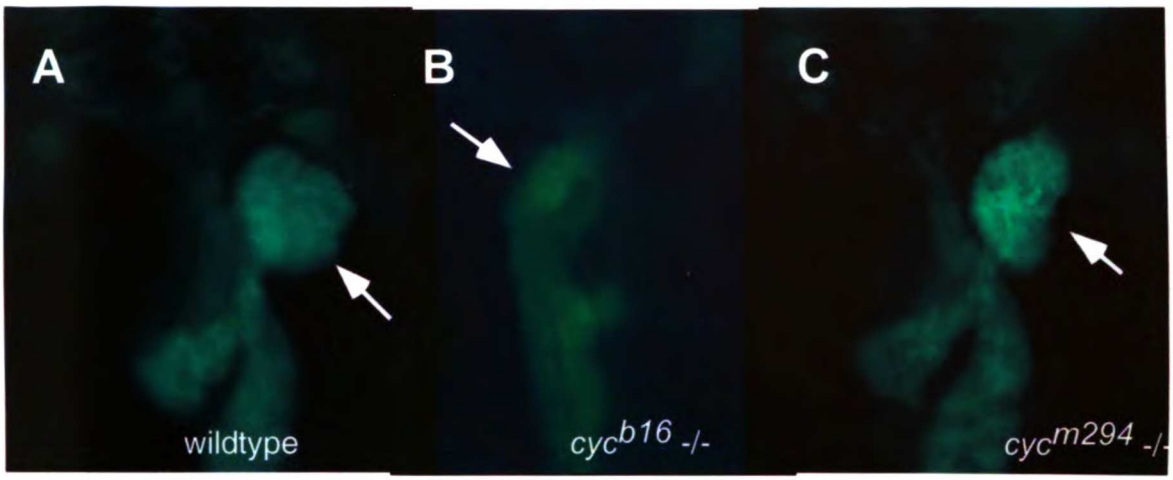

Figure A2.2. A defect in *cyc* is not responsible for the endodermal phenotype in *cyc*^{b16} mutant embryos.

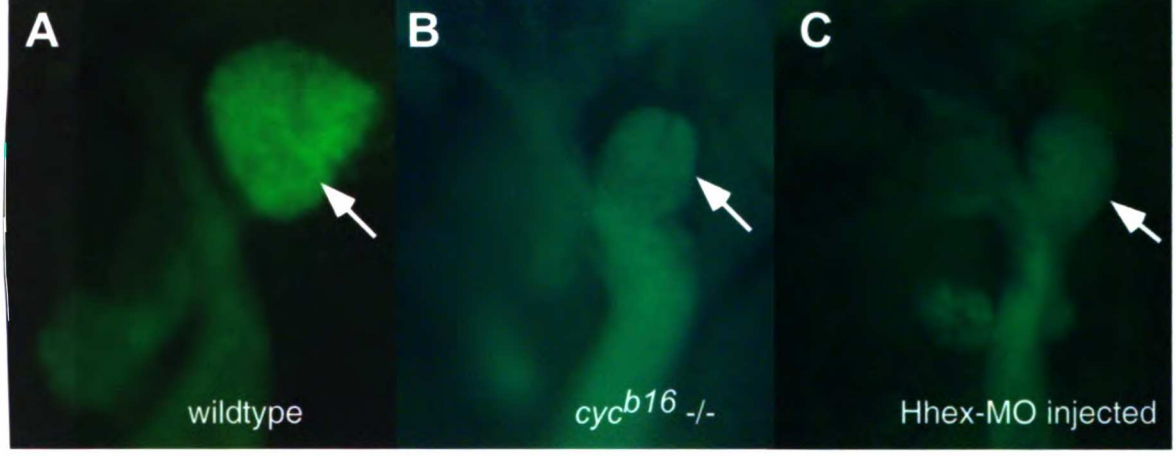

Figure A2.3. Hhex-MO phenocopies the endodermal defect seen in *cyc*^{b16} mutant embryos.

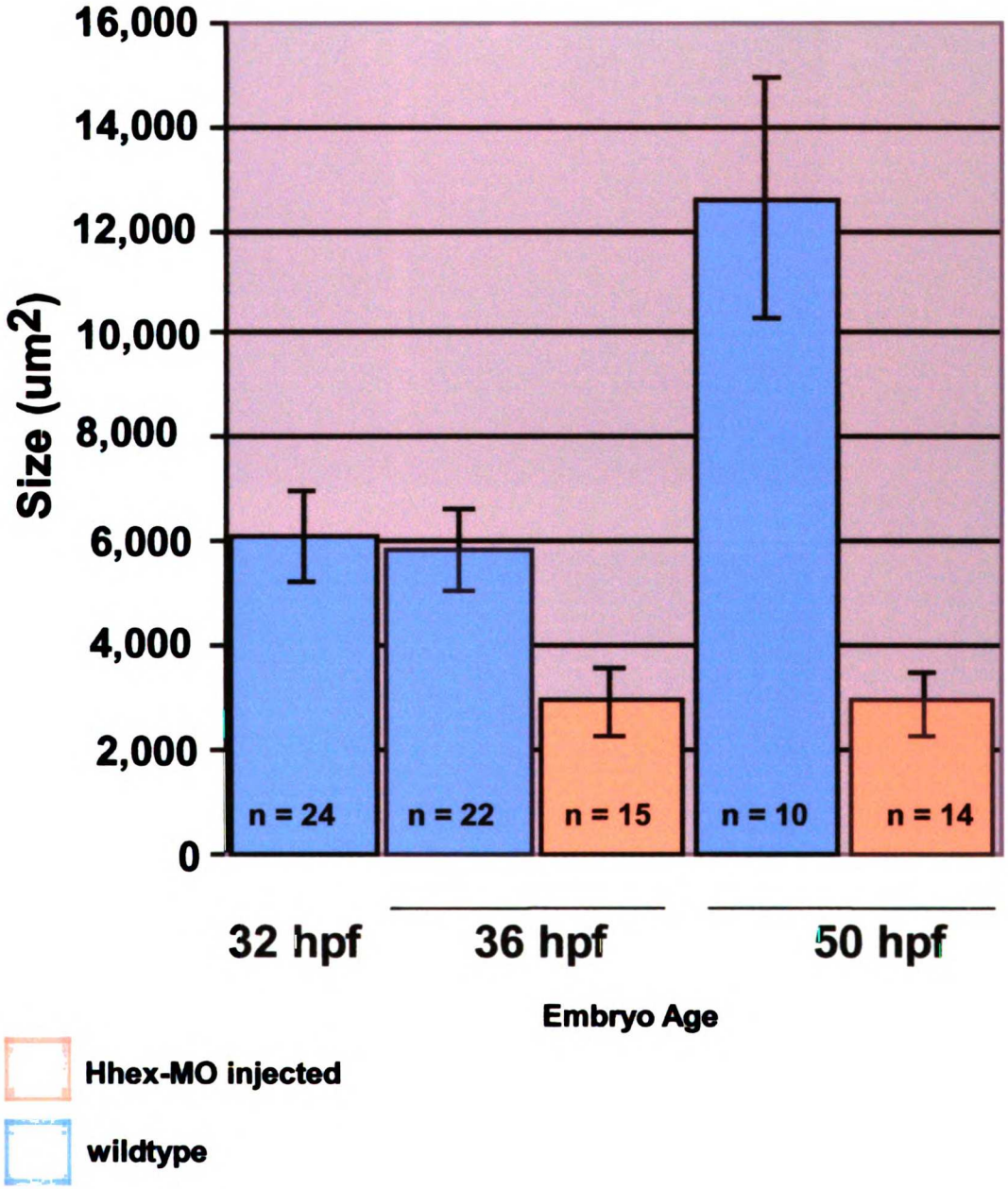

Figure A2.4. Quantitation of liver size defect in Hhex-MO injected embryos.

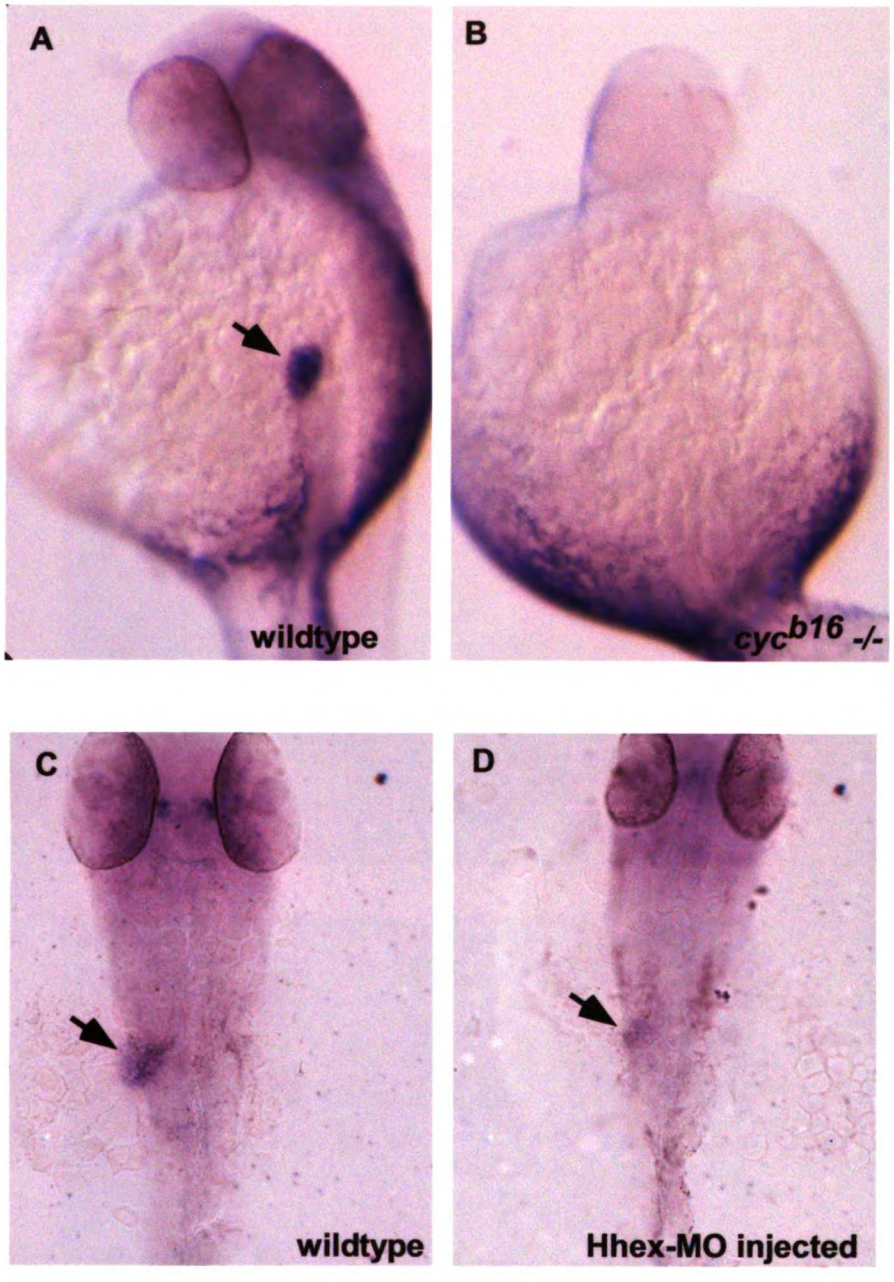

Figure A2.5. *in situ* hybridization of *cp* (A and B) and *prox1* (C and D) in embryos lacking Hhex and their wildtype siblings.

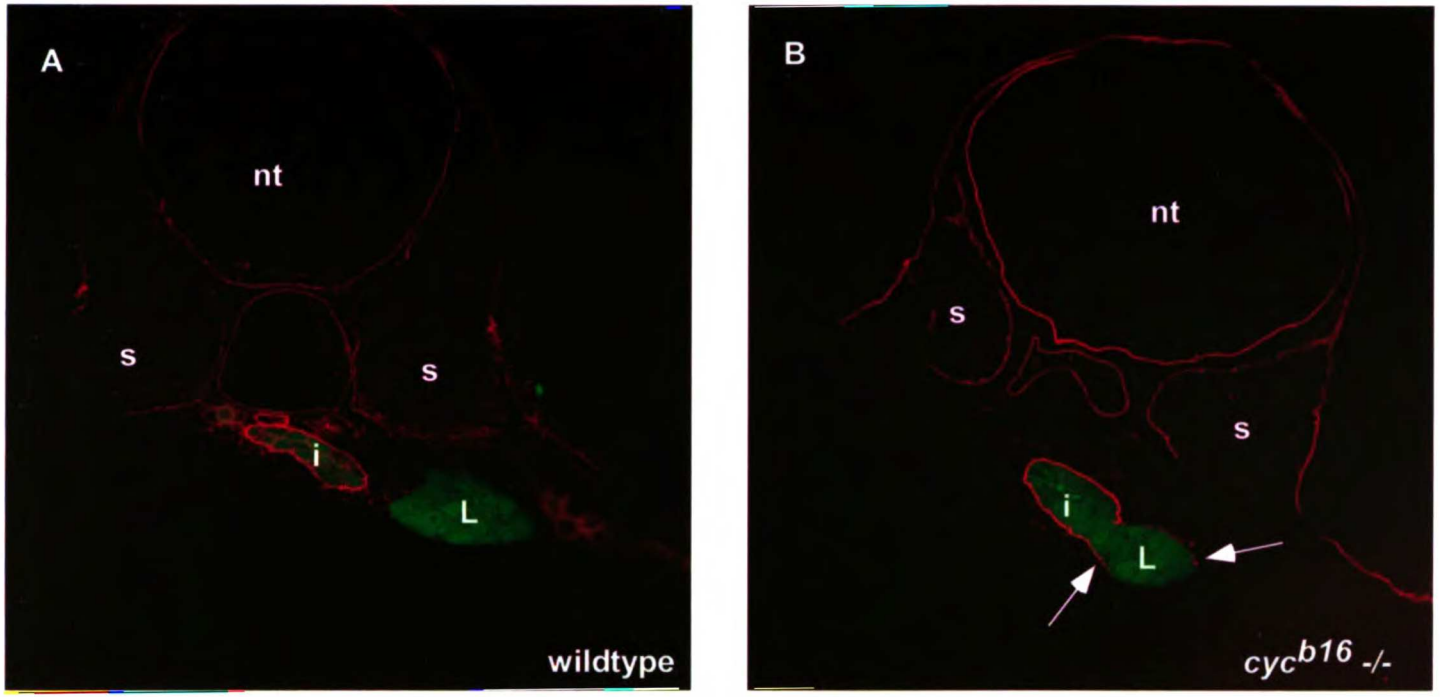

Figure A2.6. The presence of laminin around the liver perimeter of embryos lacking Hhex is debatable.

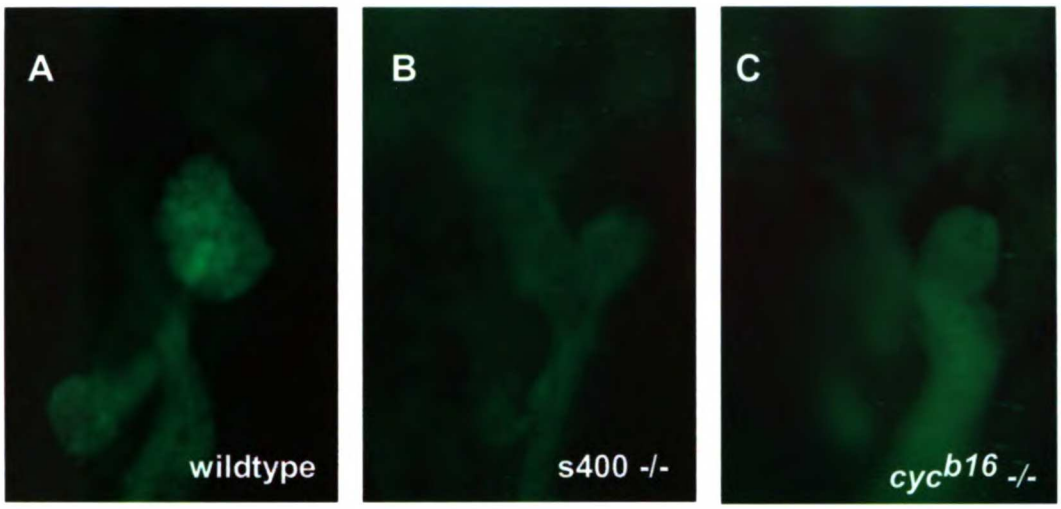

Figure A2.7. Morphology of endoderm in embryos homozygous for the s400 mutation resembles that in embryos lacking Hhex.

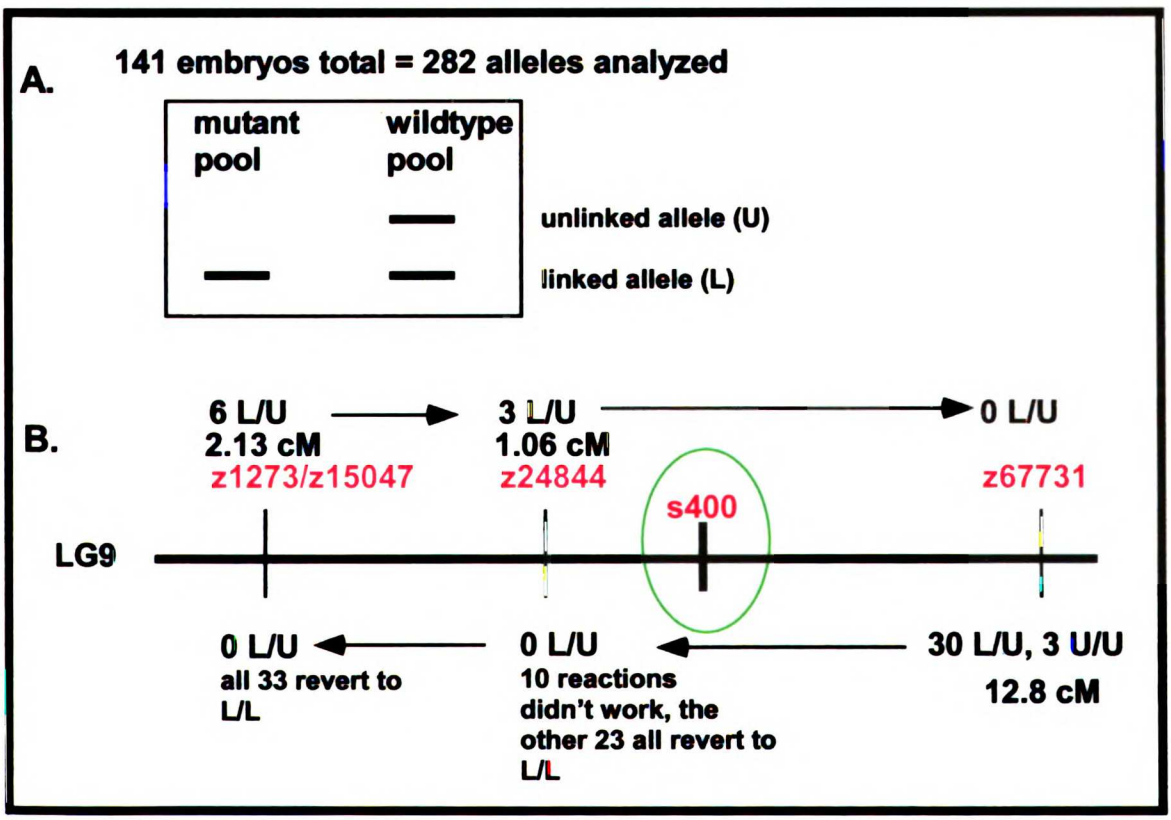

Figure A2.8. s400 maps between z24844 and z67731 on LG9; approximately 1.06cM distal to z24844 and 12.8cM proximal to z67731.

Table A2.1. Reagents useful in the study of Hhex and its role in liver development.

in situ Probes

pHexGII. Hhex cDNA cloned into the EcoRI site of pGEM-T by Chi-Yip Ho while in the Stainier Lab. Antisense promoter, sp6; antisense enzyme, NcoI.

Other useful plasmids

pcs2:Hhex. The *hhex* expression plasmid (previously called pcs2(+) pHexGII). Sense promoter, sp6; sense enzyme, Apa1.

hex:GFP. Hex promoter and enhancers driving GFP in a puc31 backbone from Rodriquez et al. (2001) Dev Biol. 234, 304-316.

pCS2(+) Cyclops. *Cyclops* orf in pCS2(+) from Michael Rebagliati. Sense promoter, sp6; sense enzyme, NotI. Can be used to inject as DNA or to make mRNA.

Appendix 3.

The role of Islet proteins in the lateral plate mesoderm

INTRODUCTION

Islet is one of the original members of the LIM homeodomain protein family. (LIM stands for lin-11, isl-1, and mec-3). All members of this family contain a cystein-histidine-rich domain called the LIM domain (Dawid et al., 1998). Islet proteins have been found in a number of organisms. The mouse genome contains two known Islet paralogs, Isl1 (Karlsson et al., 1990) and Isl2 (Kawai et al., 2001), while the zebrafish genome contains at least three, *isl-1* (Inoue et al., 1994), *isl-2* and *isl-3* (Tokumoto et al., 1995). In zebrafish, expression analyses have focused on neuronal expression (Inoue et al., 1994; Tokumoto et al., 1995). However, expression of Isl1 in chick has been reported in the endoderm, with expressing cells contributing to the oral membrane, thyroid, branchial pouches and branchial grooves (Yuan and Schoenwolf, 2000). Isl-1 is also expressed in the splanchnic mesoderm and caudal lateral plate mesoderm (LPM) bilaterally before gut rotation, and becomes restricted to mesoderm on the embryos left, along the outer curvature of the prospective caudal stomach/rostral duodenum after gut looping (Yuan and Schoenwolf, 2000). In mouse, ISL1 protein is present bilaterally in the mesodermal mesenchymal cells around the dorsal, but not the ventral, pancreatic bud (Ahlgren et al., 1997). Additionally, Isl1 expression is initiated in all four classes of pancreatic endocrine cells after they have left the cell cycle (Ahlgren et al., 1997).

In ISL1-mutant mouse embryos, the lack of ISL1 has both an autonomous affect on endocrine cell differentiation as well as a non-autonomous effect on dorsal exocrine

cells which can be rescued *in vitro* by supplying wildtype mesodermal mesenchyme, results consistent with the domains of Isl1 expression (Ahlgren et al., 1997). The function of ISL1 in the mesodermal mesenchyme is not clear, nor is the pathway through which this LIM protein functions.

RESULTS AND DISCUSSION

An antibody generated against the c-terminus of mouse ISL1 (39.4D5 from Developmental Studies Hybridoma Bank) cross-reacts with a protein in zebrafish displaying a localization pattern expected for the zebrafish Islet proteins. In a whole-mount embryo, fixed for two hours at room temperature in 3.7% Formaldehyde in PEM (0.1M Pipes, 1.0mM $MgSO_4$, 2mM EGTA, pH to 7 with NaOH), this anit-ISL1 antibody stains neuronal tissue, the dorsal pancreatic bud, and the lateral plate mesoderm posterior to the pharyngeal endoderm and anterior to the dorsal pancreatic bud (data not shown). Visualization of anti-ISL1 immunohistochemistry in transverse section clearly shows the presence of the cross-reacting protein in both the left and the right LPM as well as the endocrine cells making up the posterior pancreatic bud (Fig. A3.1).

Due to the similarity between mouse ISL1 c-terminus and the c-terminal regions of the zebrafish Islet proteins (Fig.A3.2), it was not clear which Islet protein was cross-reacting with the mouse anti-ISL1 antibody. To define the specific expression domains for each of the zebrafish *isl* genes and thus determine which Islet was being detected by the mouse antibody, I performed *in situ* hybridization to detect mRNA expression for all three *islet* genes. Three RNA probes were used, each designed to recognize only one of the *islet* paralogs (for specifics on the probes, see Table A3.1).

Endodermal expression of *isl1* has been previously described (Biemar et al., 2001). Endodermal expression initiates in bilateral patches of cells at the 12 somite stage. The expression domain condenses at the midline and is subsequently found in the dorsal cluster of cells that comprise the posterior pancreatic bud. This posterior pancreatic bud expression of *isl1* persists, while in the LPM expression is clear by 30 hpf but is not present at 22 hpf (Fig. A3.3A, D). *isl2* and *isl3* both initiate LPM localized expression by 22 hpf, but neither are expressed in the endoderm of the posterior pancreatic bud (Fig A3.3B, C). By 30 hpf tissue migration has resulted in the left and right LPM overlapping at the midline with the left LPM dorsal to the right LPM (Horne-Badovinac et al., 2003). At 30 hpf the LPM expression domains of the three *islet* genes are similar but distinct (Fig. A3.3D-F).

Due to the overlap of the left and right LPM and the fact that the sheets of LPM are folded back on themselves into a "U" shape creating two cell layers of polarized epithelium (Horne-Badovinac et al., 2003), whole-mount *in situ* hybridization does not give a clear understanding of the exact expression domains. The distinct patterns of expression observed for each gene is most-likely due to unique medial/lateral position of expression domains within the LPM (Fig. A3.3G-I).

To determine whether the endoderm influenced LPM expression of any of the *islet* genes, *in situ* hybridization of *islet* mRNA was performed on embryos homozygous for *cas*^{ta56}, a mutation which results in a near absence of endodermal cells (Alexander et al., 1999; Kikuchi et al., 2001). Embryos homozygous for the *cas*^{ta56} mutation were identified by the presence of cardio bifida. Endodermal *isl1* expression was predictably absent since these mutant embryos lack endoderm (Fig. A3.4B). In addition, 21 of the 25

mutant embryos lacked *isl1* expression in the LPM (Fig. A3.4B), with the remaining 4 of the 25 embryos showing a severe reduction in the level of expression (data not shown). In 22 of the 24 *cas* mutant embryos stained for *isl2*, expression was consistently reduced as compared to wildtype siblings (Fig. A3.4C, D). The level of *isl3* staining in the LPM of *cas* mutant embryos varied in comparison with their wildtype siblings. Seventeen of the 25 embryos assayed had a variable reduction in *isl3* levels, although none showed a complete absence of expression. These data suggest that the expression of each *islet* gene is controlled differently by the presence of endoderm.

FUTURE DIRECTIONS

To localize the expression of each *islet* gene within the LPM will require analysis on transverse sections. Transverse sections of whole-mount *in situ* hybridized embryos embedded in JB-4 plastic was inconclusive due to bleeding of the stain used to detect the probe (data not shown). Fluorescent *in situ* techniques should be employed on transverse sections to give interpretable results.

The localization of *islet* expression specifically around the region of the gut that loops suggests a role for one or multiple Islet proteins in looping and/or organ development. To test this hypothesis, dominant negative and morpholino knock-down experiments should be performed. Dr. Hitoshi Okamoto generously contributed constructs containing the LIM domains of each zebrafish *islet* gene (see Table A3.1) (Kikuchi et al., 1997; Segawa et al., 2001). Injecting these constructs at the one cell stage results in neuronal defects consistent with a dominant negative affect on Islet function (Kikuchi et al., 1997). These constructs should be used to block Islet activity so the function of each of these proteins in the LPM can be determined. Due to their similarity,

it is possible that one Islet could act redundantly in the absence of another. To rule out this possibility, the LIM constructs should be injected in all possible combinations. Both the endoderm and the LPM should be examined for developmental defects since it is not yet clear whether the primary role of Islet proteins in the LPM is autonomous to LPM development and morphogenesis, or if they are controlling a non-autonomous cascade that acts on the endoderm.

Morpholino oligos directed against *isl1* and *isl2* mRNA have been used successfully to generate neuronal phenotypes (Segawa et al., 2001). These morpholinos (see Table A3.1) should be used in addition to the dominant negative constructs to assess the role of each Islet protein by assaying the development of the endoderm and LPM in their absence.

REFERENCES

Ahlgren, U., Pfaff, S. L., Jessell, T. M., Edlund, T., and Edlund, H. (1997). Independent requirement for ISL1 in formation of pancreatic mesenchyme and islet cells. *Nature* **385,** 257-60.

Alexander, J., Rothenberg, M., Henry, G. L., and Stainier, D. Y. (1999). casanova plays an early and essential role in endoderm formation in zebrafish. *Dev Biol* **215,** 343-57.

Biemar, F., Argenton, F., Schmidtke, R., Epperlein, S., Peers, B., and Driever, W. (2001). Pancreas development in zebrafish: early dispersed appearance of endocrine hormone expressing cells and their convergence to form the definitive islet. *Dev Biol* **230,** 189-203.

Dawid, I. B., Breen, J. J., and Toyama, R. (1998). LIM domains: multiple roles as adapters and functional modifiers in protein interactions. *Trends Genet* **14,** 156-62.

Horne-Badovinac, S., Rebagliati, M., and Stainier, D. Y. (2003). A cellular framework for gut-looping morphogenesis in zebrafish. *Science* **302,** 662-5.

Inoue, A., Takahashi, M., Hatta, K., Hotta, Y., and Okamoto, H. (1994). Developmental regulation of islet-1 mRNA expression during neuronal differentiation in embryonic zebrafish. *Dev Dyn* **199,** 1-11.

Karlsson, O., Thor, S., Norberg, T., Ohlsson, H., and Edlund, T. (1990). Insulin gene enhancer binding protein Isl-1 is a member of a novel class of proteins containing both a homeo- and a Cys-His domain. *Nature* **344,** 879-82.

Kawai, J., Shinagawa, A., Shibata, K., et. al. (2001). Functional annotation of a full-length mouse cDNA collection. *Nature* **409,** 685-90.

Kikuchi, Y., Agathon, A., Alexander, J., Thisse, C., Waldron, S., Yelon, D., Thisse, B., and Stainier, D. Y. (2001). casanova encodes a novel Sox-related protein necessary and sufficient for early endoderm formation in zebrafish. *Genes Dev* **15,** 1493-505.

Kikuchi, Y., Segawa, H., Tokumoto, M., Tsubokawa, T., Hotta, Y., Uyemura, K., and Okamoto, H. (1997). Ocular and cerebellar defects in zebrafish induced by overexpression of the LIM domains of the islet-3 LIM/homeodomain protein. *Neuron* **18,** 369-82.

Segawa, H., Miyashita, T., Hirate, Y., Higashijima, S., Chino, N., Uyemura, K., Kikuchi, Y., and Okamoto, H. (2001). Functional repression of Islet-2 by disruption of

complex with Ldb impairs peripheral axonal outgrowth in embryonic zebrafish. *Neuron* **30,** 423-36.

Tokumoto, M., Gong, Z., Tsubokawa, T., Hew, C. L., Uyemura, K., Hotta, Y., and Okamoto, H. (1995). Molecular heterogeneity among primary motoneurons and within myotomes revealed by the differential mRNA expression of novel islet-1 homologs in embryonic zebrafish. *Dev Biol* **171,** 578-89.

Yuan, S., and Schoenwolf, G. C. (2000). Islet-1 marks the early heart rudiments and is asymmetrically expressed during early rotation of the foregut in the chick embryo. *Anat Rec* **260,** 204-7.

FIGURE LEGENDS

Fig. A3.1. Mouse anti-ISL1antibody staining in transverse sections of zebrafish. This antibody recognizes an antigen that is distributed in a pattern expected for the zebrafish Islet protein. At each stage depicted, images to the left are from more anterior regions in the embryo than those to the right. For all images, dorsal is to the top and left is to the reader's right. (A-C) At 30 hpf, the antibody stains neurons within the neural tube (nt) and cells within both the left and right LPM (A, B, arrows). Only the tall, columnar cells of the LPM seem to be staining. The antibody also recognizes pancreatic endocrine cells of the posterior pancreatic bud (C, asterisk). (D-F) At 36 hpf, staining is still present in the left and right LPM (D, E, arrows) which by this time have migrated over one another. Cells of the LPM adjacent to the developing anterior pancreatic bud (ab) are detected by the antibody (E), as are cells in the posterior pancreatic bud (F, asterisk). (G, H) At 40 hpf the epithelium of the LPM is starting to break down. (G) Staining is not obvious in the cells derived from the LPM that are adjacent to the developing anterior pancreatic bud (ab). (H) Staining is still present in the posterior pancreatic bud (asterisk). (I) Mesodermal mesenchyme surrounding the swim bladder (sb) stain with the anit-ISL1 antibody (arrow). Due to leftward gut looping, these cells all fall to the right side of the intestinal bulb (ib). (J) The pancreatic endocrine cells (asterisk) from the posterior pancreatic bud are still staining with the antibody at 52 hpf.

Fig. A3.2. The C-termini of the mouse ISL1 and the three zebrafish Islet proteins share similar amino acid motifs. Portions of the amino acid sequence close to and at the c-

terminus of mouse ISL1 are nearly identical to the same regions in all three of the zebrafish Isl proteins.

Fig. A3.3. Actual whole-mount mRNA expression patterns (A-F; ventral views, anterior to the top), and speculated transverse expression domains (G-H; dorsal to the top, the embryos left is to the readers right to maintain consistency with the whole-mount views), for *isl1*, *isl2* and *isl3*. (A-C) At 22 hpf, the expression domains of each zebrafish *isl* gene is distinct. (A) *isl1* is expressed within the cells that make up the posterior pancreatic bud (arrow) but LPM expression is not yet detectable. (B) *isl2* expression has initiated in the LPM (brackets). Since the left and right LPM are still lateral to the endoderm, expression appears as two stripes. (C) *isl3* expression has also initiated in the left and right LPM by 22 hpf (brackets). Expression appears as two bilateral stripes. (D-F) By 30 hpf all three *isl* genes are expressed in the LPM, but their expression patterns are unique. (D) *isl1* expression in the LPM (brackets) appears to be restricted to the embryos left. Upon close inspection, this expression domain is found to be in both the left and right LPM. The appearance of a left-only expression domain is likely due to the medial/lateral restriction of *isl1* expression within the left and right LPM. (E) *isl2* expression in the LPM at 30 hpf (brackets) also appears to be restricted to the embryos left, although the domain of expression has a two distinct patches, the right patch being slightly more anterior than the left, and the left patch stretching more posterior than the right. (F) *isl3* expression in the LPM (brackets) appears as one patch located at the embryos midline. The speculated patterns of *isl1* (G), *isl2* (H) and *isl3* (I) within the LPM are represented by cartoons of a

transverse section through the region of LPM expression. Endoderm is depicted in green, the LPM in red, and *isl* expression in blue. L, liver.

Fig. A3.4. The absence of endoderm perturbs LPM expression of each islet gene to different degrees. Whole-mount *in situ* hybridization of *isl1* (A, B), *isl2* (C, D) and *isl3* (E, F) at 28 hpf. Left dorso-lateral views, anterior to the top. (A) Both the LPM (arrow) and posterior pancreatic bud (pp) domains of *isl1* expression seen in wildtype embryos is lost in embryos lacking endoderm (B). (D) *isl2* expression in the LPM is severely reduced in the absence of endoderm, as compared to wildtype siblings (C). (F) *isl3* expression is somewhat reduced in embryos lacking endoderm, but of all the *isl* genes, it is the least severely affected by the lack of endoderm.

Table A3.1. Reagents for use in the study of Islet activity in the LPM.

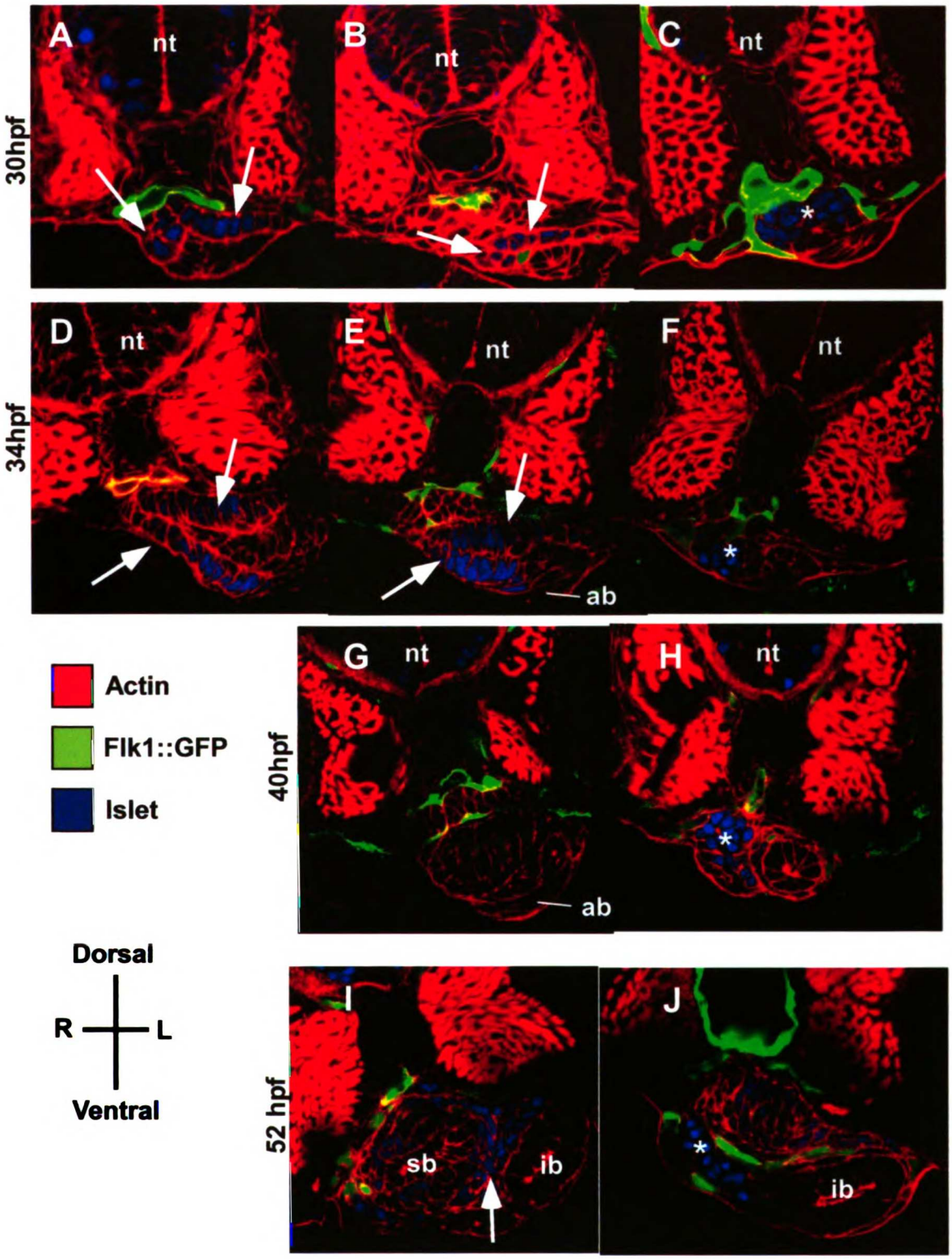

Figure A3.1. Mouse anti-ISL1 antibody staining in transverse sections of zebrafish.

```
Islet1_mouse     - MKQLQQQQ --- SSQLPDTPNSMVASPIEA  cterm
Islet1_zfish     - MKQLQQQQ --- SSQLPDTPNSMVASPIEA  cterm
Islet2_zfish     - MKQLQQQQ --- SSQLPDTPNSMVPSPVET  cterm
Islet3_zfish     - MKQLQQQ  --- SSQLPDTPNSMVPSPVET  cterm
```

Figure A3.2. The C-termini of the mouse ISL1 and the three zebrafish Islet proteins share similar amino acid motifs.

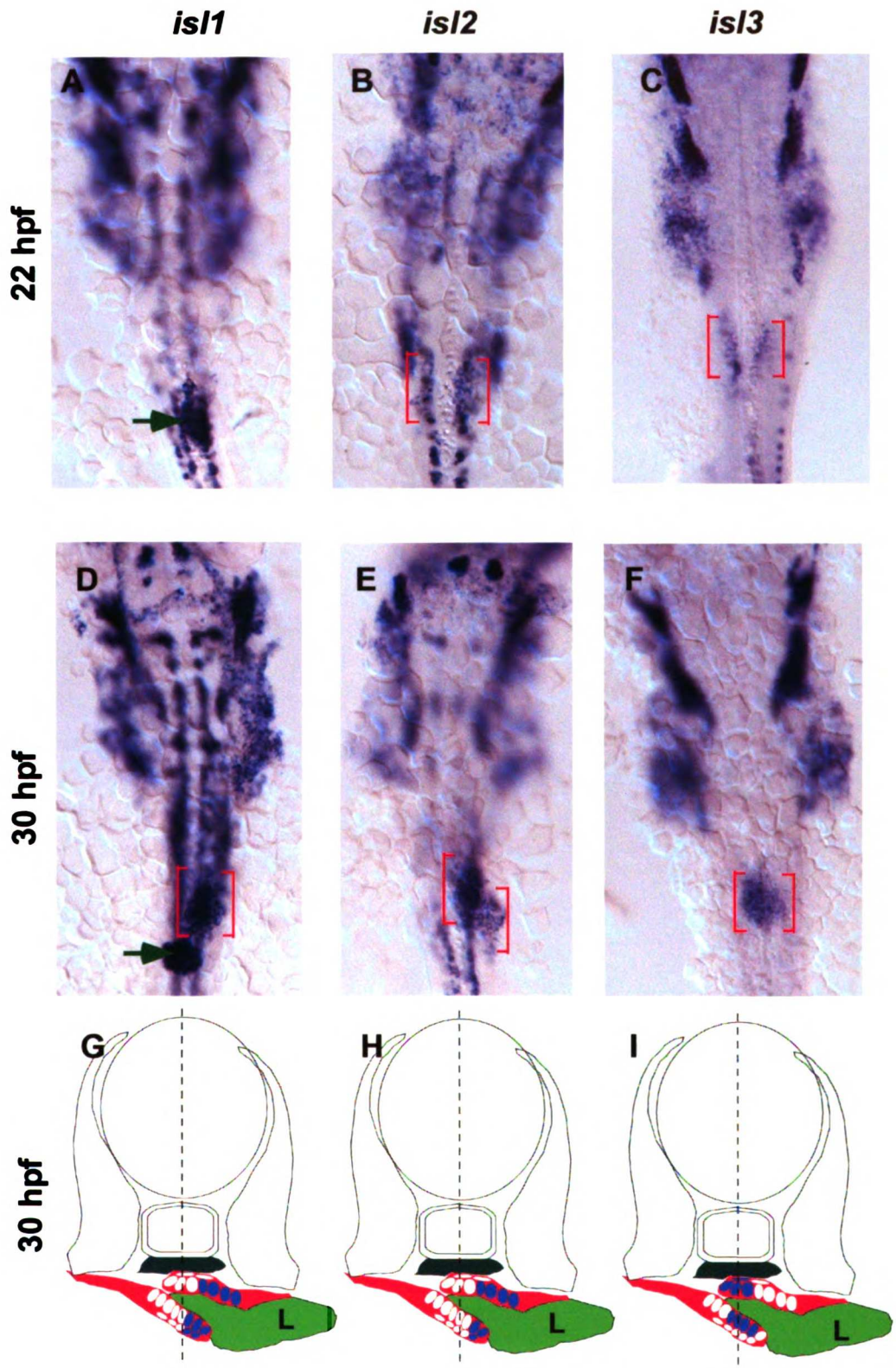

Figure A3.3. Actual whole-mount mRNA expression patterns (A-F), and speculated transverse expression domains (G-H), for *isl1*, *isl2* and *isl3*.

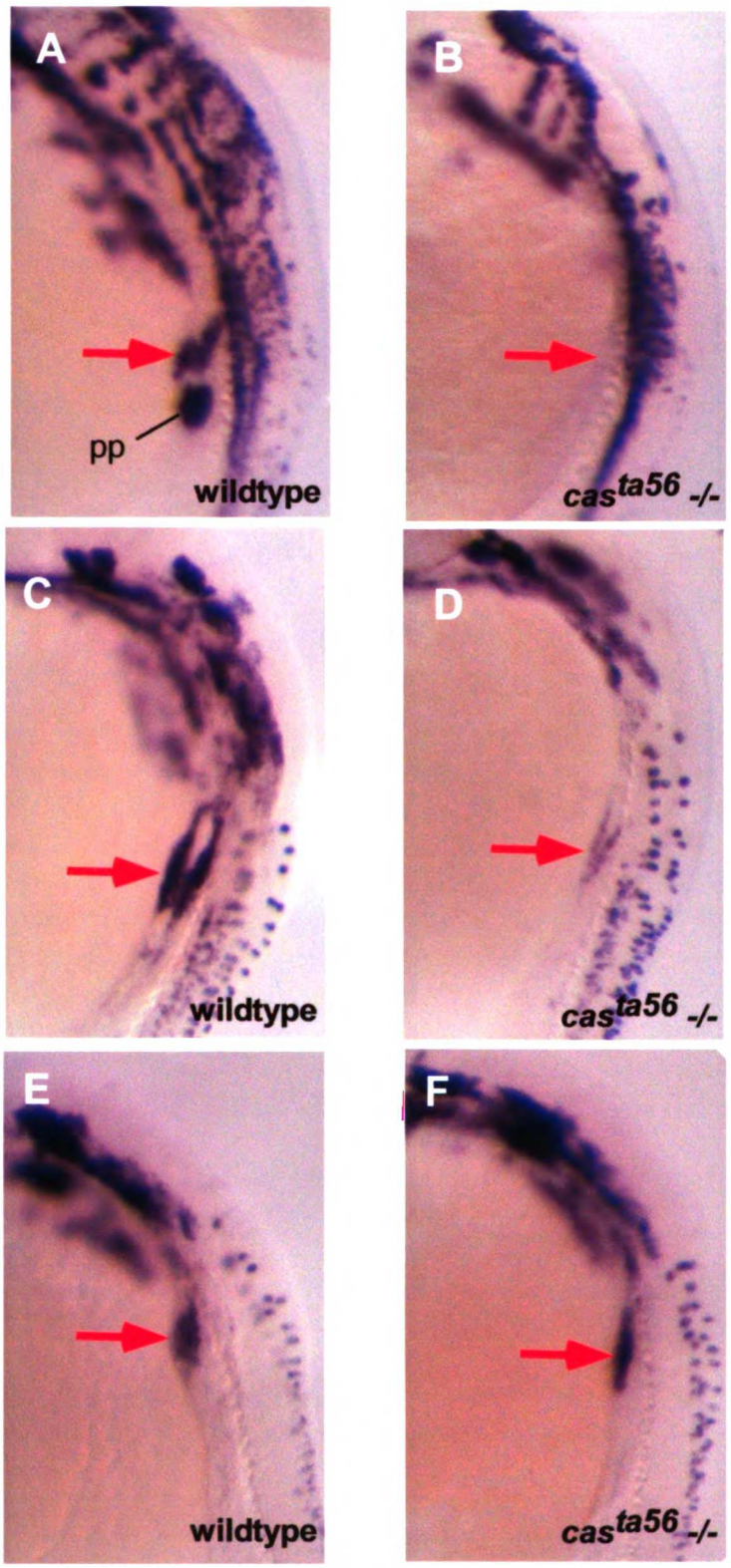

Figure A3.4. The absence of endoderm perturbs LPM expression of each *islet* gene to different degrees.

Table A3.1. Reagents for use in the study of Islet activity in the LPM

Antibodies

Anti-Islet-1 antibody. 39.4D5 from DSHB. Isotype Mouse IgG2b. Use at 8:100 dilution with 0.3% TritonX in PBS.

in situ Probes

pBS SK FL-islet1. The full length *islet1* in pBluescript SK(-) from Jose M. De Jesus. Antisense promoter, T7; antisense enzyme, EcoRI. For expression, transcribe with T3.
pBS SK FLISL2. The full length *islet2* in pBluescript SK(-) from Jose M. De Jesus. Antisense promoter, T7; antisense enzyme, EcoRI.
islet-3. From Yutaka Kikuchi. Antisense promoter, T7; antisense enzyme, BamHI.

Other useful plasmids

LIMisl1. The LIM domain of *islet1* in pCS2+ from Hiroshi Segawa. To make RNA, linearize with Not1, use sp6 promoter. Inject RNA at 1 ug/ul.
LIMisl2. The LIM domain of *islet2* in pCS2+ from Hiroshi Segawa. To make RNA, linearize with Not1, use sp6 promoter. Inject RNA at 1 ug/ul.
LIMisl3. The LIM domain of *islet3* in pCS2+ from Hiroshi Segawa. To make RNA, linearize with Not1, use sp6 promoter. Inject RNA at 1 ug/ul.
LIMisl1-myc. The LIM domain of *islet1* with one myc tag in pCS2+ from Hiroshi Segawa. To make RNA, linearize with Not1, use sp6 promoter. Inject RNA at 1 ug/ul.
LIMisl2-myc. The LIM domain of *islet2* with one myc tag in pCS2+ from Hiroshi Segawa. To make RNA, linearize with Not1, use sp6 promoter. Inject RNA at 1 ug/ul.
LIMisl3-myc. The LIM domain of *islet3* with one myc tag in pCS2+ from Hiroshi Segawa. To make RNA, linearize with Not1, use sp6 promoter. Inject RNA at 1 ug/ul.
LIMisl1-GFP. The LIM domain of *islet1* with GFP tag in pCS2+ from Hiroshi Segawa. To make RNA, linearize with Not1, use sp6 promoter. Inject RNA at 1 ug/ul.
LIMisl2-GFP. The LIM domain of *islet2* with GFP tag in pCS2+ from Hiroshi Segawa. To make RNA, linearize with Not1, use sp6 promoter. Inject RNA at 1 ug/ul.
LIMisl3-GFP. The LIM domain of *islet3* with GFP tag in pCS2+ from Hiroshi Segawa. To make RNA, linearize with Not1, use sp6 promoter. Inject RNA at 1 ug/ul.

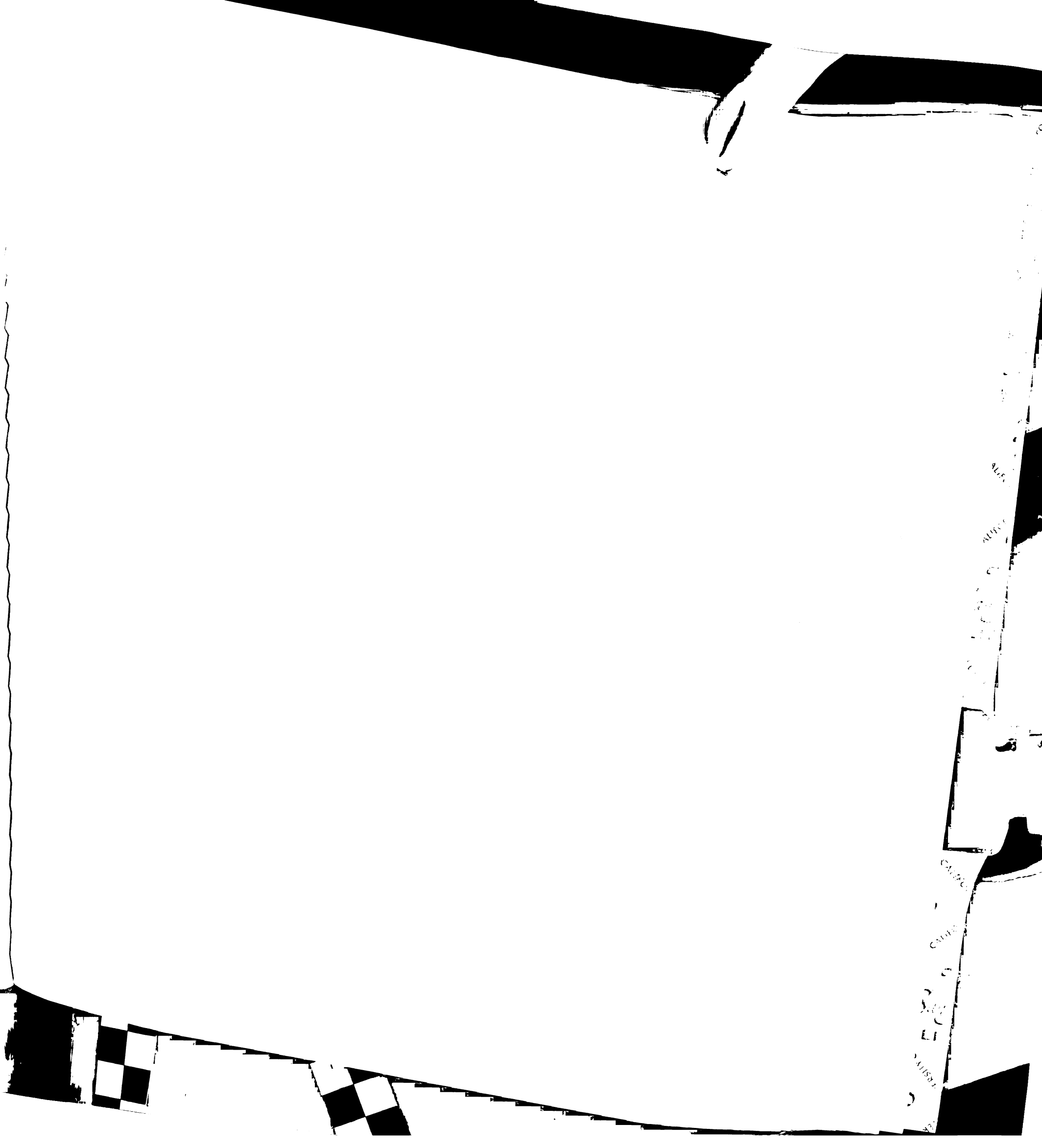

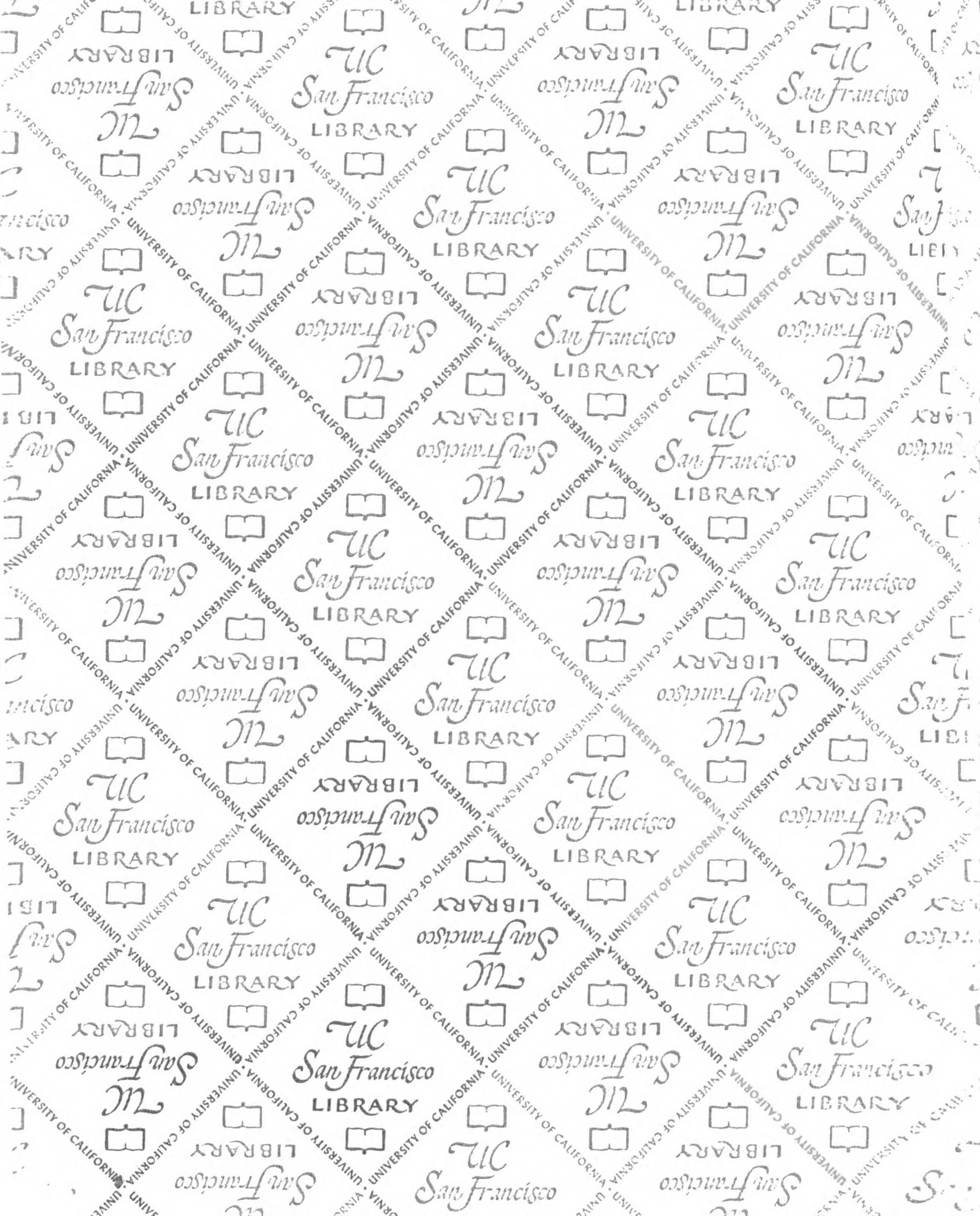
UC
San Francisco
LIBRARY
UNIVERSITY OF CALIFORNIA